

Friction Effect on Hydraulic Jump

Daniel Foroughi

Submitted to the
Institute of Graduate Studies and Research
in partial fulfillment of the requirements for the Degree of

Master of Science
in
Civil Engineering

Eastern Mediterranean University
September 2014
Gazimağusa, North Cyprus

Approval of the Institute of Graduate Studies and Research

Prof. Dr. Elvan Yılmaz
Director

I certify that this thesis satisfies the requirements as a thesis for the degree of Master of Science in Civil Engineering.

Prof. Dr. Özgür Eren
Chair, Department of Civil Engineering

We certify that we have read this thesis and that in our opinion it is fully adequate in scope and quality as a thesis for the degree of Master of Science in Civil Engineering.

Assoc. Prof. Dr. Umut Turker
Supervisor

Examining Committee

1. Assoc. Prof. Dr. Umut Türker

2. Asst. Prof. Dr. Tulin Akçaoğlu

3. Asst. Prof. Dr. Mustafa Ergil

ABSTRACT

A theoretical relationship for calculating the sequent depth ratio of the hydraulic jump formed in rectangular horizontal and roughened bed channels has been offered. This has been achieved based on considering the effect of drag force due to bed roughness in the momentum equation of hydraulic jumps. Two dimensionless parameters, dimensionless drag effect and dimensionless roughness effect are developed in order to observe the effect of roughness height on the magnitude of drag. Also, the effect of dimensionless drag effect on drag coefficient during hydraulic jump is achieved for different roughness heights at the bottom of channel. Within this study, another important physical phenomena occurring during hydraulic jumps that is the roller length as well investigated. A new model is developed for estimating the roller length in rectangular channels in terms of conjugate depths and upstream flow velocity. The developed equation has been tested for different type of rectangular cross section roughened beds as well.

Keywords: Hydraulic jump, roughened bed, rectangular channel, drag force, roller length.

ÖZ

Dikdörtgen kesitlerde taban pürüzlülüklerinin hidrolik sıçrama üzerinde yaptığı etki araştırılmış ve sıçrama öncesi ve sonrası su derinlikleri ile ilgili bağıntısı tanımlanmaya çalışılmıştır. Bağıntının elde edilmesinde hidrolik sıçrama anında momentumun korunumu ilkesi baz alınmış ve momentumun korunumu denklemi çözülerek kanal tabanındaki pürüzlülük ile sürüklenme (drag) kuvveti arasında bir ilişki kurulmuştur. Boyutsuz parametreler, boyutsuz sürüklenme etkisi ve boyutsuz pürüzlülük etkisi, kullanılarak pürüz yüksekliğinin hidrolik sıçramaya yaptığı etki gözlemlenmiştir. Bu çalışmada ayrıca hidrolik sıçramalar sırasında ortaya çıkan bir diğer önemli fiziksel fenomen olan sıçrama uzunluğu da bir model geliştirilerek eşlenik derinlikler ve menba akış hızı cinsinden yazılmış ve Dikdörtgen kesitlerde sıçrama uzunluğunu tahmin etmek için geliştirilmiştir. Geliştirilen bu denklem farklı pürüzlülük katsayısına sahip olan ortamlar için test edilmiş ve hidrolik sıçrama uzunluğu Dikdörtgen kesitler için modellenmiştir.

Anahtar Kelimeler: Hidrolik Sıçrama, pürüzlü yatak, dikdörtgen kanal, sürüklenme kuvveti, sıçrama uzunluğu.

DEDICATION

To My Family

ACKNOWLEDGMENT

I would like to thank Assoc. Prof. Dr. Umut Turker for his continuous support and guidance in the preparation of this study. Without his invaluable supervision, all my efforts could have been short-sighted.

I owe quite a lot to my family who allowed me to travel all the way from Iran to Cyprus and supported me all throughout my studies. I would like to dedicate this study to them as an indication of their significance in this study as well as in my life.

TABLE OF CONTENTS

ABSTRACT	iii
ÖZ	iv
DEDICATION	v
ACKNOWLEDGMENT	vi
LIST OF TABLES	ix
LIST OF FIGURES	x
LIST OF SYMBOLS	xiii
1 INTRODUCTION	1
1.1 Introduction	1
1.2 The Outcome of This Study	3
1.3 Literatures Review	4
2 FUNDAMENTAL DEFINITIONS	7
2.1 Hydraulic Jump	7
2.1.1 Types of Hydraulic Jump.....	8
2.1.2 Basic Characteristic of Hydraulic Jump	10
2.2 Drag and Its Effects	15
2.2.1 Friction Drag and Pressure Drag	15
2.2.2 Drag Coefficient	16
2.2.3 Roughness and Drag Effects on Hydraulic Jump	16
3 THEORETICAL CONSIDERATION	20
3.1 Depth Ratio in Hydraulic Jumps	20
3.2 Roller Length in Hydraulic Jumps	25
3.3 coefficient of determination, (R^2).....	27

3.4 Calculation of the Errors	28
4 RESULTS AND DISCUSSION	29
4.1 Friction Effect Analysis, Drag Force Coefficient and Drag Force.....	29
4.1.1 The obtained relationship between the dimensionless Drag Effect, (β) and the dimensionless Roughness Effect, ($K_s/\Delta E$)	30
4.1.2 The relationship between $K_s/\Delta E$ and β with respect to type of the jump..	34
4.1.2.b Steady Jump Condition.....	36
4.1.2.c Strong Jump Condition	40
4.1.3 Relationship between upstream Froude number, Fr_1 and dimensionless drag effect, β	42
4.1.4 Relationship between α and dimensionless drag effect, β	46
4.1.5 Relationship between drag coefficient, C_D and drag force, F_d	49
4.2 Roller Length.....	53
4.2.1 Relationship between dimensionless roller length, L_r/y_1 , and $K/\Delta E$	53
4.2.2 Relationship between dimensionless roller length, L_r/y_1 , and depth ratio ($y_2/y_1 - 1$) v_1	55
5 CONCLUSION	59
REFERENCES.....	62
APPENDICES	65
Appendix 1: Hughes, W.C and Flack, J.E's (1984) Data.....	66
Appendix 2: Ead, S.A and Rajaratnam, N.'s (2002) Data.....	73
Appendix 3: Evcimen, T.U.'s (2005) Data	74
Appendix 4: Carollo, F.G, Ferro, V. and Pampalone, V.'s (2007) Data	78

LIST OF TABLES

Table 4.1: Generated equations for dimensionless drag effect, β and dimensionless roughness effect, $K_s/\Delta E$ (Carollo et al. 2007).....	31
Table 4.2: Derived equations for dimensionless drag effect, β and dimensionless roughness effect, $K_s/\Delta E$ (Hughes and Flack, (1984), Ead and Rajaratnam (2002), Evcimen (2005)).....	33
Table 4.3: Generated equations for dimensionless drag effect, β and dimensionless roughness effect, $K_s/\Delta E$ in oscillating jump condition (Carollo et al. (2007), Hughes and Flack (1984)).	36
Table 4.4: Generated equations for dimensionless drag effect, β and dimensionless roughness effect, $K_s/\Delta E$ in steady jump condition (Carollo et al. (2007), Hughes and Flack (1984), Ead and Rajaratnam (2002), Evcimen, (2005)).....	39
Table 4.5: Generated equations for dimensionless drag effect, β and dimensionless roughness effect, $K_s/\Delta E$ in strong condition (Carollo et al. (2007), Evcimen, (2005)).	41
Table 4.6: Generated equations for dimensionless drag effects, β and upstream Froude number	45
Table 4.7: Generated drag coefficient, C_D , for each kind of roughness height, K_s ,... ..	49
Table 4.8: Generated drag force, F_d , for each kind of drag coefficient, C_D	52
Table 4.9: Dimensionless roller length equation.....	55
Table 4.10: Generated equations for dimensionless roller length.....	58

LIST OF FIGURES

Figure 2.1: Hydraulic jump's situation (Potter et. al., 2010)	7
Figure 2.2: Various types of hydraulic jump (Potter et. al., 2010)	9
Figure 2.3: Schematic representative of hydraulic jump with roller length.....	12
Figure 2.4: Parameters of a hydraulic jump on a rectangular prismatic channel.....	13
Figure 2.5: Different types of roughness at the channel bed.....	18
Figure 3.1: Schematic representative of hydraulic jump and its rectangular cross section.....	20
Figure 4.1: The relationship between dimensionless drag effect, β and dimensionless roughness effect, $K_s/\Delta E$, (Carollo. et al., 2007)	31
Figure 4.2: The relationship between dimensionless drag effect, β and dimensionless roughness effect, $K_s/\Delta E$ (Hughes and Flack, 1984)	32
Figure 4.3: The relationship between dimensionless drag effect, β and dimensionless roughness effect, $K_s/\Delta E$ (Ead and Rajaratnam, 2002)	32
Figure 4.4: The relationship between dimensionless drag effect, β and dimensionless roughness effect, $K_s/\Delta E$ (Evcimen, 2005).....	33
Figure 4.5: The relationship between dimensionless drag effect, β and dimensionless roughness effect, $K_s/\Delta E$ in oscillating jump condition (Carollo. et. al., 2007).....	35
Figure 4.6: The relationship between dimensionless drag effect, β and dimensionless roughness effect, $K_s/\Delta E$ in oscillating jump condition (Hughes and Flack, 1984).....	35
Figure 4.7: The relationship between dimensionless drag effect, β and dimensionless roughness effect, $K_s/\Delta E$ in steady jump condition (Carollo. et. al., 2007)	37

Figure 4.8: The relationship between dimensionless drag effect, β and dimensionless roughness effect, $K_s/\Delta E$ in steady jump condition (Hughes and Flack, 1984)	37
Figure 4.9: The relationship between dimensionless drag effect, β and dimensionless roughness effect, $K_s/\Delta E$ in steady jump condition (Ead and Rajaratnam, 2002)	38
Figure 4.10: The relationship between dimensionless drag effect, β and dimensionless roughness effect, $K_s/\Delta E$ in steady jump cond.(Evcimen, 2005)	38
Figure 4.11: The relationship between dimensionless drag effect, β and dimensionless roughness effect, $K_s/\Delta E$ in strong jump. (Carollo et al., 2007)	40
Figure 4.12: The relationship between dimensionless drag effect, β and dimensionless roughness effect, $K_s/\Delta E$ in strong jump cond. (Evcimen, 2005)	41
Figure 4.13: The relationship between upstream Froude number, Fr_1 and dimensionless drag effect, β (Carollo et. al., 2007)	43
Figure 4.14: The relationship between upstream Froude number, Fr_1 and dimensionless drag effect, β (Hughes and Flack, 1984)	43
Figure 4.15: The relationship between upstream Froude number, Fr_1 and dimensionless drag effect, β (Ead and Rajaratnam, 2002)	44
Figure 4.16: The relationship between upstream Froude number, Fr_1 and dimensionless drag effect, β (Evcimen, 2005)	44
Figure 4.17: The relationship between α and dimensionless drag effect, β (Carollo et. al., 2007)	46
Figure 4.18: The relationship between α and dimensionless drag effect, β (Hughes and Flack, 1984)	47

Figure 4.19: The relationship between α and dimensionless drag effect, β (Ead and Rajaratnam, 2002).....	47
Figure 4.20: The relationship between α and dimensionless drag effect, β (Evcimen, 2005).....	48
Figure 4.21: The relationship between drag coefficient, C_D and drag force, F_d (N) (Carollo et. al., 2007).....	50
Figure 4.22: The relationship between drag coefficient, C_D and drag force, F_d (N) Hughes and Flack, 1984).....	50
Figure 4.23: The relationship between drag coefficient, C_D and drag force, F_d (N) (Ead and Rajaratnam, 2002).....	51
Figure 4.24: The relationship between drag coefficient, C_D and drag force, F_d (N) Evcimen, 2005).....	51
Figure 4.25: The relationship between $K/\Delta E$ and dimensionless roller length, L_r/y_1 (Carollo et. al., 2007).....	54
Figure 4.26: The relationship between $K/\Delta E$ and dimensionless roller length, L_r/y_1 (Hughes and Flack, 1984).....	54
Figure 4.27: Relationship between dimensionless roller length, L_r/y_1 and $(y_2/y_1 - 1)v_1$ (Carollo et. al. 2007).....	56
Figure 4.28: Relationship between dimensionless roller length, L_r/y_1 and $(y_2/y_1 - 1)v_1$ for different K_s values separately (Carollo et. al., 2007).....	56
Figure 4.29: Relationship between dimensionless roller length, L_r/y_1 and $(y_2/y_1 - 1)v_1$ (Hughes and Flack, 1984).....	57
Figure 4.30: Relationship between dimensionless roller length, L_r/y_1 and $(y_2/y_1 - 1)v_0$ for different K_s values separately (Hughes and Flack, 1984).....	57

LIST OF SYMBOLS

a_1	The coefficient relating dimensionless drag effect and dimensionless roughness effect
a_2	The coefficient relating dimensionless drag effect and upstream Froude number
a_3	The coefficient relating dimensionless drag effect and upstream Froude number
a_4	The coefficient relating drag force and drag coefficient
a_5	The coefficient relating dimensionless roller length and $(K/\Delta E)$
a_6	The coefficient relating dimensionless roller length and $(y_2/y_1 - 1)$
A	Area of the channel cross section [m^2]
B	Channel width of rectangular channel [m]
C_{Df}	Frictional drag coefficient
d_{50}	Average diameter size of the particles [m]
ΔE	Amount of energy lost between upstream to downstream energies [m]
E_1	Upstream energy [m]
E_2	Downstream energy [m]
F_d	Drag force [N]
F_f	Friction force [N]
F_l	Lift force [N]

F_{df}	Frictional drag force [N]
F_{dp}	Pressure drag force [N]
F_{p1}	Upstream pressure force [N]
F_{p2}	Downstream pressure force [N]
Fr_1	Upstream Froude number
Fr_{s1}	Effective upstream Froude number
F_w	Weight force [N]
g	Gravitational acceleration [m/s^2]
h_{c1}	Centroid height of upstream cross section [m]
h_{c2}	Centroid height of downstream cross section [m]
I	Roughness density
K	Retarding force coefficient
K_s	Roughness height [m]
L_r	Roller length [m]
l_j	Hydraulic jump length [m]
L	Length [m]
m	Mass [Kg]
M	Momentum [$kg.m/s^2$]
P	Pressure [N/m^2]
Q	Unit discharge [m^2/s]
Q	Discharge [m^3/s]
S_0	Bed slope
Re	Reynolds number
T	Time [s]
v_1	Upstream flow velocity [m/s]

v_2	Downstream flow velocity [m/s]
V	Volume of a rectangular channel [m ³]
W	The distance between two consecutive bars in roughened bed [m]
\bar{y}	The mean value of dependent variables
y_1	Upstream depth of the hydraulic jump [m]
y_2	Downstream depth of the hydraulic jump [m]
z	Height of a prismatic cubic bar in Hughes-Flack's experiment [m]
ρ	Density [kg/m ³]
τ_w	Shear stress [N/m ²]
μ	Dynamic viscosity [kg/(m.s)]
δ	Kinetic energy correction factor
γ	Specific weight [N/m ³]
β	Dimensionless drag effect

Chapter 1

INTRODUCTION

1.1 Introduction

Whenever the water is not capable to control its power, it releases its excess energy and rearranges itself into a new balanced state. This phenomenon occurs naturally and can be easily observed while wave breaks at coastal areas and where hydraulic jump occurs in open channel flows.

Different researchers (Chow, 1959; Munson, 1990) have defined hydraulic jump several times and in general, all these definitions can be simplified by defining the jump as a rapid transition of flow from a high velocity condition into slower motion.

The hydraulic jump behavior of water in open channels can be used artificially in order to get benefits for engineering applications. It can be used for energy dissipation purposes at hydraulic structures in order to minimize the damages caused by scouring. The increase in water levels after the hydraulic jump helps obtaining higher heads for water distribution purposes like in irrigation channels. The chaotic behavior of water during the jump helps to mix different chemicals without extra energy requirements especially at water purification works. Among these applications, energy dissipation is the most important phenomenon; and for this purpose, roughened beds like corrugated bed, stilling basins, gravel bed, or combination of these are generally designed. Generally, fixing the location of the hydraulic jump, increasing the rate of the energy dissipation during the hydraulic

jump and minimizing the cost of the hydraulic structures are the main design motivations in hydraulics engineering.

Two dominant hydraulic jump characteristics are the length of the jump and the conjugate depths before and after the jump. These characteristics are usually used to illustrate the amount of energy dissipation during the jump. The length of a jump can be defined as the interim between the front face of the jump and the point exactly after the jump where subcritical state has been formed whereas conjugate depths are the depths exactly before and after the jump (figure 2.1) (Chow, 1959).

Rajaratnam (1968) has shown that the roughness of the surfaces decreases the length of the jump and the tailwater depth in open channels. The decrease in the length of the jump on the other hand helps to decrease the length of the stilling basins just at the dam's downstream side and cause to minimize the cost of this structure.

Ead and Rajaratnam (2002) improved the roughness studies by using corrugated beds and illustrated that length of the jump on corrugated beds is half of the jump length on smooth beds.

So far, several times it is proved that rough beds lead to reduction of the length of the jump and depth of the tailwater (Rajaratnam, 1968; Hughes and Flack, 1984; Negm, 1996; Ead and Rajaratnam, 2002). It is obvious that, whenever the interaction of the rough bed with flow occurs, shear stress increases and more energy dissipate consequently.

In this current study, the momentum equation is used together with the drag force relationship to obtain a reasonable drag coefficient in different rough bed characteristics. For applying this, a coefficient β is introduced to the momentum equation, which is modified by the drag force as a retarding force. The β values gave the reasonable drag coefficients (C_D), which are related to the geometry of the roughness.

1.2 The Outcome of This Study

The substantial goal of the present study is to apprehend the influences of roughness on hydraulic jumps by means of drag coefficient derived from momentum equations.

In chapter two, hydraulic jump characteristics in different situations were discussed. Furthermore, the drag force and its effects explained. In addition, in literature review, the studies carried out before related to the roughness effects on hydraulic jumps were illustrated. In chapter 3, theoretical studies about the effect of the roughness on the hydraulic jump characteristics, such as sequent depths ratio with respect to drag force and the roller length and the relationship between them were expressed. In chapter 4, graphical illustrations of the effects of roughness elements on the jump characteristics were presented. In chapter 5, the results were summarized.

In Appendices, all experimental data, which was used for this study, is given.

1.3 Literatures Review

Rajaratnam (1968) carried out the early studies on hydraulic jump regarding rough beds. In this work, relative roughness was considered as basin parameter and upstream Froude number was chosen as flow parameter. His conclusion initiated new discussions on hydraulic jump phenomena while searching for the effect of roughness and Froude number on conjugate depths.

Later, Hughes and Flack (1984) in their laboratory experiments, assessed the effects of impervious rough bed on hydraulic jump properties. Their experiments held in horizontal rectangular flume with two different roughness geometries, one with prismatic bars and another with gravels cemented on the basin. The laboratory observation showed that both sequent depth and the length of the hydraulic jump reduced due to the boundary roughness's.

Huger and Bremen (1989) have studied on depth ratio change due to wall friction. They have obtained that the Blanger equation is not valid for hydraulic jumps occurring over rough beds. In their study, the determined limit for the scaling deviation in between experimental data and theoretical calculation was 5 percent. It was summed up that, observed deviation is due to scaling effects because of reducing down the model dimensions, also those deviations exceeding these limits are brought by the fluid viscosity effects.

Alhamid and Negm (1996) perused on hydraulic jump over rectangular, roughened stilling basin and they have tested the effects of slope of the stilling basin on the flow characteristic, such as the relationship in between the conjugate depths.

Ead and Rajaratnam (2002) investigated hydraulic jumps on corrugated beds for a range of Froude number from 4 to 10 and three different relative roughness values from 0.25 to 0.5. They concluded that the downstream water depths in hydraulic jumps over corrugated basins are significantly smaller than jumps on smooth beds, and the length of the jump on corrugated basins are half of the jumps on smooth ones.

Evcimen (2005) investigated the influences of non-stuck out prismatic bars on jump while altering the Froude numbers. He obtained that with given upstream condition, the length of the jump and the depth of the tail water on roughened bed is shorter and smaller than those on smooth beds.

Carollo et al. (2007) investigated the hydraulic jump on horizontal rough beds experimentally. Experiments carried out to study the efficacy of roughened channel surface on the sequent depths ratio and roller length. They have solved the momentum equation and find its relationship with sequent depths, upstream Froude number, Fr_1 , and the ratio between the roughness height, K_s , and the upstream flow depth, y_1 . Results showed that, bed roughness diminishes the conjugate depth ratio, also the roller length, L_r , decreases when roughness height, K_s , augments. As a result, one boundary shear coefficient that can be approximated by the ratio between the upstream supercritical depth, y_1 and roughness height, K_s has been offered. They suggested the following equation as drag roughness coefficient (C_D),

$$C_D = \frac{2}{\pi} \arctan \left(0.8 \left(\frac{K_s}{y_1} \right)^{0.75} \right) \quad (1.1)$$

Afzal et al. (2011) offered an effective upstream Froude number which yields universal predictions for sequent depth ratio, jump length, roller length, jump profile,

and the other hydraulic jump characteristics that are definitely independent of bed roughness drag. They offered the conjugate depth ratio as

$$\frac{y_2}{y_1} = \frac{1}{2} \left[-1 + \sqrt{1 + 8Fr_{s1}^2} \right] \quad (1.2)$$

where, Fr_{s1} is the effective upstream Froude number where

$$Fr_{s1} = [(1 - C_D)(1 + \delta)]^{\frac{1}{2}} Fr_1 \quad (1.3)$$

where, δ is the kinetic energy correction factor, and also they suggested drag force coefficient (C_D) as follows,

$$C_D = 1 - \exp \left[-0.55 \left(\frac{K_s}{y_1} \right)^{0.75} \right] \quad (1.4)$$

Chapter 2

FUNDAMENTAL DEFINITIONS

2.1 Hydraulic Jump

When a flow passes from super critical regime to subcritical regime in open channels hydraulic jump definitely occurs (Fig. 2.1). This phenomenon happens frequently in the nature and also in man made structures such as at the regulation sluice, at the foot of spillways or at a place where a steep slope channel suddenly changes into mild slope. There are several hydraulic jump applications like, energy dissipation at the downstream of a dam or at the sluice gate, or increasing the water depth within the irrigation canal so as to divert the water to side canal or field; or to increase the water depth in an apron to counteract the uplift pressure, also for mixing the chemicals and for aeration in water distribution systems.

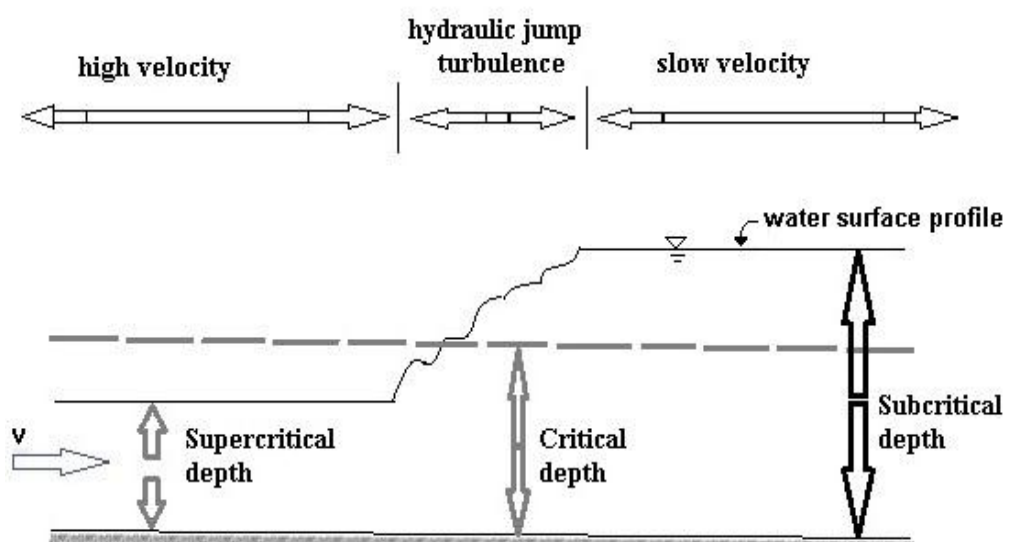


Figure 2.1: Hydraulic jump's situation (Potter et. al., 2010)

2.1.1 Types of Hydraulic Jump

Hydraulic jump on horizontal surface can be conveniently classified in the following categories according to Froude numbers (Figure 2.2); where Froude number can be defined as the ratio of inertial forces to gravitational forces.

For incoming Froude number equal to 1 ($Fr_1 = 1$), the flow is critical and therefore no jump can form.

For $1 < Fr_1 \leq 1.7$, the undulations are shown by water surface and the jump is called *undular jump*.

For $1.7 < Fr_1 \leq 2.5$, series of small roller form and the downstream water surface remains smooth and the energy loss during this jump is low. This jump is called *weak jump*.

For $2.5 < Fr_1 \leq 4.5$, an oscillating jet enters to the bottom of the hydraulic jump to surface with no periodicity. This jump is called *oscillating jump*.

For $4.5 < Fr_1 \leq 9$, that is insensitive to downstream conditions. This jump is a well-balanced jump that offers best performance. This jump is called *steady jump*.

For $Fr_1 > 9.0$, jump is intermittent but has good performance. This jump is called *strong jump*.






Types of Jump	Fr_1 range	Description	Energy Dissipation	Schematic
Undular Jump	$1 < Fr_1 \leq 1.7$	Undulation are shown by water surface	<5%	
Weak Jump	$1.7 < Fr_1 \leq 2.5$	Small roller forms but downstream water surface remains smooth	5% - 15%	
Oscillating Jump	$2.5 < Fr_1 \leq 4.5$	Unstable, Oscillating jet enters to the bottom of the jump, creates large waves	15% - 45%	
Steady Jump	$4.5 < Fr_1 \leq 9$	Well balanced jump which offers best performance	45% - 70%	
Strong Jump	$Fr_1 > 9.0$	jump is intermittent but good performance	70% - 85%	

Figure 2.2: Various types of hydraulic jumps (Potter et. al., 2010)

2.1.2 Basic Characteristic of Hydraulic Jump

Hydraulic jump leads to a significant turbulence and dissipation of energy wherever it occurs. The important parameters of the hydraulic jump are the conjugate depth, the length of the jump and the energy dissipation.

a) Conjugate depth

Conjugate depth refers to the upstream depth or the super critical depth (y_1) and the downstream or the subcritical depth (y_2) of the hydraulic jump.

The equation (Eq. 2.1), that demonstrates the conjugate depth ratio in hydraulic jump, is known as Belanger equation, and is valid in smooth rectangular channels.

$$\frac{y_2}{y_1} = \frac{1}{2} \left(\sqrt{1 + 8Fr_1^2} - 1 \right) \quad (2.1)$$

where y_1 is the upstream depth and y_2 is the downstream depth of the jump, Fr_1 is the upstream Froude number, which is

$$Fr_1 = \frac{v_1}{\sqrt{gy_1}} \quad (2.2)$$

where “ v_1 ” is the average velocity of the upstream flow and “ g ” is the gravitational acceleration.

Belanger equation is valid for smooth rectangular channels where the effect of friction is neglected. As soon as the bed roughness's become significant Belanger equation needs to be modified and a new definitions must be proposed.

b) Length of the hydraulic jump and roller length

In the literature, two definitions are widely used for the length of the jump. In the first definition, length of the jump is treated as the distance between the starting point of the jump at the upstream of the flow and the point immediately after the last roller at the downstream of the flow (roller length). The second definition is the distance

from the toe of the jump in supercritical side to the point where the flow surface states in completely level (Chow, 1959).

In most of the publications, the length of hydraulic jump is not given in terms of equations and usually defined either as a function of conjugate depths or as a function of Froude Numbers. An example is the jump length that varies from $4.5y_2$ to $6.5y_2$ for Froude numbers between 4 and 15 (Potter et. al., 2010). In general, it is preferred to define the length of hydraulic jump by means of experimental studies. Seldom, there are numerical studies concentrated on proving a relationship for hydraulic jump length (Ebrahimi et. al., 2013; Zhao and Misra, 2004; Abbaspour et. al., 2009). Roller length is the length from the toe of the jump where the surface roller starts until the last roller in downstream of the flow where the jump is going to be completed at subcritical level (Figure 2.3).

Chow (1973) defines guidelines about how to estimate the roller length of hydraulic jump as a function of upstream flow conditions. Hager et al. (1990) reviewed a wider datasets and correlations. They suggested the following correlation (Equation 2.3) for wide channel (i.e. $\frac{y_1}{B} < 0.10$) (Chanson, 2004), as:

$$\frac{L_r}{y_1} = 160 \tanh\left(\frac{Fr_1}{20}\right) - 12 \quad 2 < Fr_1 < 16 \quad (2.3)$$

where L_r is the roller length in meters. This equation is valid for rectangular horizontal channels.

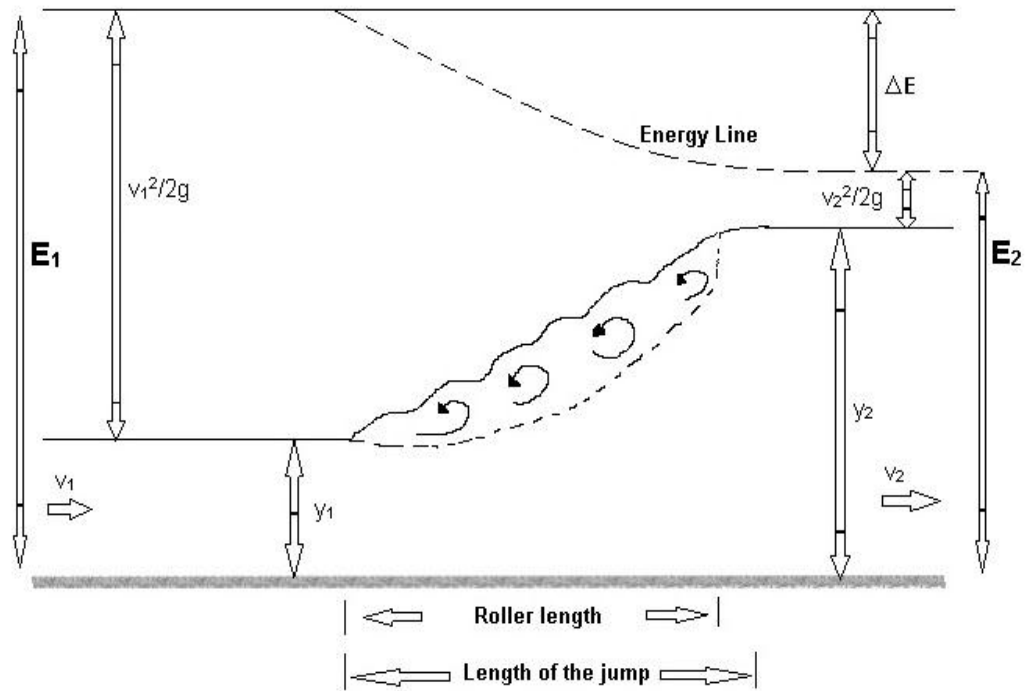


Figure 2.3: Schematic representation of hydraulic jump with roller length

c) Hydraulic jump as an energy dissipater

Hydraulic jump is a useful phenomenon to dissipate excess energy of upstream supercritical flow. It quickly reduces the velocity of the flow on a paved apron to where the flow does not have the ability for scouring the downstream channel bed below overflow spillways, chutes, and sluice gates (Chow, 1959).

The loss of energy in hydraulic jump is the difference between the specific energies before and after the jump as shown in Figure 2.3.

The energy loss during hydraulic jump can be obtained from the following path,

$$\Delta E = E_1 - E_2 \quad (2.4)$$

Writing down the energy terms in an open forum results in,

$$y_1 + \frac{v_1^2}{2g} - \left(y_2 + \frac{v_2^2}{2g} \right) \quad (2.5)$$

And also velocity, (v) can be expressed as (Q/A), hence, equation (2.4) is redefined as,

$$\Delta E = y_1 - y_2 + \left(\frac{Q^2}{2gB^2y_1^2} + \frac{Q^2}{2gB^2y_2^2} \right) \quad (2.6)$$

For the simplification of the above computations, unit discharge (q) can be replaced the total discharge, Q of the flow. Unit discharge is defined as the total discharge (Q) per unit width (B) of the channel. Hence,

$$\Delta E = y_1 - y_2 + \frac{q^2}{2g} \left(\frac{y_2^2 - y_1^2}{y_1^2 y_2^2} \right) \quad (2.7)$$

On the other hand, in fluid dynamics the momentum-force balance over a control volume is

$$M_1 + M_2 = F_w + F_d + F_{p1} + F_{p2} \quad (2.8)$$

which is shown in Figure 2.4.

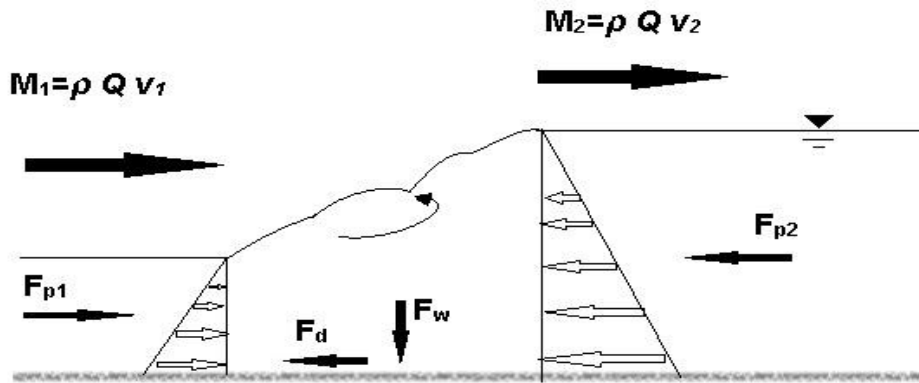


Figure 2.4: Parameters of a hydraulic jump on a rectangular prismatic channel

where, M is the momentum per unit time (mL/t^2), F_w is gravitational force due to weight of water (mL/t^2), F_d is force due to friction drag (mL/t^2) and F_p is pressure force (mL/t^2). Subscripts 1 and 2 represent upstream and downstream locations, respectively and units $L = \text{length}$, $t = \text{time}$ and $m = \text{mass}$.

Applying the momentum-force balance in the direction of flow, in a horizontal bed channel (i.e. $F_w = 0$) and neglecting the frictional force (smooth channel bed and walls) equation (2.8) can be written as follows:

$$M_{1x} + M_{2x} = F_{p1x} + F_{p2x} \quad (2.9)$$

Substituting the components of momentum per unit time and pressure force (with their respective positive or negative directions)

$$M_{1x} = m_r v_{1x} = -\rho Q v_1 \quad \text{and} \quad F_{p1x} = \bar{P}_1 A_1 \quad (2.10)$$

$$M_{2x} = m_r v_{2x} = -\rho Q v_2 \quad \text{and} \quad F_{p2x} = \bar{P}_2 A_2 \quad (2.11)$$

Finally the equation becomes

$$-\rho Q v_1 + \rho Q v_2 = \bar{P}_1 A_1 - \bar{P}_2 A_2 \quad (2.12)$$

where, m_r is the mass flow rate (m/t), ρ is the fluid density (m/L³), Q is the flow rate or discharge within the channel (L³/t), v is flow velocity (L/t), \bar{P} is the average pressure (m/Lt²) and A is the cross sectional area of the flow (L²). Subscripts 1 and 2 represent upstream and downstream locations, respectively.

The equation 2.8, which is called the momentum equation, can be written as

$$F_{p1} - F_{p2} = \rho Q (v_2 - v_1) \quad (2.13)$$

where, F_{p1} is the pressure force at upstream of the flow, F_{p2} is the pressure force at the downstream.

Finally, from the momentum equation (Eq. 2.13) one can have,

$$\rho g \frac{y_1}{2} y_1 B - \rho g \frac{y_2}{2} y_2 B = \rho Q \left(\frac{Q}{y_2 B} - \frac{Q}{y_1 B} \right) \quad (2.14)$$

Dividing both side of equation by B, ρ and g leads to

$$y_1^2 - y_2^2 = \frac{2q^2}{g} \left[\frac{y_1 - y_2}{y_2 y_1} \right] \quad (2.15)$$

Simplifying this equation will give,

$$\frac{q^2}{g} = \frac{y_1 y_2 (y_1 + y_2)}{2} \quad (2.16)$$

Substituting Eq. 2.16 in Eq. 2.7 results

$$\Delta E = y_1 - y_2 + \left[\frac{y_1 y_2 (y_1 + y_2) (y_2 - y_1) (y_1 + y_2)}{4 y_1^2 y_2^2} \right]$$

Finally, it simplifies as

$$\Delta E = \frac{(y_2 - y_1)^3}{4 y_1 y_2} \quad (2.17)$$

2.2 Drag and Its Effects

When a particle passes through a fluid, an interaction happens between body of the particle and the fluid; this effect results in forces between fluid and body joint; which can be explained in terms of two kinds of stresses that are the wall shear stress τ_w , due to viscous effects and the normal stresses due to the pressure (P). Any particle passing through a fluid is experiencing a drag, F_d which is a net force in the flow direction due to the shear forces and the pressure on the surface of the particle.

2.2.1 Friction Drag and Pressure Drag

Friction drag (F_{df}) occurs due to the shear stress (τ_w). The friction drag on a flat plate of width B and length L can be calculated from

$$F_{df} = \frac{1}{2} \rho v_{av}^2 B L C_D \quad (2.18)$$

where C_D is the drag force coefficient. The magnitude of the drag force coefficient depends on the Reynolds number and the relative roughness. Reynolds number can be determined from the ratio of inertia forces and viscous forces whereas the relative

roughness, which is the result of the boundary layer analysis, can be determined through experiments.

Pressure drag (F_{dp}), is that part of the drag which is due to the pressure (P), on the object. Pressure drag usually refers as *form drag*, because it depends to the shape of the object.

2.2.2 Drag Coefficient

As it is mentioned before, the net drag is due to both pressure and shear stress effects. In most situations, these two effects are taken into account and a drag coefficient (C_D) which is defined in equation 2.13, is used. Information about the drag coefficient covers compressible and incompressible viscous flows over any shape of interest in both artificial and natural channels.

The analysis and effects of drag on objects is usually determined by means of numerous experiments with water tunnels, wind tunnels, towing tanks etc. Almost all of these studies concentrated on investigating drag on scale models. The gathered data from these information can be put into dimensionless form and the results can be further rationed for calculations. Typically, the resultant drag coefficient equation for a special shaped object is given as

$$C_D = \frac{F_d}{\frac{1}{2} \rho v_{av}^2 A} \quad (2.19)$$

Munson (1990) said that, drag coefficient depends on several factors such as shape of the surface, Reynolds number, compressibility, surface roughness and Froude number.

2.2.3 Roughness and Drag Effects on Hydraulic Jump

Rajaratnam (1968) has done first investigations on how rough beds affect the hydraulic jump. He mentioned that conjugate depth depends on roughness height.

The other researchers such as Hughes and Flack (1984), Huger and Bremen (1990), Negm (1996) , Ead (2002), Evcimen (2005), Carollo et al. (2007) and Afzal (2011) carried out their studies to analyze the effects of roughness in hydraulic jump and they have concluded with different results for different bed roughness characteristics. As a simplification, it can be said that, when hydraulic jump occurs at a rough bed, conjugate depth y_2 and the length of the jump will be shorter than those jumps passing through smooth beds.

To develop a hydraulic jump and to augment energy dissipation, roughness elements can be utilized over a channel surface. Roughness elements are in different shapes, such as corrugated beds, gravels (pebbles and stones) and rectangular prismatic bars (cubic bars).

Hughes and Flacks (1984) and Evcimen (2005) analyzed the energy dissipation at hydraulic jumps in the presence of prismatic cubic bars with height “ z ”, and length of “ X ” (Figure 2.5a). The bars were located at the distance of “ W ” in strip form, coating the total breadth of the channel bed (Figure 2.5b) or formed in reeled shape, which is illustrated in Figure 2.5c.

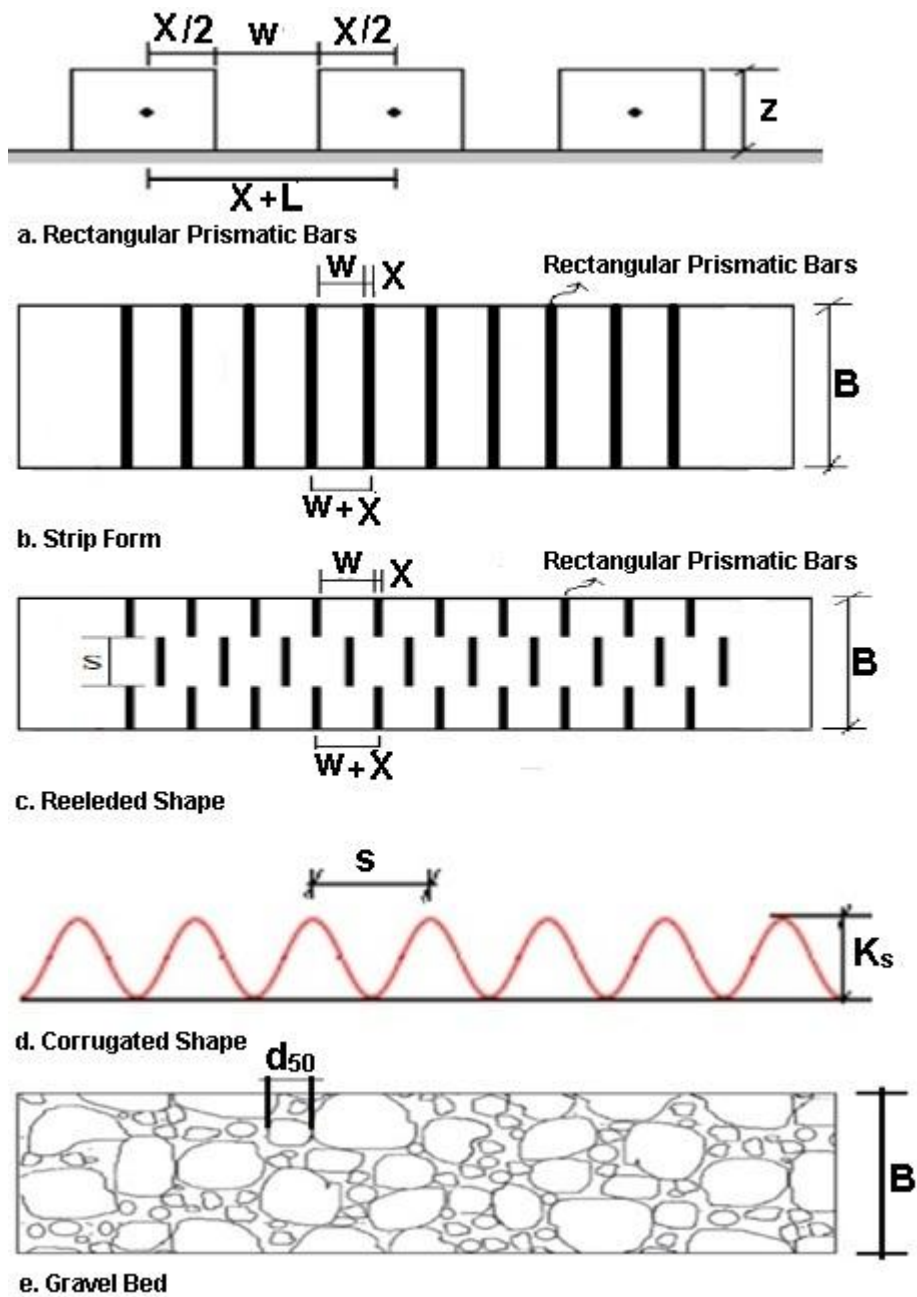


Figure 2.5: Different types of roughness at the channel bed

Ead and Rajaratnam (2002) studied the effects of corrugation with a wave shape with wavelength of “ s ” and amplitude of “ K_s ” (Figure 2.5d). It also can be placed to cover the whole length of the basin.

Sometimes pebbles are considered as roughness elements. Gravel is favored because of its cheap price, its availability in natural environment and easy transportation

possibilities. Generally, the median diameter size, d_{50} , agreed as estimated roughness height, K_s , for pebbles and gravels. On the other hand, there are no definite ways to assess the average interim between gravel grains. Thus, the most significant property on a gravel bed is the median diameter of the gravel grains that are considered as roughness height, K_s . Gravel grains are placed to coat the entire bed surface as can be observed in Figure 2.5e.

There is a lack of information about friction drag coefficient in different type of bed materials in hydraulic jump situation, which is clarified in this study.

Chapter 3

THEORETICAL CONSIDERATION

3.1 Depth Ratio in Hydraulic Jumps

Momentum equation, which has been discussed before, is as follow,

$$F_{p1} - F_{p2} - F_d - F_w = \rho Q(v_2 - v_1)$$

In case of mild slope where the slope is approximately zero, weight component can be dropped, $F_w = 0$, in which

$$F_{p1} - F_{p2} - F_d = \rho Q(v_2 - v_1) \quad (3.1)$$

F_{p1} and F_{p2} are the hydrostatic pressure forces. F_d is the drag force as it introduced before in Equation 2.8.

$$F_{p1} = \gamma h_{c1} A_1 \quad (3.2)$$

$$F_{p2} = \gamma h_{c2} A_2 \quad (3.3)$$

where, h_{c1} is the distance from the water surface to the centroid of the upstream rectangular cross section (Figure 3.1) which is $\frac{y_1}{2}$, h_{c2} is the centroid of the downstream rectangular cross section which is $\frac{y_2}{2}$, γ is the specific weight of water which is $\gamma = \rho g$, A_1 is the cross sectional area of upstream part of the jump, A_2 is the cross sectional area of downstream part of the jump.

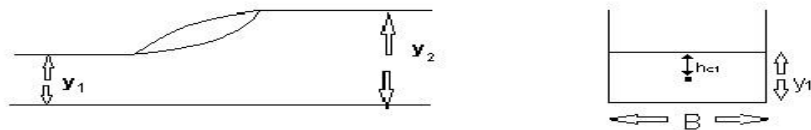


Figure 3.1: Schematic representation of hydraulic jump and its rectangular cross section

Substituting F_{p1} and F_{p2} in momentum equation (Eq. 3.1) will result;

$$\gamma h_{c1}A_1 - \gamma h_{c2}A_2 = \frac{\gamma}{g} Q(v_2 - v_1) + F_d \quad (3.4)$$

Dividing all the terms by γ ;

$$h_{c1}A_1 - h_{c2}A_2 = \frac{Q}{g}(v_2 - v_1) + \frac{F_d}{\gamma} \quad (3.5)$$

Inserting $\frac{Q}{A} = v$ in terms of v_1 and v_2 results in;

$$h_{c1}A_1 - h_{c2}A_2 = \frac{Q^2}{A_2g} - \frac{Q^2}{A_1g} + \frac{F_d}{\gamma} \quad (3.6)$$

which can be re-arranged as,

$$\frac{Q^2}{A_1g} + h_{c1}A_1 = \frac{Q^2}{A_2g} + h_{c2}A_2 + \frac{F_d}{\gamma} \quad (3.7)$$

The term $(\frac{Q^2}{A_ig} + h_{ci}A_i)$ is known as specific force. In the case of rectangular channels

where $A=By$ the discharge can be define in terms of unit discharge, q . Then unit discharge is the ratio between the discharge and the width of the rectangular channel.

Therefore, equation (3.7) can be re-arranged by replacing Q with qB , and since B is constant along the channel;

$$B \left[\frac{q^2}{y_1g} + h_{c1}y_1 - \frac{q^2}{y_2g} - h_{c2}y_2 \right] = \frac{F_d}{\gamma} \quad (3.8)$$

Substituting $h_{c1} = \frac{y_1}{2}$ and $h_{c2} = \frac{y_2}{2}$ into above equation will give;

$$\frac{q^2}{g} \left[\frac{y_2 - y_1}{y_1y_2} \right] + \frac{y_1^2}{2} - \frac{y_2^2}{2} = \frac{F_d}{\gamma B} \quad (3.9)$$

Decomposing 2nd degree y terms into 1st degree gives,

$$B \left[\frac{q^2}{y_1g} + h_{c1}y_1 - \frac{q^2}{y_2g} - h_{c2}y_2 \right] = \frac{F_d}{\gamma} \quad (3.10)$$

$$(y_1 - y_2) \left[\left[-\frac{q^2}{gy_1y_2} \right] + \frac{1}{2}(y_1 + y_2) \right] = \frac{F_d}{\gamma B} \quad (3.11)$$

In rectangular open channel flows, the discharge can be defined as

$$Q = Byv \quad (3.12)$$

which can be simplified into

$$q = yv \quad (3.13)$$

Thus above equation can be re-written in terms of water depth and flow velocity as;

$$(y_1 - y_2) \left[\frac{1}{2} (y_1 + y_2) - Fr_1^2 \frac{y_1^2}{y_2} \right] = \frac{F_d}{\gamma B} \quad (3.14)$$

Taking all the terms out of brackets,

$$\frac{1}{2} (y_1^2 - y_2^2) - Fr_1^2 \frac{y_1^2}{y_2} (y_1 - y_2) = \frac{F_d}{\gamma B} \quad (3.15)$$

Collecting Froude number into brackets gives,

$$y_1^2 \left[\frac{1}{2} - Fr_1^2 \frac{y_1}{y_2} + Fr_1^2 \right] - \frac{1}{2} y_2^2 = \frac{F_d}{\gamma B} \quad (3.16)$$

then, can be writing drag force as a subject of the formula,

$$F_d = \gamma B \left[y_1^2 Fr_1^2 \left(\frac{y_2 - y_1}{y_2} \right) + \frac{1}{2} y_1^2 - \frac{1}{2} y_2^2 \right] \quad (3.17)$$

$$F_d = \gamma B \left[y_1^2 Fr_1^2 \left(\frac{y_2 - y_1}{y_2} \right) + \frac{1}{2} (y_1 - y_2)(y_1 + y_2) \right] \quad (3.18)$$

Rewriting drag force in open form and substituting in the above equation leads to

$$F_d = \frac{1}{2} C_D \rho v_{av}^2 A_{bed} \quad (3.19)$$

$$\gamma B \left[y_1^2 Fr_1^2 \left(\frac{y_2 - y_1}{y_2} \right) + \frac{1}{2} (y_1 - y_2)(y_1 + y_2) \right] = \frac{1}{2} C_D \rho v_{av}^2 A_{bed} \quad (3.20)$$

Dividing all terms by γ and y_1^2 gives,

$$\frac{B}{y_1^2} \left[2y_1^2 Fr_1^2 \left(\frac{y_2 - y_1}{y_2} \right) + (y_1 - y_2)(y_1 + y_2) \right] = \frac{v_{av}^2}{g} C_D A_{bed} \frac{1}{y_1^2} \quad (3.21)$$

$$2Fr_1^2 \left(\frac{y_2 - y_1}{y_2} \right) + \left(\frac{y_1^2 - y_2^2}{y_1^2} \right) = \frac{v_{av}^2}{y_1^2 g} C_D \frac{A_{bed}}{B} \quad (3.22)$$

The term on the right hand side of the equation is equal to β (dimensionless drag effect),

$$\beta = \frac{v_1^2}{y_1^2 g} C_D \frac{A_{bed}}{B} \quad (3.23)$$

Previous equation becomes;

$$2Fr_1^2 \left(\frac{y_2 - y_1}{y_2} \right) + \left(\frac{y_1^2 - y_2^2}{y_1^2} \right) = \beta \quad (3.24)$$

A_{bed} can be expressed as the multiplication of bottom width, B and length of the jump, l_j .

Hence,

$$1 - \beta = \left(\frac{y_2}{y_1} \right)^2 - 2Fr_1^2 + 2Fr_1^2 \left(\frac{y_1}{y_2} \right) \quad (3.25)$$

Multiplying both side of equation with $\left(\frac{y_2}{y_1} \right)$ will give,

$$\left(\frac{y_2}{y_1} \right)^3 = 2Fr_1^2 \left(\frac{y_2}{y_1} \right) - 2Fr_1^2 + \left(\frac{y_2}{y_1} \right) - \beta \left(\frac{y_2}{y_1} \right) \quad (3.26)$$

Bringing all terms to left hand side results

$$\left(\frac{y_2}{y_1} \right)^3 - (2Fr_1^2 + 1 - \beta) \left(\frac{y_2}{y_1} \right) + 2Fr_1^2 = 0 \quad (3.27)$$

If β is 0 where C_D is 0

$$\left(\frac{y_2}{y_1} \right)^3 - (2Fr_1^2 + 1) \left(\frac{y_2}{y_1} \right) + 2Fr_1^2 = 0 \quad (3.28)$$

If uniform flow, then $\frac{y_2}{y_1} = 1$ and $y_2 = y_1$.

If no, then

$$\left[\left(\frac{y_2}{y_1} \right)^2 + \left(\frac{y_2}{y_1} \right) - 2Fr_1^2 \right] \left[\left(\frac{y_2}{y_1} \right) - 1 \right] = 0 \quad (3.29)$$

let $\frac{y_2}{y_1} = x$ then the above equation can be written as;

$$[x^2 + x - 2Fr^2][x - 1] = 0 \quad (3.30)$$

Since the second term cannot be equal to zero except at $y_1=y_2$ (which means no hydraulic jump) then $[x^2 + x - 2Fr^2]$ must be equal to zero. The roots of the equation can be find simply by

$$x_1, x_2 = \frac{-b \pm \sqrt{b^2 - 4ac}}{2a} \quad (3.31)$$

which gives

$$x_1 = \frac{y_2}{y_1} = \frac{1}{2} \left[-1 + \sqrt{1 + 8Fr_1^2} \right] \quad (3.32)$$

The above equation is the famous Blanger hydraulic jump relationship for frictionless environments.

However, If $\beta \neq 0$ where $C_D \neq 0$

$$\left(\frac{y_2}{y_1}\right)^3 - (2Fr_1^2 + 1 - \beta) \left(\frac{y_2}{y_1}\right) + 2Fr_1^2 = 0 \quad (3.33)$$

where

$$\beta = \frac{v_{av}^2}{y_1^2 g} C_D \frac{A_{bed}}{B}$$

$$\beta = \frac{v_{av}^2}{y_1 g} C_D \frac{l_j}{y_1} \quad (3.34)$$

According to Alhamid and Negm (1996), in the case of consecutive blocks as the distributed roughness elements, the blocks are below the entire length of the jump and the correct approach is to calculate the drag force due to each block, then integrate them to obtain the total drag force to use in the momentum equation. The average velocity at upstream section can be used as a representative velocity v_I , as an assumption for simplicity of driving the model, because v_I can be easily determined by dividing the measured discharge by the cross sectional area at upstream section which is well known. Rechecking the derived model with the experimental results

proved that this assumption works well. Therefore, the average velocity can be accepted to be equivalent to upstream velocity (v_1).

Therefore, substituting Fr_1^2 instead of $\frac{v_1^2}{y_1 g}$ causes,

$$\beta = Fr_1^2 C_D \frac{l_j}{y_1} \quad (3.35)$$

Suppose

$$Fr_1^2 \frac{l_j}{y_1} = \alpha \quad (3.36)$$

Then,

$$\beta = \alpha C_D \quad (3.37)$$

3.2 Roller Length in Hydraulic Jumps

The experimental studies of Pietrkowski (1932), Smetana (1937) and (Hager 1992) suggest that one can assume roller length, L_r proportional to the difference between the sequent depths as

$$\frac{L_r}{y_1} = a \left[\frac{y_2}{y_1} - 1 \right] \quad (3.38)$$

in which coefficient a is equal to 6, 5.5 and 5.2 according to Smetana (1937), Citrini (1939), Mavis and Luksck (Hager et al. 1990) respectively. Carollo et al. (2007) performed experiments and rewrote this equation and compared the findings with the results of Hughes and Flack (1984) and Hager et al. (1990). Carollo et al. (2007) concluded with one single number representing the coefficient, (a) as 4.616. Findings attained a coefficient of determination equivalent to 0.92. In this study, a theoretical approach will be carried out instead of experimental approach in order to define formulation of roller length.

The net force occurring during the action of drag force on a solid surface is the famous Newtonian second law where drag force proportionally depends on the velocity of the flow.

$$F_{net} = m \cdot a = +F_d = -Kv \quad (3.39)$$

Considering a column of liquid passing over a rough surface, mass can be written as $\rho\Delta V$ and the acceleration as $\frac{dv}{dt}$, as the flow will act in the x-direction. The resultant equation can be given as,

$$\rho\Delta V \frac{dv}{dt} = -F_d \quad (3.40)$$

The drag force is function of density, ρ , velocity, v and the area, A as,

$$F_d = f(\rho, v, A) \quad (3.41)$$

Therefore,

$$F_d = -K\rho vA \quad (3.42)$$

where K is retarding force coefficient. Rewriting the Equation 3.40 will give

$$\rho\Delta V \frac{dv}{dt} = -K\rho vA \quad (3.43)$$

For a fluid particle of cubic shape acting on an area of $\Delta x\Delta z$, Equation 3.43 can be rewritten as

$$\rho\Delta y\Delta x\Delta z \frac{dv}{dt} = -\rho v\Delta x\Delta zK \quad (3.44)$$

Simplifying the above equation leads to Equation 3.45

$$\Delta y \frac{dv}{dt} = -vK \quad (3.45)$$

$$\frac{dv}{v} = \frac{-K}{\Delta y} dt \quad (3.46)$$

Solving Equation 3.46 results;

$$v = v_0 e^{\left(-\frac{K}{\Delta y}\right)t} \quad (3.47)$$

Since $v = \frac{dx}{dt}$; Equation 3.28 can be defined as

$$\frac{dx}{dt} = v = v_0 e^{\left(-\frac{K}{\Delta y}\right)t}$$

$$dx = v_0 e^{\left(-\frac{K}{\Delta y}\right)t} dt \quad (3.48)$$

Integrating equation 3.48 in which $dx = x_2 - x_1$ defines the roller length (L_r) as

$$\frac{L_r}{y_1} = \frac{1}{K} \left[\frac{y_2}{y_1} - 1 \right] v_{av} \quad (3.49)$$

As it is mentioned before $v_{av} = v_1$; and final roller length equation can be defined as;

$$\frac{L_r}{y_1} = \frac{1}{K} \left[\frac{y_2}{y_1} - 1 \right] v_1 \quad (3.50)$$

3.3 coefficient of determination, (R^2)

In statistics, the coefficient of determination, (R^2) is a number that indicates how well data fit a statistical model, sometimes simply a line or curve. It is a statistic used in the context of statistical models whose main purpose is either the prediction of future outcomes or the testing of hypotheses, on the basis of other related information. It provides a measure of how well observed outcomes are replicated by the model, as the proportion of total variation of outcomes explained by the model (Glantz et. al., 1990). The coefficient of determination ranges from 0 to 1 and it can be calculated by the Equation 3.51.

$$R^2 \equiv 1 - \frac{SS_{res}}{SS_{tot}} \quad (3.51)$$

Also SS_{res} and SS_{tot} are total sum of squares and sum of squares of residuals respectively and can be calculated by following equations.

$$SS_{tot} = \sum_i (y_i - \bar{y})^2 \quad (3.52)$$

$$SS_{res} = \sum_i (y_i - f(x_i))^2 \quad (3.53)$$

Where \bar{y} is mean, y_i is the i^{th} value of the variable to be predicted, x_i is the i^{th} value of the explanatory variable, and $f(x_i)$ is the predicted value of y_i .

3.4 Calculation of the Errors

Calculation of the Errors has been done based on mean absolute percentage error (MAPE) method. In statistics, the mean absolute percentage error is the computed average of percentage errors by which forecasts of a model differ from actual values of the quantity being forecast.

The formula for the mean absolute percentage error is

$$\text{MAPE (\%)} = \frac{100}{n_o} \sum_{i=1}^n \frac{|f_i - a_i|}{|a_i|} \quad (3.54)$$

where a_i is the actual value of the quantity being forecast, f_i is the forecast, and n_o is the number of different times for which the variable is forecast (Khan and Bartley, 2003).

Magnitude of mean absolute percentage error by considering the distance between actual data and approximated data shows how large the error actually is; i.e, 100% of MAPE says that the interim between forecasted value and actual value is two times bigger than actual value; on the other hand, 1% of MAPE shows that the forecasted value and actual value are 99% similar and the error in estimation between the forecasted value and the actual value is negligible. It can be said that, the MAPE has an inverse relationship with data accuracy; i.e., the smaller the mean absolute error, the closer the forecasted data are to actual data; conversely, the larger mean absolute percent error, the greater the difference in the forecasted value and the actual value.

Chapter 4

RESULTS AND DISCUSSION

4.1 Friction Effect Analysis, Drag Force Coefficient and Drag Force

The relationship between parameters derived in previous chapters is analyzed in this section. In general, the relationship between dimensionless drag effect (β) and dimensionless roughness effects ($K_s/\Delta E$) are studied with respect to different roughness heights and different Froude numbers. The relationship is developed for the data series given by Carollo et al. (2007), Hughes and Flack (1986), Ead and Rajaratnam (2002), and Evcimen (2005). As it can be seen in Equation 3.35, dimensionless drag effect, (β) is a function of upstream Froude number, (Fr_1) also. Hence, the relationship between upstream Froude number, (Fr_1) and the dimensionless drag effect, (β) was studied. This relationship carried out for the same datasets. Then, according to Equation 3.37, the relationship between coefficient α and dimensionless drag effect, (β) used for finding drag coefficient, (C_D) with respect to all roughness heights. Finally, according to Equation 3.20, the relationship between drag coefficient, (C_D) and the drag force, (F_d) figured out for all datasets.

4.1.1 The obtained relationship between the dimensionless Drag Effect, (β) and the dimensionless Roughness Effect, ($K_s/\Delta E$)

The variation of the dimensionless drag effect, (β) and the dimensionless roughness effect ($K_s/\Delta E$) is given in Figure 4.1. The figure is plotted using the experimental dataset of Carollo et al. (2007). The general trend of β with respect to ($K_s/\Delta E$) shows an inverse relationship. As β increases $K_s/\Delta E$ approaches zero, while $K_s/\Delta E$ goes to infinity as β diminishes. The solid lines in Figure 4.1 shows the best fit line through experimental data for different K_s values. The equation of best fit lines for different K_s values are given in Table 4.1. It is clear from Figure 4.1 that, the best fit line between β and $K_s/\Delta E$ through experimental data can be represented by

$$\beta = a_1 \left(\frac{K_s}{\Delta E} \right)^n \quad (4.1)$$

In which a_1 and n are constants with n always being less than zero. The best linear fit equations in respect of the present empirical models along with the coefficient of determination (R^2) are given in Table 4.1. Higher values of R^2 associated with the β and $K_s/\Delta E$ reflects the fact that, their functional dependence is acceptable. For comparative purposes, the utility of functional representation of other models (Hughes and Flack (1986), Ead and Rajaratnam (2002), and Evcimen (2005)) were examined and their results were interpreted as well.

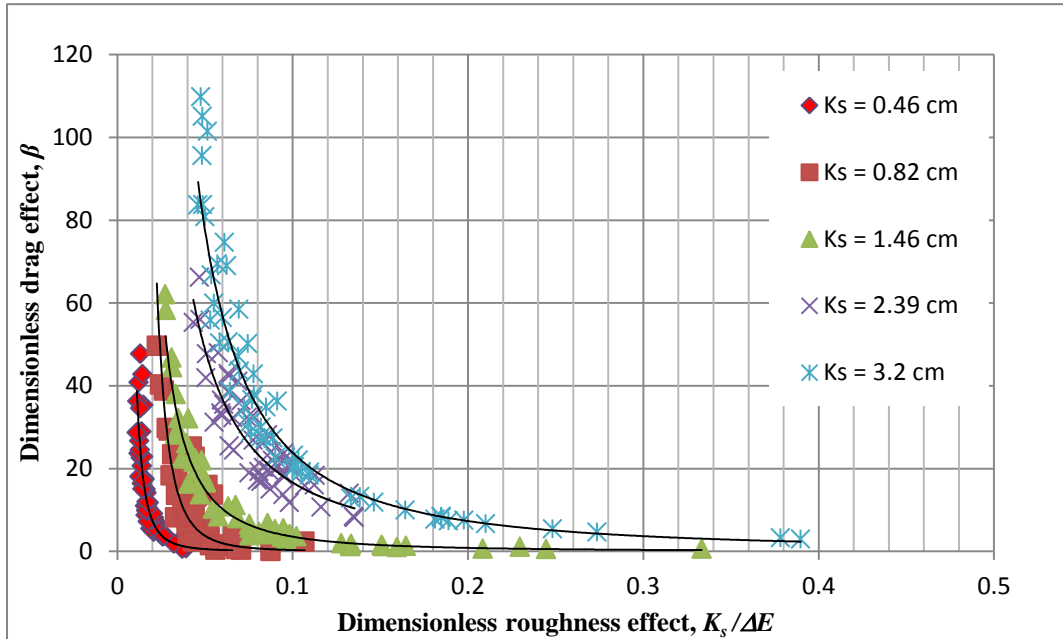


Figure 4.1: The relationship between dimensionless drag effect, β and dimensionless roughness effect, $K_s/\Delta E$, (Carollo. et al., 2007)

Figure 4.1 is based on Carollo, et. al. (2007) dataset and it illustrates the trend line obtained for each roughness height (K_s). Generated equations with coefficient of determination and the mean absolute percentage error values are given in following Table 4.1.

Table 4.1: Generated equations for dimensionless drag effect, β and dimensionless roughness effect, $K_s/\Delta E$ (Carollo et al. 2007)

figure number; dimensionless drag effect	roughness height, K_s (cm)	equation type	coefficients of equation, a_1, n ; correlation coefficient, R^2 ; MAPE (%)	data set reference
4.1; β	0.46		$a_1 = 0.0001, n^* = -2.83$; $R^2 = 0.94$; MAPE=26.2	Carollo et al., (2007)
4.1; β	0.82		$a_1 = 9E-05, n = -3.57$; $R^2 = 0.81$; MAPE=221.1	
4.1; β	1.46	$\beta = a_1(K_s/\Delta E)^n$	$a_1 = 0.0297, n = -2.08$; $R^2 = 0.97$; MAPE=56.75	
4.1; β	2.39		$a_1 = 0.4661, n = -1.55$; $R^2 = 0.81$; MAPE=22.43	
4.1; β	3.2		$a_1 = 0.4736, n = -1.70$; $R^2 = 0.97$; MAPE=11.99	

*n, is a constant

Figures (4.2 - 4.4) has depicted based on Hughes and Flack's data (1986), Ead and Rajaratnam (2002) and Evcimen (2005) and the equation of obtained trend line for each roughness height (K_s) value is given in Table 4.2. MAPE value for different K_s magnitudes show that the suggested equations are reliable for K_s values except $K_s=0.82$ cm.

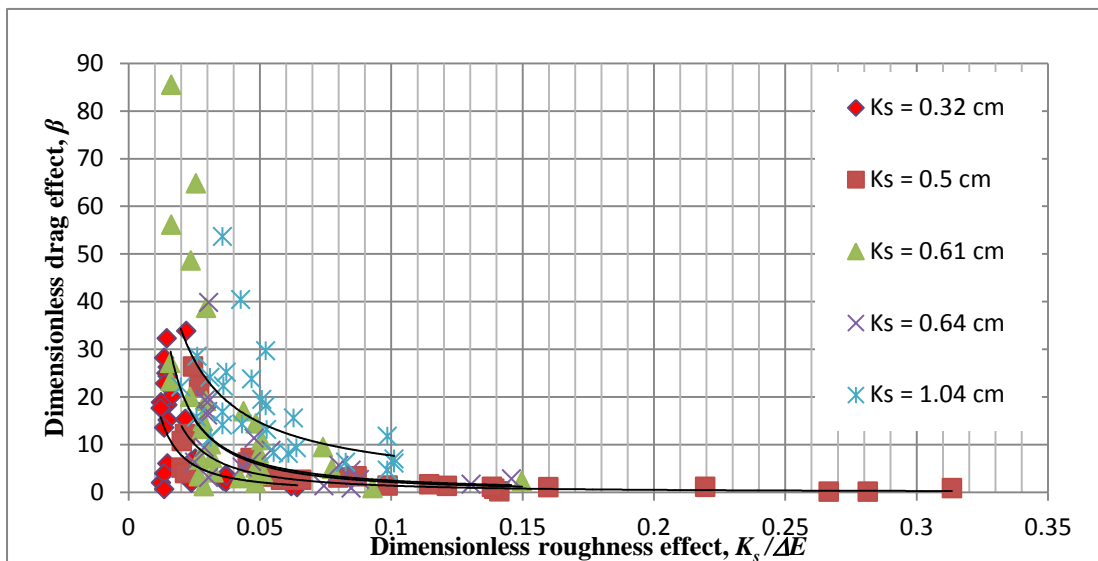


Figure 4.2: The relationship between dimensionless drag effect, β and dimensionless roughness effect, $K_s/\Delta E$ (Hughes and Flack, 1984)

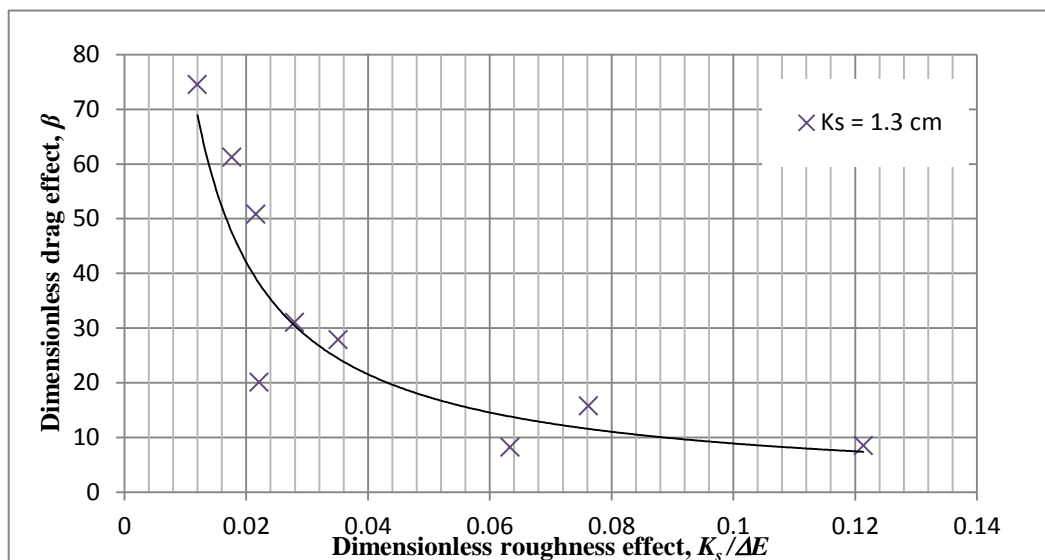


Figure 4.3: The relationship between dimensionless drag effect, β and dimensionless roughness effect, $K_s/\Delta E$ (Ead and Rajaratnam, 2002)

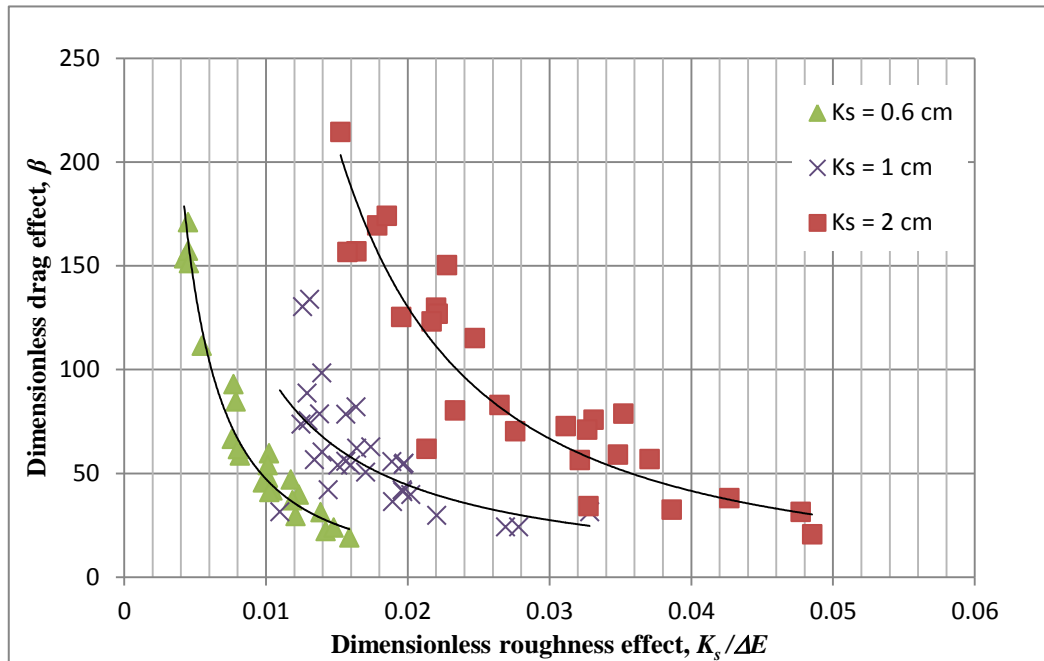


Figure 4.4: The relationship between dimensionless drag effect, β and dimensionless roughness effect, $K_s/\Delta E$ (Evcimen, 2005)

Table 4.2: Derived equations for dimensionless drag effect, β and dimensionless roughness effect, $K_s/\Delta E$ (Hughes and Flack, (1984), Ead and Rajaratnam (2002), Evcimen (2005)).

figure number; dimensionless drag effect	roughness height, K_s (cm)	equation type	coefficients of equation, a_1, n ; correlation coefficient, R^2 ; MAPE (%)	data set reference
4.2; β	0.32		$a_1 = 0.0295, n^* = -1.43$; $R^2 = 0.34$; MAPE=145.21	
4.2; β	0.5		$a_1 = 0.0507, n = -1.44$; $R^2 = 0.73$; MAPE=81.46	Hughes and Flack, (1984)
4.2; β	0.61	$\beta = a_1 (K_s/\Delta E)^n$	$a_1 = 0.0796, n = -1.43$; $R^2 = 0.42$; MAPE=99.83	
4.2; β	0.64		$a_1 = 0.1158, n = -1.31$; $R^2 = 0.22$; MAPE=54.63	
4.2; β	1.04		$a_1 = 0.9229, n = -0.92$; $R^2 = 0.46$; MAPE=36.86	
4.3; β	1.3	$\beta = a_1 (K_s/\Delta E)^n$	$a_1 = 0.9642, n = -0.965$; $R^2 = 0.82$; MAPE=29.46	
4.4; β	0.6		$a_1 = 0.0383, n = -1.55$; $R^2 = 0.95$; MAPE=12.24	Evcimen, (2005)
4.4; β	1	$\beta = a_1 (K_s/\Delta E)^n$	$a_1 = 0.4365, n = -1.18$; $R^2 = 0.48$; MAPE=20.07	
4.4; β	2		$a_1 = 0.2064, n = -1.65$; $R^2 = 0.82$; MAPE=20.99	

* n, is a constant

Regarding obtained R^2 and MAPE values for the datasets, it can be said that the suggested equation is not satisfying results of Hughes-Flacks' experiments.

4.1.2 The relationship between $K_s/\Delta E$ and β with respect to type of the jump

Previous analyses demonstrate good fit while predicting the relationship between β and $K_s/\Delta E$. On the other hand, since β is a function of dimensionless Froude number, it should have a significant effect on the relationship between the two parameters. Thereafter, it is decided to analyze the relationship between the β and $K_s/\Delta E$ parameters for different hydraulic jump conditions. This has been achieved through working at oscillating jump ($2.5 < Fr < 4.5$); steady jump ($4.5 < Fr < 9$) and strong jump ($9 < Fr$) conditions. This has been applied to Carollo et al. 2007; Hughes and Flack (1986), Ead and Rajaratnam (2002), and Evcimen (2005). For oscillating jump condition only Carollo et al. (2007) and Hughes and Flack (1984) dataset respecting their Froude numbers can be utilized. In steady jump condition, all datasets can be used. Moreover, for strong jump condition where upstream Froude number should be greater than 9, just Carollo et al. (2007) and Evcimen (2005) can be used. Similar to previous section, as β increases $K_s/\Delta E$ approaches zero, while $K_s/\Delta E$ goes to infinity β diminishes. The solid lines in coming figures show the best fit line through experimental data for different K_s values. In addition, the best fit line between β and $K_s/\Delta E$ through experimental data can be represented by the same equation 4.1.

Figure 4.5 and 4.6 represents the relationship between β and $K_s/\Delta E$ for the dataset of Carollo et al. (2007) and Hughes and Flack (1984), respectively. Solid lines in those figures show the best fit line and the related equations for these lines have been given in following table 4.3.

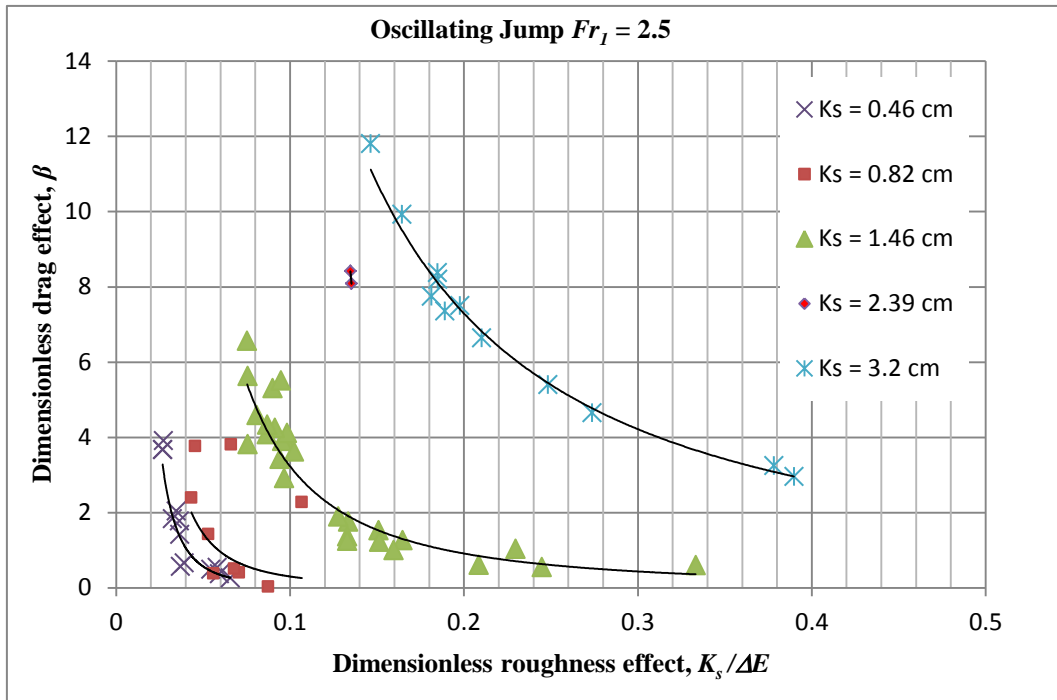


Figure 4.5: The relationship between dimensionless drag effect, β and dimensionless roughness effect, $K_s/\Delta E$ in oscillating jump condition (Carollo. et. al., 2007)

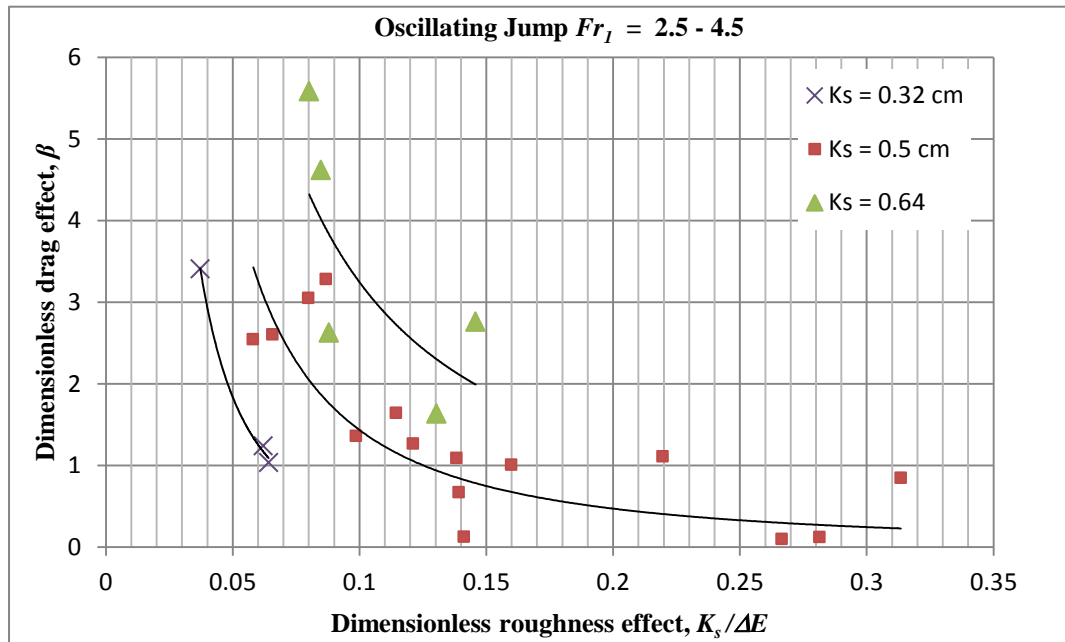


Figure 4.6: The relationship between dimensionless drag effect, β and dimensionless roughness effect, $K_s/\Delta E$ in oscillating jump condition (Hughes and Flack, 1984)

Table 4.3: Generated equations for dimensionless drag effect, β and dimensionless roughness effect, $K_s/\Delta E$ in oscillating jump condition (Carollo et al. (2007), Hughes and Flack (1984)).

figure number; dimensionless drag effect	roughness height, K_s (cm)	equation type	coefficients of equation, a_1, n ; correlation coefficient, R^2 ; MAPE (%)	data set reference
4.5; β	0.46		$a_1 = 0.0001, n^{**} = -2.79$; $R^2 = 0.87$; MAPE=32.13	
4.5; β	0.82		N/A*	
4.5; β	1.46	$\beta = a_1(K_s/\Delta E)^n$	$a_1 = 0.0486, n = -1.83$; $R^2 = 0.9$; MAPE=97.7	Carollo et al., (2007)
4.5; β	2.39		N/A	
4.5; β	3.2		$a_1 = 0.829, n = -1.35$; $R^2 = 0.99$; MAPE=7.66	
4.6; β	0.32		$a_1 = 0.0035, n = -2.09$; $R^2 = 0.99$; MAPE=3.73	Hughes and Flack, (1984)
4.6; β	0.5	$\beta = a_1(K_s/\Delta E)^n$	$a_1 = 0.0358, n = -1.60$; $R^2 = 0.52$; MAPE=84.62	
4.6; β	0.64		$a_1 = 0.1649, n = -1.29$; $R^2 = 0.53$; MAPE=41.68	

* Represents no correlation between dependent and independent variables.

** n, is a constant

Looking at Carollo's experiment analysis shows that for $K_s=1.46$, MAPE value is high even though $R^2=0.9$. Hence the obtained equation is not proper for this situation.

4.1.2.b Steady Jump Condition

Figures (4.7 – 4.10) bring out relationships between dimensionless drag effect, β and dimensionless roughness height, $K_s/\Delta E$ for all data series when Froude number is between 4.5 and 9 (steady jump condition). Solid lines show the best fit line and the obtained equations for this line has been brought in following table 4.4. Similar to previous results in this section, as β increases $K_s/\Delta E$ approaches to zero, while $K_s/\Delta E$ goes to infinity as β decreases. But it is obvious that since in this situation Froude number increases in comparison with oscillating jump condition the effect of low K_s

values on the flow decrease and there is weaker relationship and somewhere unpredictable relationship between β and $K_s/\Delta E$ in most of the cases.

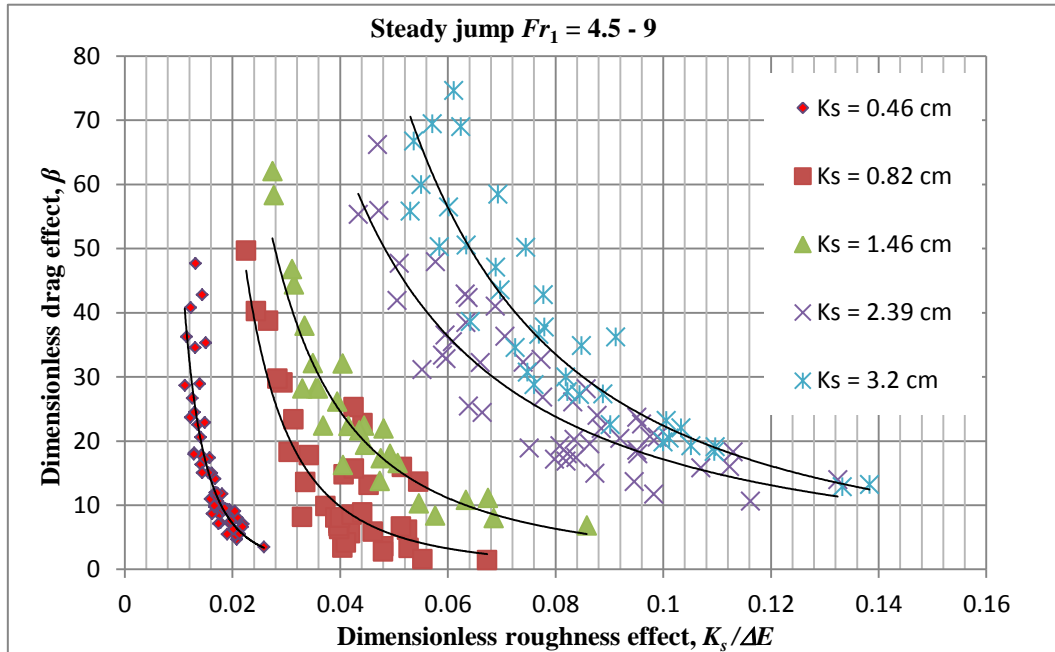


Figure 4.7: The relationship between dimensionless drag effect, β and dimensionless roughness effect, $K_s/\Delta E$ in steady jump condition (Carollo et al., 2007)

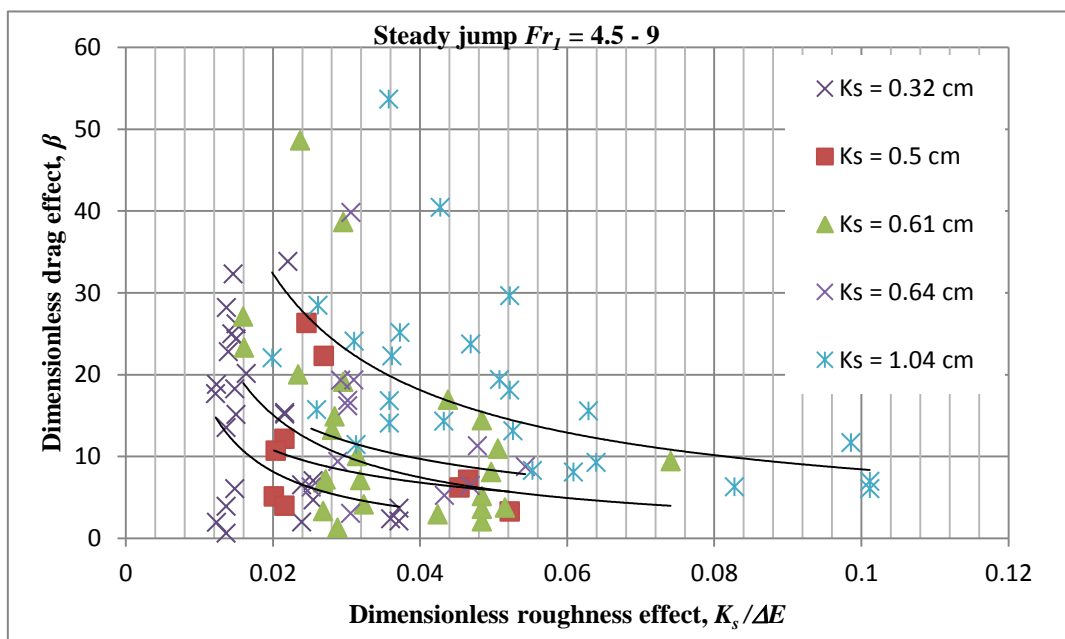


Figure 4.8: The relationship between dimensionless drag effect, β and dimensionless roughness effect, $K_s/\Delta E$ in steady jump condition (Hughes and Flack, 1984)

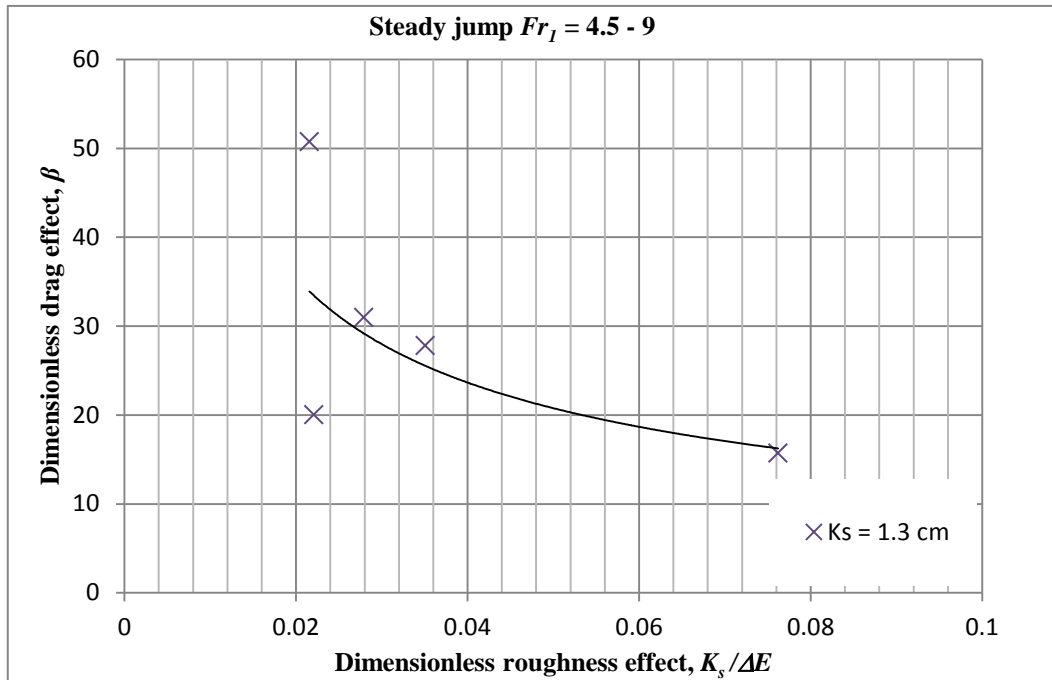


Figure 4.9: The relationship between dimensionless drag effect, β and dimensionless roughness effect, $K_s/\Delta E$ in steady jump condition (Ead and Rajaratnam, 2002)

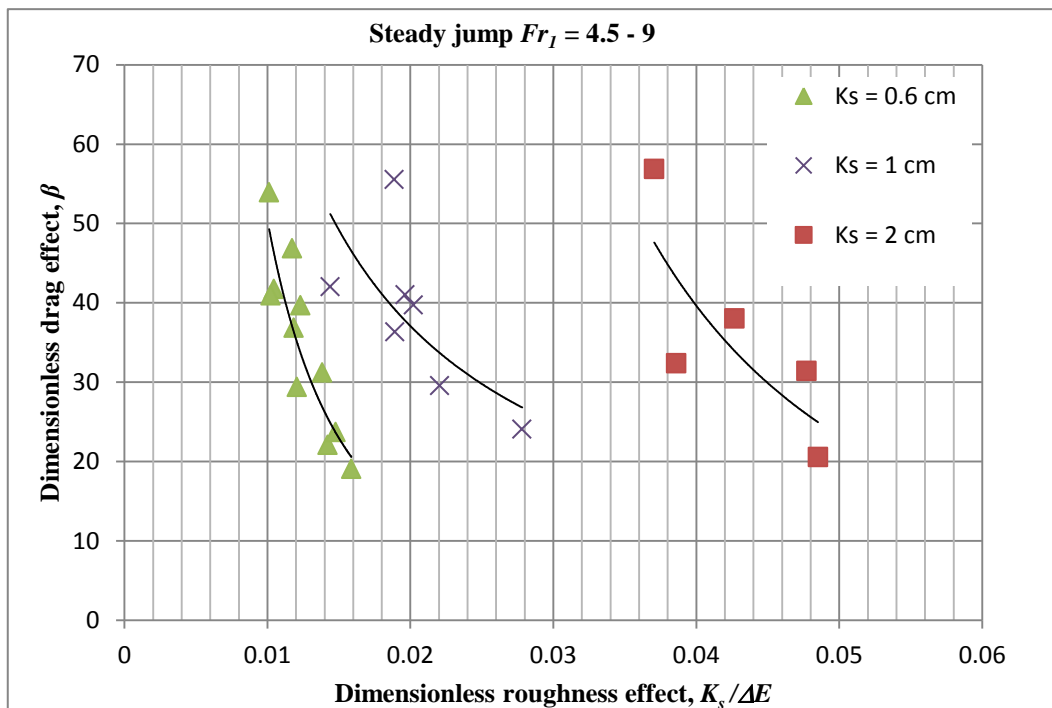


Figure 4.10: The relationship between dimensionless drag effect, β and dimensionless roughness effect, $K_s/\Delta E$ in steady jump condition (Evcimen, 2005)

Table 4.4: Generated equations for dimensionless drag effect, β and dimensionless roughness effect, $K_s/\Delta E$ in steady jump condition (Carollo et al. (2007), Hughes and Flack (1984), Ead and Rajaratnam (2002), Evcimen, (2005)).

figure number; dimensionless drag effect	roughness height, K_s (cm)	equation type	coefficients of equation, a_1, n ; correlation coefficient, R^2 ; MAPE (%)	data set reference
4.7; β	0.46		$a_1 = 7E-05, n^{**} = -2.96$; $R^2 = 0.82$; MAPE=20.27	Carollo et al., (2007)
4.7; β	0.82		$a_1 = 0.0016, n = -2.72$; $R^2 = 0.57$; MAPE=40.5	
4.7; β	1.46	$\beta = a_1(K_s/\Delta E)^n$	$a_1 = 0.0448, n = -1.96$; $R^2 = 0.9$; MAPE=15.74	
4.7; β	2.39		$a_1 = 0.5815, n = -1.47$; $R^2 = 0.77$; MAPE=18.4	
4.7; β	3.2		$a_1 = 0.3488, n = -1.81$; $R^2 = 0.89$; MAPE=14.01	
4.8; β	0.32		N/A*	Hughes and Flack, (1984)
4.8; β	0.5		N/A	
4.8; β	0.61	$\beta = a_1(K_s/\Delta E)^n$	N/A	
4.8; β	0.64		N/A	
4.8; β	1.04		$a_1 = 1.235, n = -0.84$; $R^2 = 0.4$; MAPE=36.86	
4.9; β	1.3	$\beta = a_1(K_s/\Delta E)^n$	$a_1 = 3.6228, n = -0.58$; $R^2 = 0.45$; MAPE=23.56	Ead- Rajaratnam, (2002)
4.10; β	0.6		$a_1 = 0.0065, n = -1.94$; $R^2 = 0.81$; MAPE=11.97	Evcimen, (2005)
4.10; β	1	$\beta = a_1(K_s/\Delta E)^n$	$a_1 = 0.7934, n = -0.98$; $R^2 = 0.52$; MAPE=14.29	
4.10; β	2		$a_1 = 0.0177, n = -2.40$; $R^2 = 0.63$; MAPE=19.83	

* Represents no correlation between dependent and independent variables

** n, is a constant

Considering MAPE and R^2 values, it is obvious that in steady jump condition the suggested equation cannot be valid for most of the experiment results except Carollo's in which the R^2 and MAPE are illustrating a good result for suggested equation.

4.1.2.c Strong Jump Condition

Figures 4.11 and 4.12 show the relationship between dimensionless drag effect, β and dimensionless roughness height, $K_s/\Delta E$ for Carollo et al. (2007) and Evcimen (2005) when Froude number is greater than 9 (strong jump condition). As it is mentioned before, in this condition high speed flow governs the flow condition and given the figures it can be seen that there is no relationship for Carollo et al. (2007) data. Solid lines show the best fit line and the obtained equations for this line has been brought in following table 4.5. For strong jump conditions, it can be concluded that Froude increases extremely in comparison with oscillating jump conditions and the effect of small K_s values on the flow becomes negligible predicting uncertain relationship for Carollo et al. (2007) data.

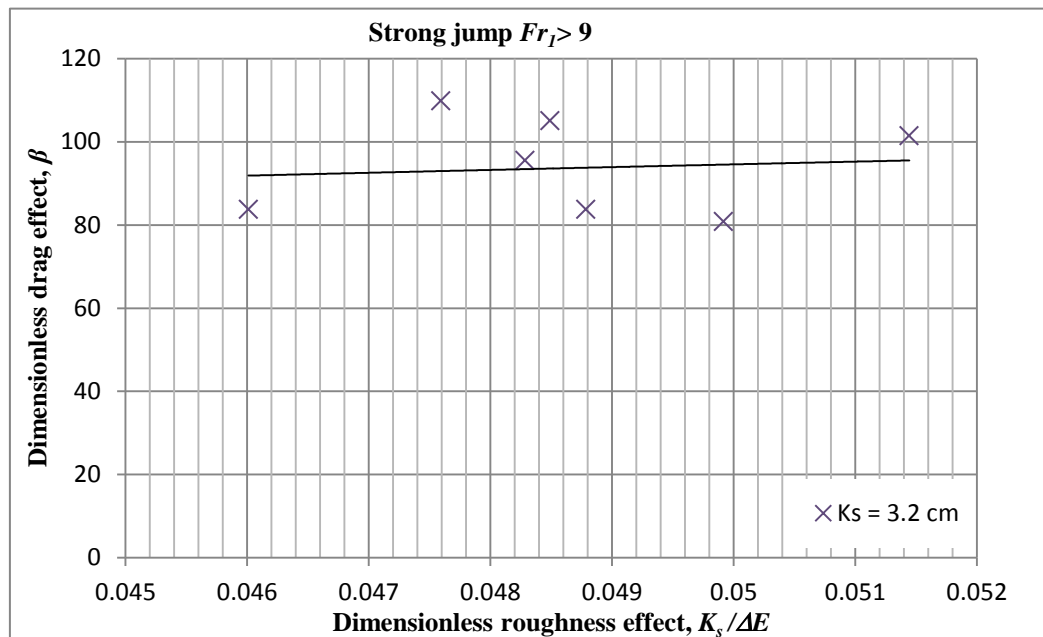


Figure 4.11: The relationship between dimensionless drag effect, β and dimensionless roughness effect, $K_s/\Delta E$ in strong jump condition (Carollo et al., 2007)

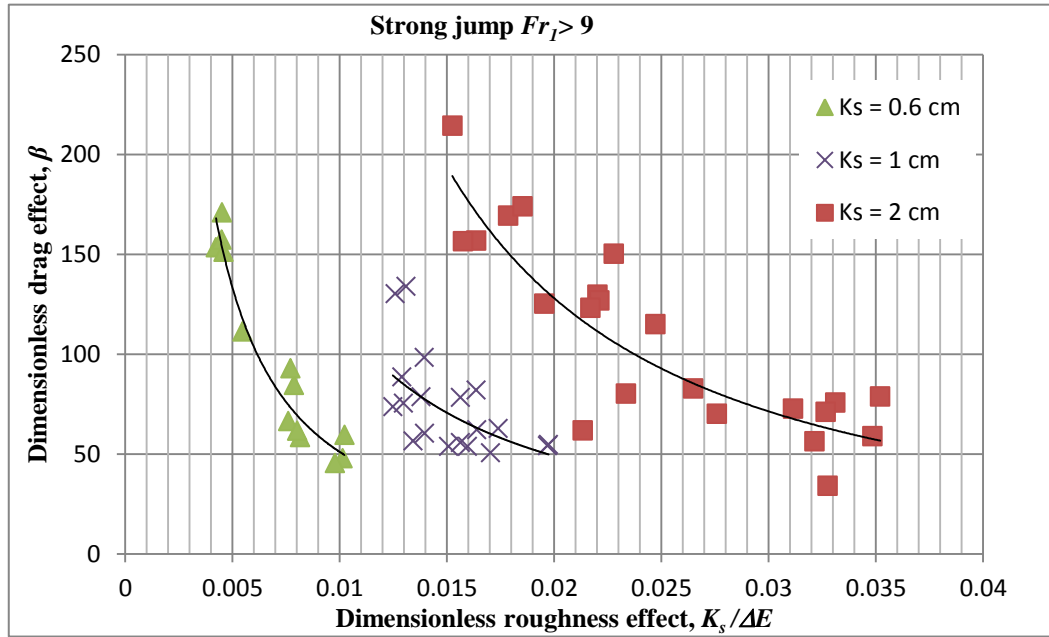


Figure 4.12: The relationship between dimensionless drag effect, β and dimensionless roughness effect, $K_s/\Delta E$ in strong jump condition (Evcimen, 2005)

Table 4.5: Generated equations for dimensionless drag effect, β and dimensionless roughness effect, $K_s/\Delta E$ in strong condition (Carollo et al. (2007), Evcimen, (2005)).

figure number; dimensionless drag effect	roughness height, K_s (cm)	equation type	coefficients of equation, a_1, n ; correlation coefficient, R^2 ; MAPE (%)	data set reference
4.11; β	0.46	N/A^*	N/A	Carollo et al., (2007)
4.11; β	0.82	N/A	N/A	
4.11; β	1.46	N/A	N/A	
4.11; β	2.39	N/A	N/A	
4.11; β	3.2	N/A	N/A	
4.12; β	0.6		$a_1= 0.0873, n^{**} = -1.38;$ $R^2= 0.92; MAPE=11.04$	Evcimen, (2005)
4.12; β	1	$\beta = a_1(K_s / \Delta E)^n$	N/A	
4.12; β	2		$a_1= 0.457, n = -1.44;$ $R^2= 0.7012; MAPE=20.58$	

* Represents no correlation between dependent and independent variables

** n, is a constant

With respect to R^2 and MAPE values for presented data, it can be said that this equation is satisfying Evcimen's experimental results in most of the cases.

As it can be seen in relationship between $K_s/\Delta E$ and β , there is a concave shape power type trend line with good regression for most of the data sets. Totally, as the $K_s/\Delta E$ decreases β tends to infinity. Even though the R^2 value is near to one in some situations, high MAPE value shows that the suggested equations are not fitting the data well.

4.1.3 Relationship between upstream Froude number, Fr_1 and dimensionless drag effect, β

The performance of the formulization given for dimensionless drag effect is a function of Froude number. Following figures show plots between β and Fr_1 for different K_s values. Results show that for small and constant Froude numbers β increases as the K_s value increases. However, as the occurrence of strong hydraulic jump increases, steep increase on β is observed independent of the magnitude of K_s . The effect of strong hydraulic jump is presented in Figure 4.16. This shows the linear increase of dimensionless drag coefficient, β , independent of changes in K_s . It can be also observed from other figures that for $Fr > 9$ conditions the dimensionless drag effect and Froude number behaves independent of roughness, K_s and thus the relationship between the parameters becomes unpredictable. As a result, the scatter of data in Figures (4.13 - 4.15) indicates that β is not only a function of Fr but also affected from the magnitude of K_s . The best fit line of experimental results, coefficient of correlation, R^2 and mean absolute percentage error, (MAPE) can be represented by power equation as given in Table 4.6.

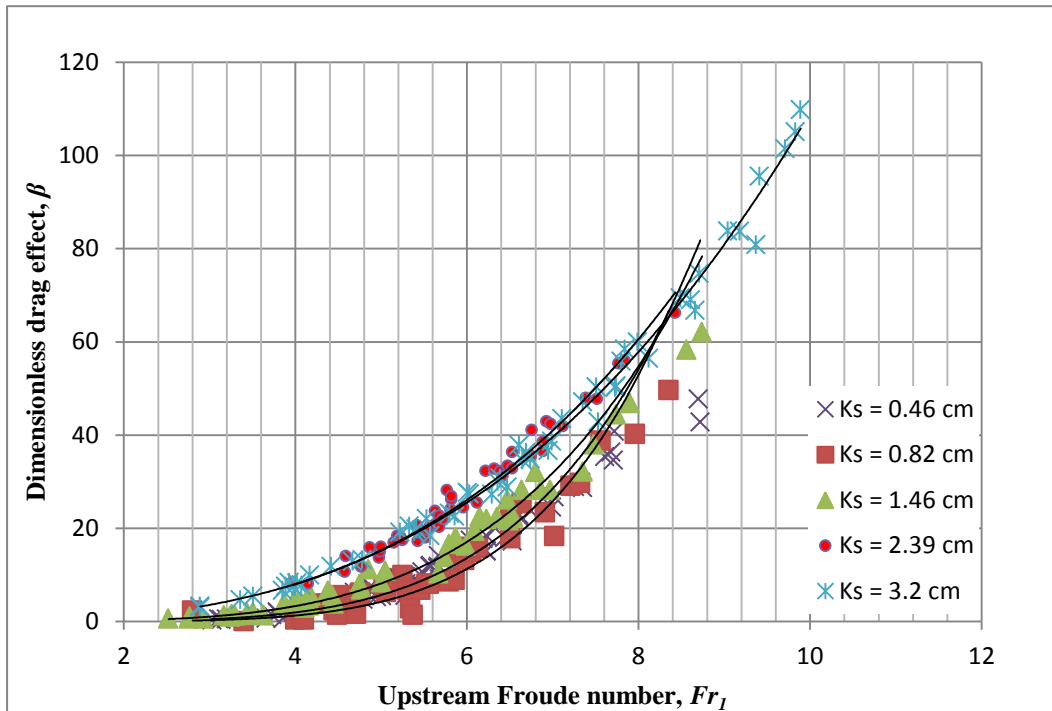


Figure 4.13: The relationship between upstream Froude number, Fr_1 and dimensionless drag effect, β (Carollo et. al., 2007)

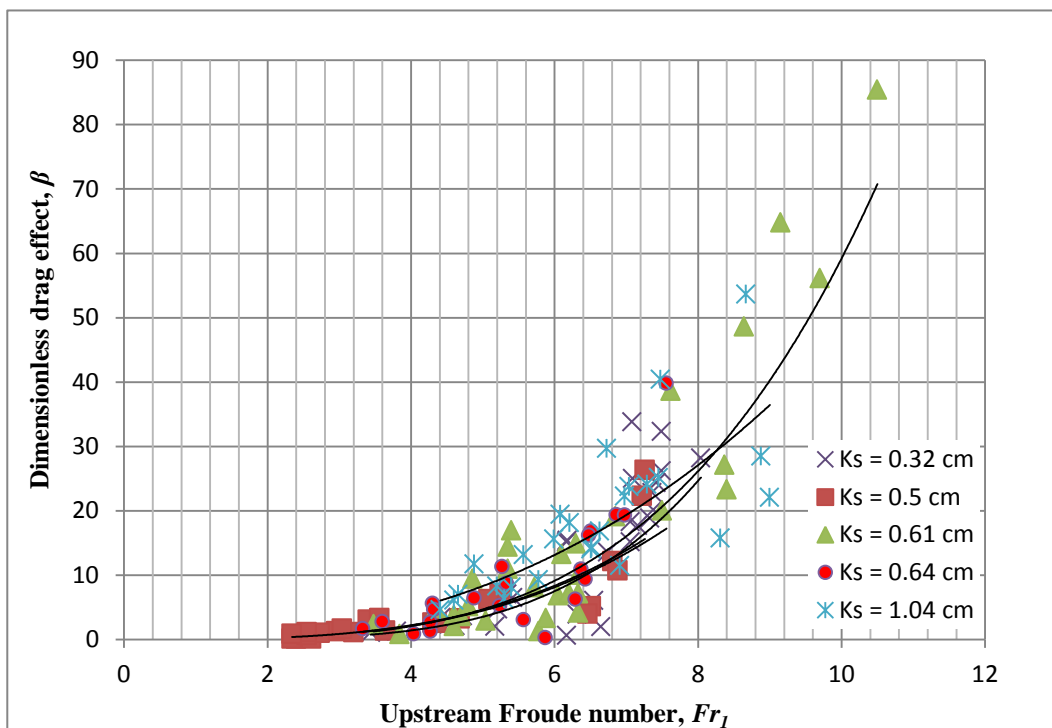


Figure 4.14: The relationship between upstream Froude number, Fr_1 and dimensionless drag effect, β (Hughes and Flack, 1984)

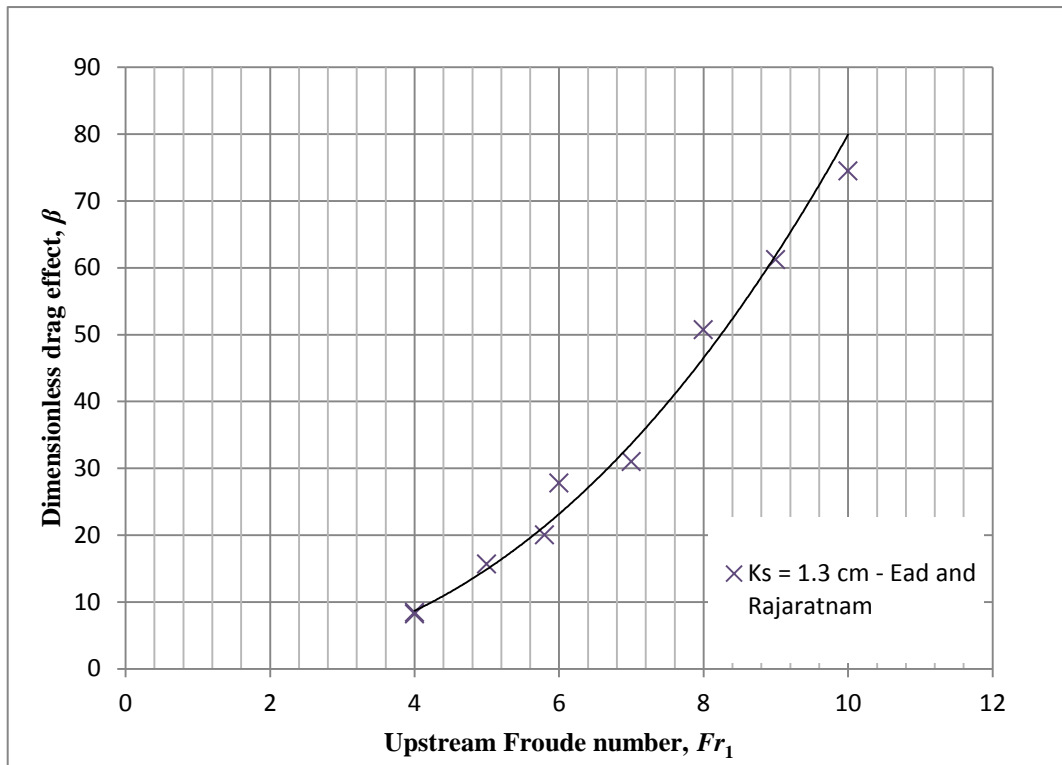


Figure 4.15: The relationship between upstream Froude number, Fr_1 and dimensionless drag effect, β (Ead and Rajaratnam, 2002)

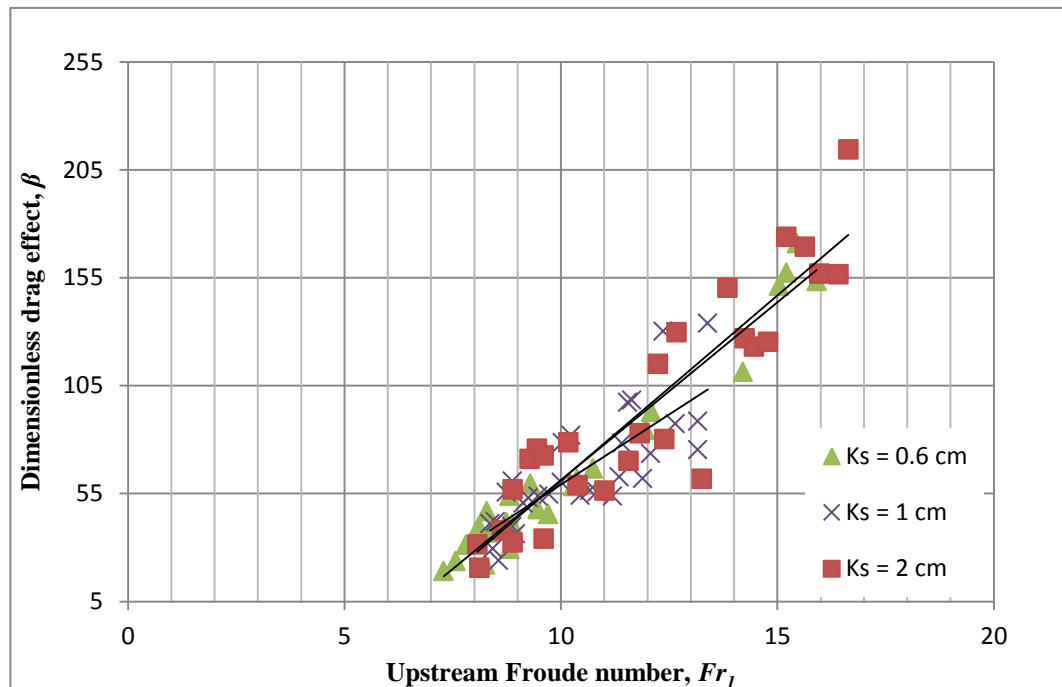


Figure 4.16: The relationship between upstream Froude number, Fr_1 and dimensionless drag effect, β (Evcimen, 2005)

Table 4.6: Generated equations for dimensionless drag effects, β and upstream Froude number

figure number; dimensionless drag effect	roughness height, K_s (cm)	equation type	coefficients of equation, a_2, a_3, n_2, b_3 ; correlation coefficient, R^2 ; MAPE (%)	data set reference
4.13; β	0.46		$a_2 = 0.0025, n_2 = 4.79$; $R^2 = 0.94$; MAPE=22.59	
4.13; β	0.82		$a_2 = 0.0025, n_2 = 4.79$; $R^2 = 0.94$; MAPE=94	
4.13; β	1.46	$\beta = a_2(Fr_1)^{n_2}$	$a_2 = 0.0121, n_2 = 4.05$; $R^2 = 0.97$; MAPE=17.34	Carollo et al., (2007)
4.13; β	2.39		$a_2 = 0.1561, n_2 = 2.84$; $R^2 = 0.996$; MAPE=6.29	
4.13; β	3.2		$a_2 = 0.1372, n_2 = 2.93$; $R^2 = 0.97$; MAPE=5.34	
4.14; β	0.32		$a_2 = 0.0045, n_2 = 4.14$; $R^2 = 0.62$; MAPE=91.38	
4.14; β	0.5		$a_2 = 0.0232, n_2 = 3.28$; $R^2 = 0.78$; MAPE=71.26	Hughes and Flack, (1984)
4.14; β	0.61	$\beta = a_2(Fr_1)^{n_2}$	$a_2 = 0.0129, n_2 = 3.66$; $R^2 = 0.72$; MAPE=64.42	
4.14; β	0.64		$a_2 = 0.0236, n_2 = 3.26$; $R^2 = 0.39$; MAPE=39.96	
4.14; β	1.04		$a_2 = 0.1445, n_2 = 2.52$; $R^2 = 0.71$; MAPE=27.63	
4.15; β	1.3	$\beta = a_2(Fr_1)^{n_2}$	$a_2 = 0.3011, n_2 = 2.42$; $R^2 = 0.99$; MAPE=6.99	Ead-Rajaratnam, (2002)
4.16; β	0.6		$a_3 = 16.465, b_3 = 103.3$; $R^2 = 0.96$; MAPE=12.94	
4.16; β	1	$\beta = a_3(Fr_1) + b_3$	$a_3 = 12.986, b_3 = 70.65$; $R^2 = 0.62$; MAPE=20.04	Evcimen, (2005)
4.16; β	2		$a_3 = 17.131, b_3 = 110.17$; $R^2 = 0.84$; MAPE=21.83	

* n_2 is a constant

β gradually increases with increasing upstream Froude number until some value then it increases with steeper slope or sharper with increasing Froude number. It shows that after some Froude numbers the effects of K_s decreases and beta suddenly increases. Also, it can be seen in Figures (4.13 – 4.15) that when K_s has smaller value, the curvature of the fit lines is intense with more bend, but when the K_s increases this trend line tends to shape as straight line. MAPE and R^2 values show

that except some cases such as Carollo's $K_s=0.82$ and Hughes and Flack's dataset where the MAPE value is greater than satisfactory level even with high R^2 , it's an acceptable relationship between upstream Froude number, Fr_l and dimensionless drag effect, β .

4.1.4 Relationship between α and dimensionless drag effect, β

According to Equation 3.37, it comes to search about drag coefficient, C_D from relating dimensionless drag effect, β and α . Figures (4.17 – 4.20) show the relationship between β and α and it is obvious as β increases α increases also. The solid lines in coming Figures show the best fit line through experimental data for different K_s values. The equation of best fit lines obtained through the regression analysis of experimental data has been figured out in Table 4.7. The table summarizes the magnitudes of drag coefficient, C_D during the hydraulic jump. The result shows reliable C_D values for different K_s values.

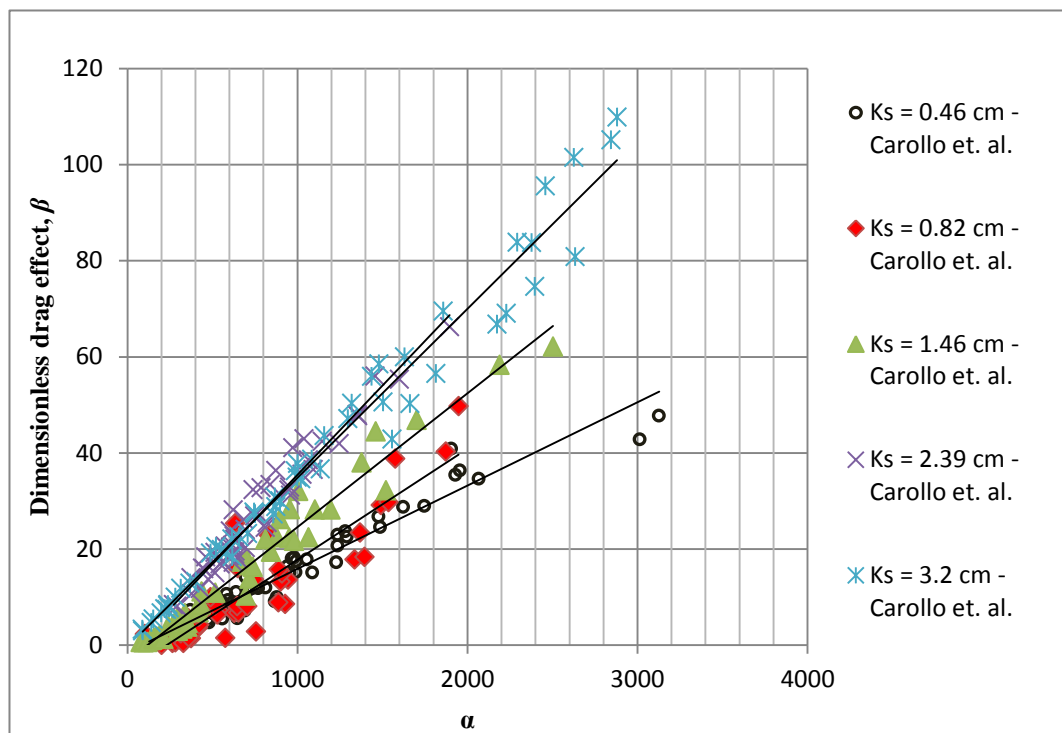


Figure 4.17: The relationship between α and dimensionless drag effect, β (Carollo et. al., 2007)

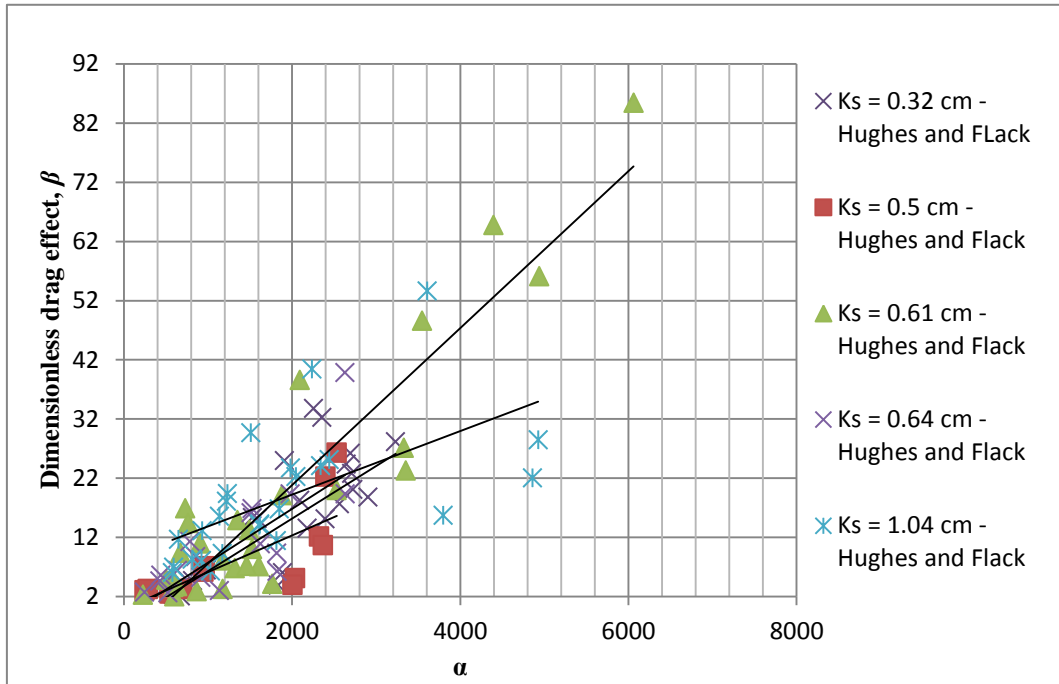


Figure 4.18: The relationship between α and dimensionless drag effect, β (Hughes and Flack, 1984)

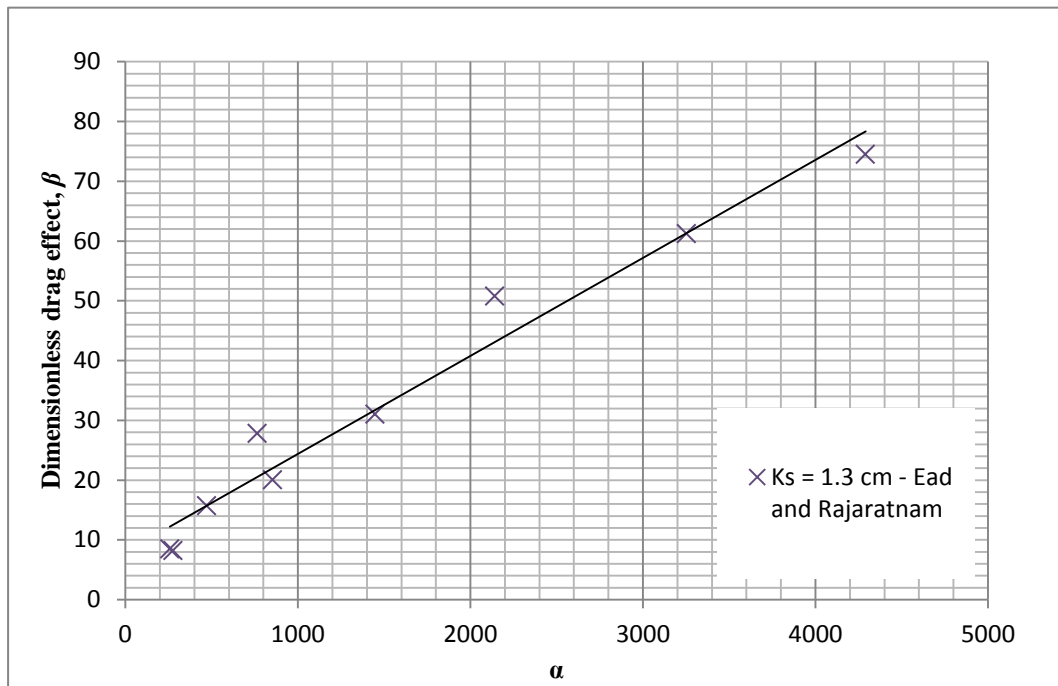


Figure 4.19: The relationship between α and dimensionless drag effect, β (Ead and Rajaratnam, 2002)

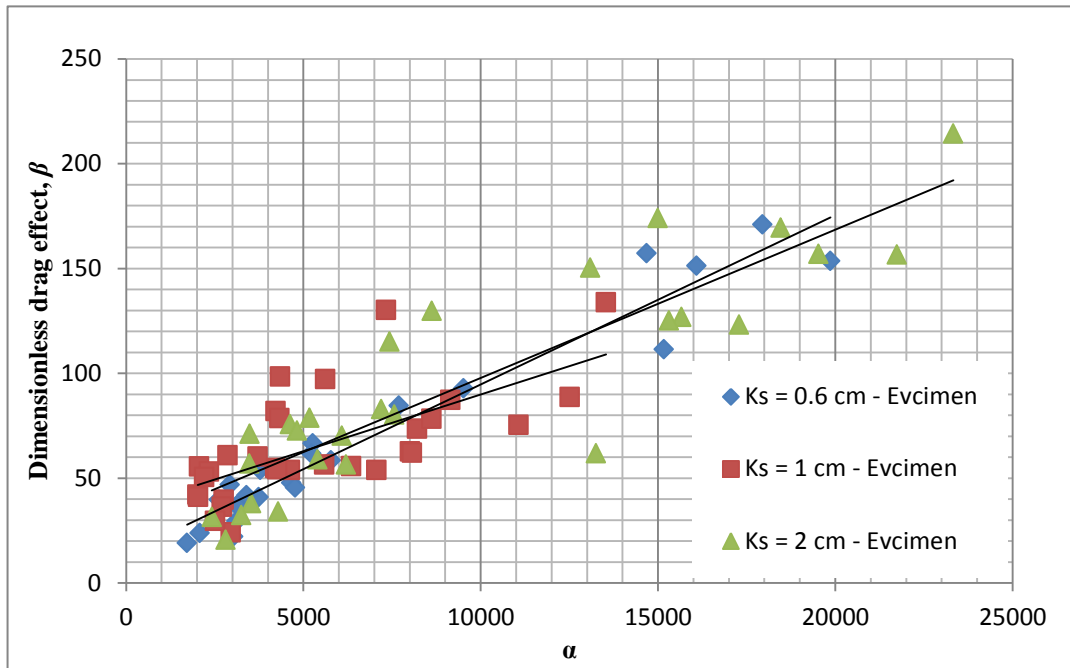


Figure 4.20: The relationship between α and dimensionless drag effect, β (Evcimen, 2005)

Obtained equations from trend lines with correlation coefficients regarding their roughness height, K_s value has been figured out in table 4.7. As it can be observed from the table, obtained linear equation cannot be valid for Hughes and Flack's experimental results and when K_s is 0.82 cm for Carollo's experimental results this is because R^2 value is not near to 1 and MAPE value is high. The suggested linear equation for fitting trend line can be valid for the other experimental data.

Table 4.7: Generated drag coefficient, C_D , for each kind of roughness height, K_s .

figure number; dimensionless drag effect	roughness height, K_s (cm)	equation type	coefficients of equation, C_D , b_4 ; correlation coefficient, R^2 ; MAPE (%)	data set reference
4.17; β	0.46		$C_D = 0.0173$, $b_4^* = -1.44$; $R^2 = 0.95$; MAPE=33.81	Carollo et al., (2007)
4.17; β	0.82		$C_D = 0.0231$, $b_4 = -5.28$; $R^2 = 0.83$; MAPE=129.6	
4.17; β	1.46	$\beta = C_D(\alpha) + b_4$	$C_D = 0.0279$, $b_4 = -3.28$; $R^2 = 0.97$; MAPE=31.64	
4.17; β	2.39		$C_D = 0.0371$, $b_4 = -1.60$; $R^2 = 0.95$; MAPE=9.95	
4.17; β	3.2		$C_D = 0.0351$, $b_4 = -0.21$; $R^2 = 0.97$; MAPE=6.88	
4.18; β	0.32		$C_D = 0.0089$, $b_4 = -2.61$; $R^2 = 0.56$; MAPE=145.71	Hughes and Flack, (1984)
4.18; β	0.5		$C_D = 0.0062$, $b_4 = -0.07$; $R^2 = 0.69$; MAPE=75.56	
4.18; β	0.61	$\beta = C_D(\alpha) + b_4$	$C_D = 0.0132$, $b_4 = -5.64$; $R^2 = 0.85$; MAPE=102.75	
4.18; β	0.64		$C_D = 0.0091$, $b_4 = -1.34$; $R^2 = 0.55$; MAPE=54.63	
4.18; β	1.04		$C_D = 0.0054$, $b_4 = -8.52$; $R^2 = 0.35$; MAPE=39.75	
4.19; β	1.3	$\beta = C_D(\alpha) + b_4$	$C_D = 0.0164$, $b_4 = 7.99$; $R^2 = 0.96$; MAPE=17.54	Ead-Rajaratnam, (2002)
4.20; β	0.6		$C_D = 0.0081$, $b_4 = 13.94$; $R^2 = 0.94$; MAPE=17.08	Evcimen, (2005)
4.20; β	1	$\beta = C_D(\alpha) + b_4$	$C_D = 0.0054$, $b_4 = 35.87$; $R^2 = 0.45$; MAPE=26.05	
4.20; β	2		$C_D = 0.0071$, $b_4 = 27.01$; $R^2 = 0.79$; MAPE=27.58	

* b_4 is a constant

4.1.5 Relationship between drag coefficient, C_D and drag force, F_d

The relationship between drag force, F_d calculated by the help of equation 3.20 and drag coefficient C_D is searched out in this section.

In general there is a linear relationship between the drag force and drag coefficient. Following plots attempts to define the correlation between the two parameters in case of hydraulic jump. In most of the plots, the data are not satisfactorily distributed

along a solid line, derived from regression analysis. However, except small K_s values of Carollo et al. (2007) and Hughes and Flack (1984), poor correlation between the drag coefficient and drag force is observed. The equation of the best fit lines obtained and has been brought in Table 4.8.

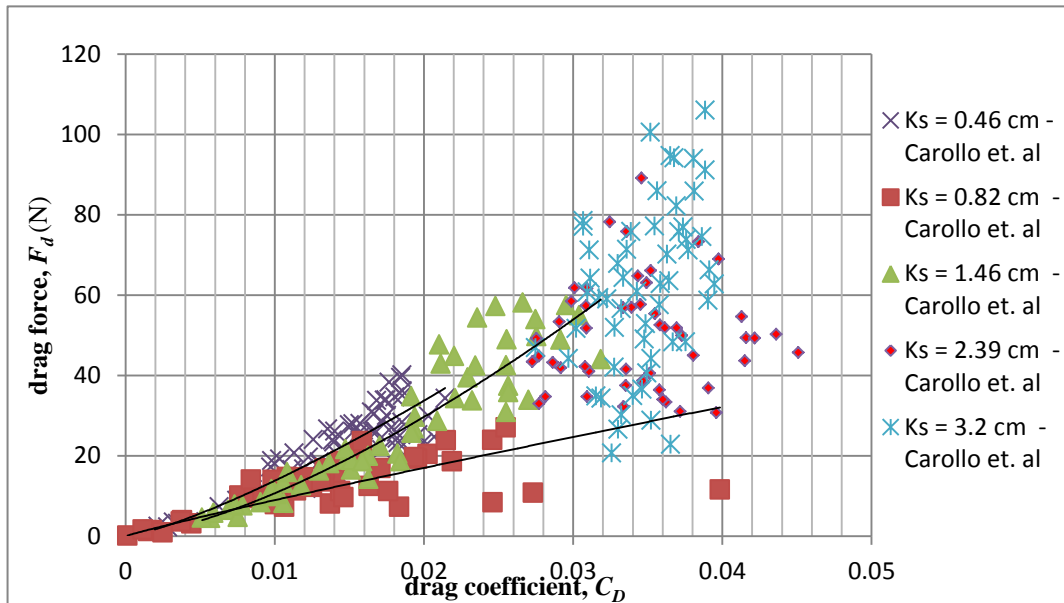


Figure 4.21: The relationship between drag coefficient, C_D and drag force, F_d (N) (Carollo et. al., 2007)

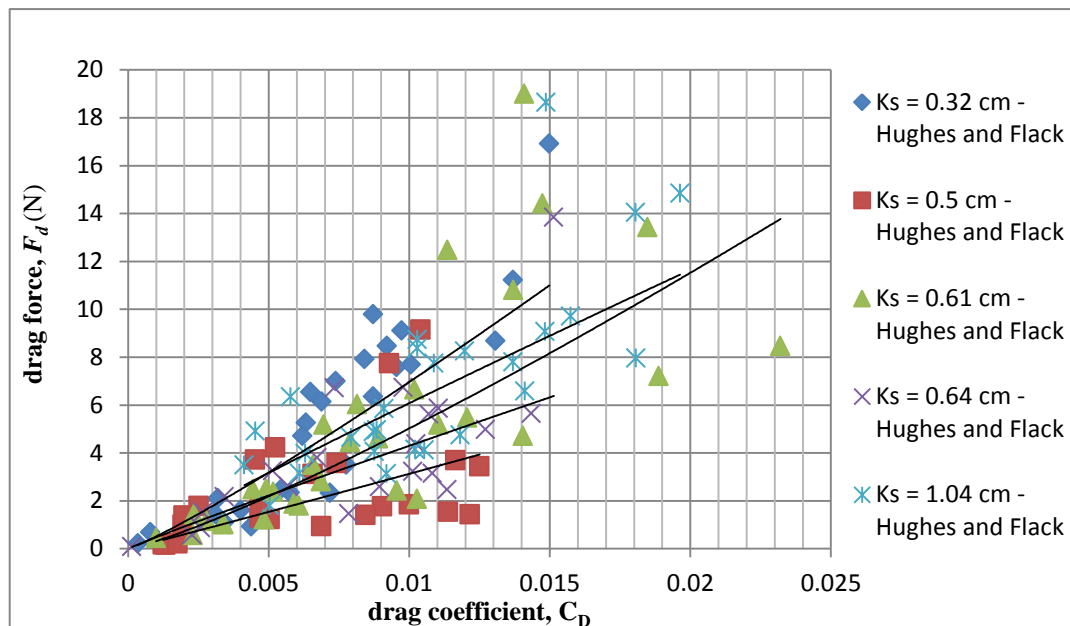


Figure 4.22: The relationship between drag coefficient, C_D and drag force, F_d (N) (Hughes and Flack, 1984)

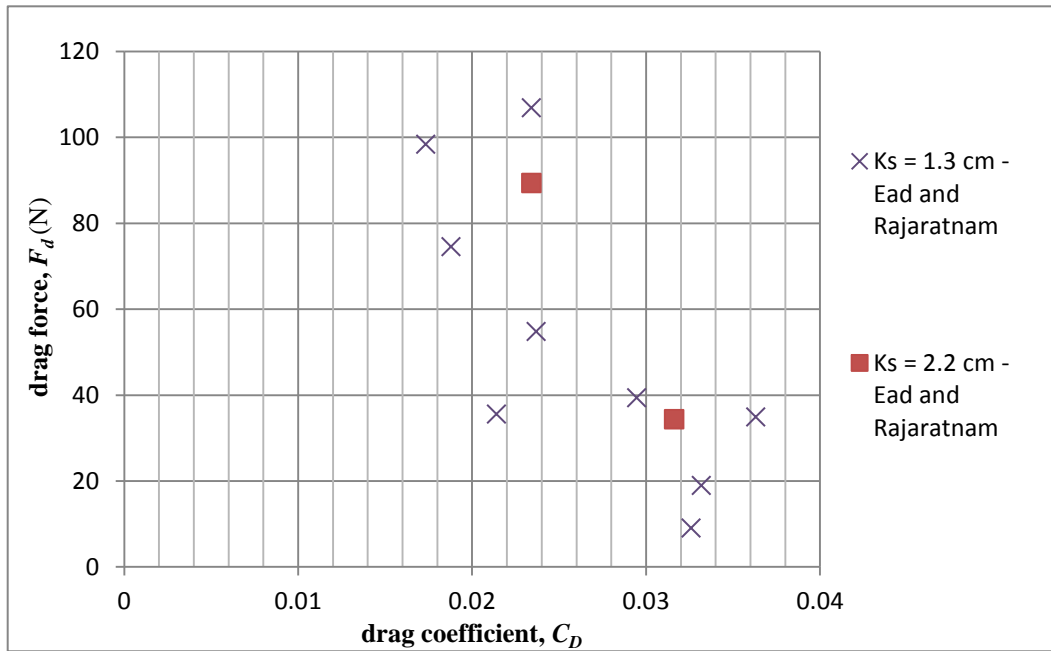


Figure 4.23: The relationship between drag coefficient, C_D and drag force, F_d (N) (Ead and Rajaratnam, 2002)

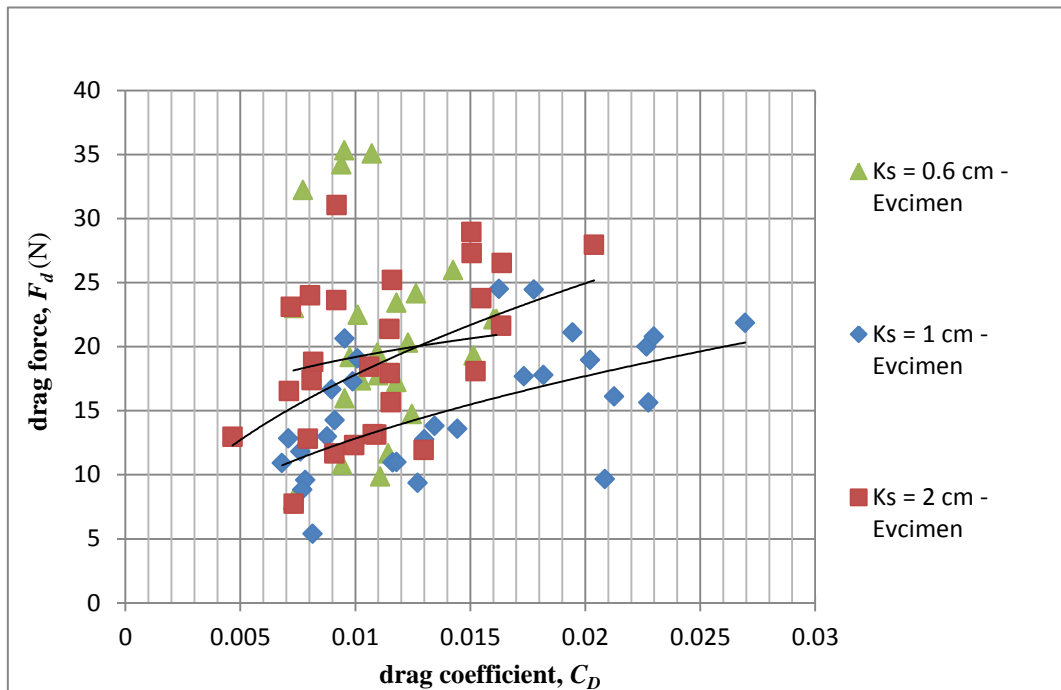


Figure 4.24: The relationship between drag coefficient, C_D and drag force, F_d (N) (Evcimen, 2005)

Obtained equations from trend lines with correlation coefficients regarding their roughness height, K_s and mean absolute percentage error, MAPE, has been figured out in Table 4.8.

Table 4.8: Generated drag force, F_d , for each kind of drag coefficient, C_D

figure number; drag force (N)	roughness height, K_s (cm)	equation type	coefficients of equation, a_4, n_3 ; correlation coefficient, R^2 ; MAPE (%)	data set reference
4.21; F_d	0.46		$a_4= 5191.1, n_3^{**}= 1.79$; $R^2 = 0.93$; MAPE=15.59	
4.21; F_d	0.82		$a_4= 622.2, n_3= 0.92$; $R^2 = 0.85$; MAPE=34.74	
4.21; F_d	1.46	$F_d = a_4(C_D)^{n_3}$	$a_4= 9377.2, n_3= 1.47$; $R^2 = 0.93$; MAPE=15.24	Carollo et al., (2007)
4.21; F_d	2.39		N/A *	
4.21; F_d	3.2		N/A	
4.22; F_d	0.32		$a_4= 1267.3, n_3= 1.13$; $R^2 = 0.84$; MAPE=38.32	
4.22; F_d	0.5		$a_4= 347.18, n_3= 1.02$; $R^2 = 0.53$; MAPE=67.25	Hughes and Flack, (1984)
4.22; F_d	0.61	$F_d = a_4(C_D)^{n_3}$	$a_4= 1248, n_3= 1.20$; $R^2 = 0.7$; MAPE=38.83	
4.22; F_d	0.64		$a_4= 342.92, n_3= 0.95$; $R^2 = 0.83$; MAPE=37.94	
4.22; F_d	1.04		$a_4= 458.22, n_3= 0.94$; $R^2 = 0.57$; MAPE=28.09	
4.23; F_d	1.3	N/A	N/A	Ead-Rajaratnam, (2002)
4.23; F_d	2.2	N/A	N/A	
4.24; F_d	0.6	N/A	N/A	
4.24; F_d	1	N/A	N/A	
4.24; F_d	2	N/A	N/A	Evcimen, (2005)

* Represents no correlation between dependent and independent variables.

** n_3 is a constant

Considering MAPE and R^2 values, from the above graphs, it can be observed that drag force increases as drag coefficient increases and there are meaningful relationship between them as long as K_s has got small values. In figure 4.21, it is obvious that for $K_s=2.39$ and $K_s=3.2$ there is no relationship between drag force and drag coefficient.

4.2 Roller Length

As it is mentioned in previous chapter, the roller length studies are nowadays motivated to find an equation for roller length as a function of hydraulic jump properties. Based on Equation 3.50 derived in Chapter 3, roller length was defined as dimensionless, together with upstream water depth. In general, the relationship between dimensionless roller length, L_r/y_1 and $K/\Delta E$ ratio in which K is the coefficient of the equation, is searched out with respect to different roughness height (K_s). This investigation has been done with the help of data series given by Carollo et al. (2007), Hughes and Flack (1986). In first section of this part it showed how dimensionless roller length, L_r/y_1 behaves with changing $K/\Delta E$ ratio. The aim was to find coefficient K to be used in the Equation 3.50 for different bed roughnesses.

4.2.1 Relationship between dimensionless roller length, L_r/y_1 , and $K/\Delta E$

The variation of dimensionless roller length, L_r/y_1 and $K/\Delta E$ ratio is given in Figures (4.25-4.26). The figures are depicted with all experimental results, which have been pointed out before. The trend of L_r/y_1 with respect to ($K/\Delta E$) is obeying an inverse relationship. As L_r/y_1 increases, $K/\Delta E$ approaches zero, coinciding while $K/\Delta E$ goes to infinity L_r/y_1 decreases. The solid line is the best fit line for different K_s values. The equation of best fit lines for different K_s values are given in Table 4.9. It is clear from Figures (4.25-4.26) that, the best fit line between L_r/y_1 and $K/\Delta E$ through experimental data can be represented by Equation 4.2.

$$\frac{L_r}{y_1} = a_5 \left(\frac{K}{\Delta E} \right)^{n_4} \quad (4.2)$$

In which a_5 and n_4 are constants with n_4 always being less than zero (0). The best linear fit equations with the coefficient of determination (R^2) and mean absolute percentage error, MAPE are given in Table 4.9. Higher values of R^2 associated with the L_r/y_1 and $K/\Delta E$ reflects the fact that their functional dependence is acceptable.

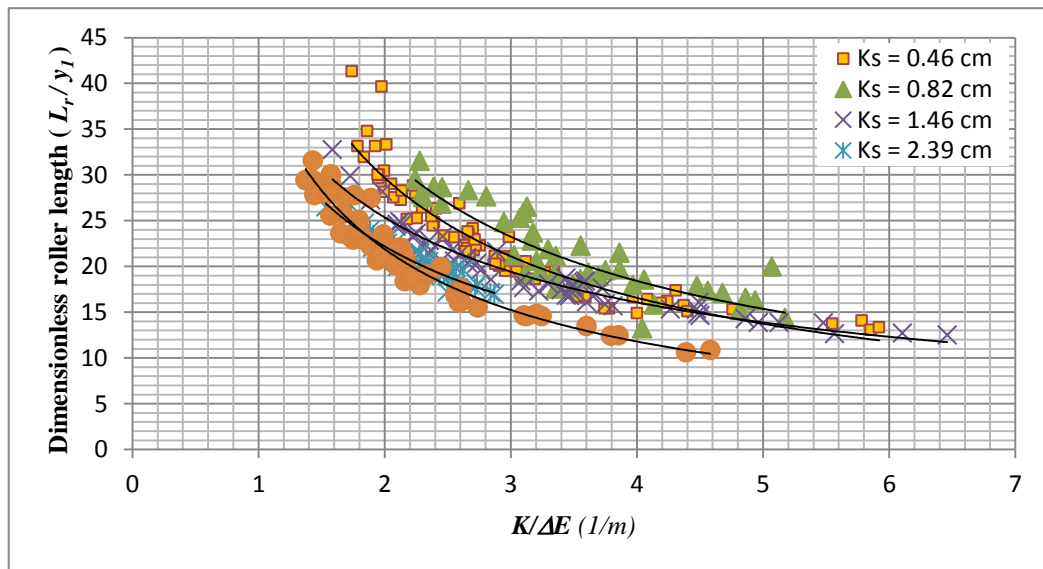


Figure 4.25: The relationship between $K/\Delta E$ and dimensionless roller length, L_r/y_1 (Carollo et. al., 2007)

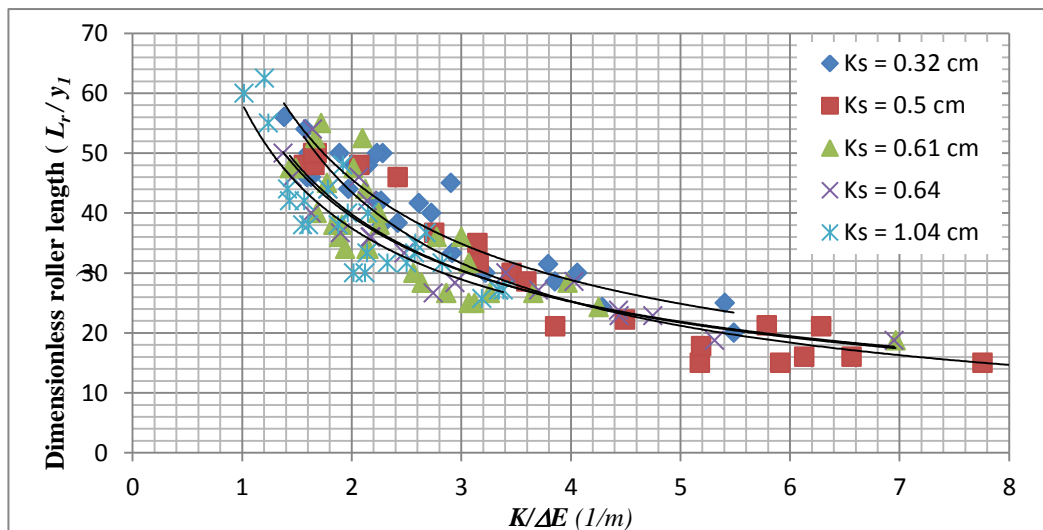


Figure 4.26: The relationship between $K/\Delta E$ and dimensionless roller length, L_r/y_1 (Hughes and Flack, 1984)

Table 4.9: Dimensionless roller length equation

figure number; dimensionless roller length	roughness height, K_s (cm)	equation type	coefficients of equation, a_5, n_4 ; correlation coefficient, R^2 ; MAPE (%)	Data set reference	
4.25; L_r/y_1	0.46		$a_5 = 53.137, n_4^* = -0.84$ $R^2 = 0.9216; MAPE = 5.51$		
4.25; L_r/y_1	0.82		$a_5 = 56.558, n_4 = -0.81$ $R^2 = 0.7679; MAPE = 8.08$		
4.25; L_r/y_1	1.46	$\frac{L_r}{y_1} = a_5 \left(\frac{K}{\Delta E} \right)^{n_4}$	$a_5 = 39.983, n_4 = -0.66$ $R^2 = 0.9557; MAPE = 3.77$	Carollo et al., (2007)	
4.25; L_r/y_1	2.39		$a_5 = 36.614, n_4 = -0.72$ $R^2 = 0.8614; MAPE = 3.26$		
4.25; L_r/y_1	3.2		$a_5 = 40.629, n_4 = -0.89$ $R^2 = 0.9518; MAPE = 4.81$		
4.26; L_r/y_1	0.32		$a_5 = 72.243, n_4 = -0.66$ $R^2 = 0.8579; MAPE = 8.25$		Hughes and Flack, (1984)
4.26; L_r/y_1	0.5		$a_5 = 74.906, n_4 = -0.78$ $R^2 = 0.9288; MAPE = 10.85$		
4.26; L_r/y_1	0.61	$a_5 = 62.934, n_4 = -0.66$ $R^2 = 0.742; MAPE = 11.38$			
4.26; L_r/y_1	0.64	$a_5 = 61.538, n_4 = -0.64$ $R^2 = 0.9035; MAPE = 7.59$			
4.26; L_r/y_1	1.04	$a_5 = 58.29, n_4 = -0.64$ $R^2 = 0.787; MAPE = 8.9$			

* n_4 is a constant

Considering R^2 and MAPE values, it can be said that suggested equation (4.2) is acceptable to calculate dimensionless roller length for the datasets.

4.2.2 Relationship between dimensionless roller length, L_r/y_1 , and depth ratio

$$(y_2 / y_1 - 1)v_1$$

According to Equation 3.50, a relationship between dimensionless roller length, L_r/y_1 and depth ratio, $(y_2 / y_1 - 1)v_1$ to figure out coefficient K and clarify how does it behave. For this purpose, coming Figures (4.27-4.30) depicted to show the coefficient K differences with respect to different roughness height K_s values. It is clear from figures when dimensionless roller length, L_r/y_1 increases coinciding depth ratio, $(y_2 / y_1 - 1)v_1$ increases. Figures show that there are linear relationship between L_r/y_1 and $(y_2 / y_1 - 1)v_1$ as follows.

$$\frac{L_r}{y_1} = a_6 \left(\frac{y_2}{y_1} - 1 \right) v_1 + b_5 \quad (4.3)$$

The solid lines in coming Figures show the best fit line through experimental data for different K_s values. The equation of best fit lines obtained through the regression analysis of experimental data with the coefficient of correlation, R^2 and MAPE values has been figured out in Table 4.10.

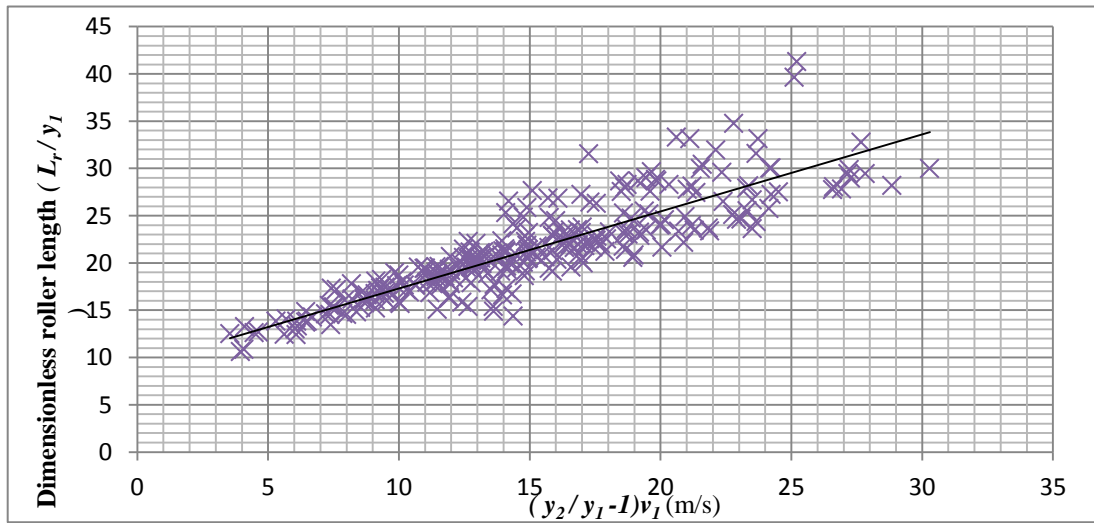


Figure 4.27: Relationship between dimensionless roller length, L_r/y_1 and $(y_2/y_1 - 1)v_1$ for all K_s values (Carollo et. al., 2007)

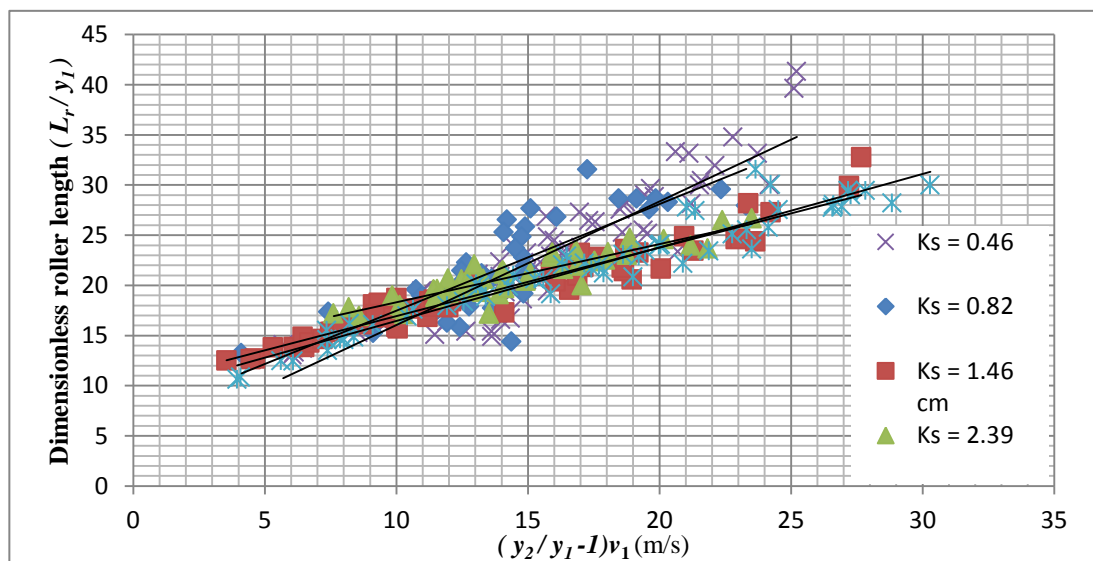


Figure 4.28: Relationship between dimensionless roller length, L_r/y_1 and $(y_2/y_1 - 1)v_1$ for different K_s values separately (Carollo et. al., 2007)

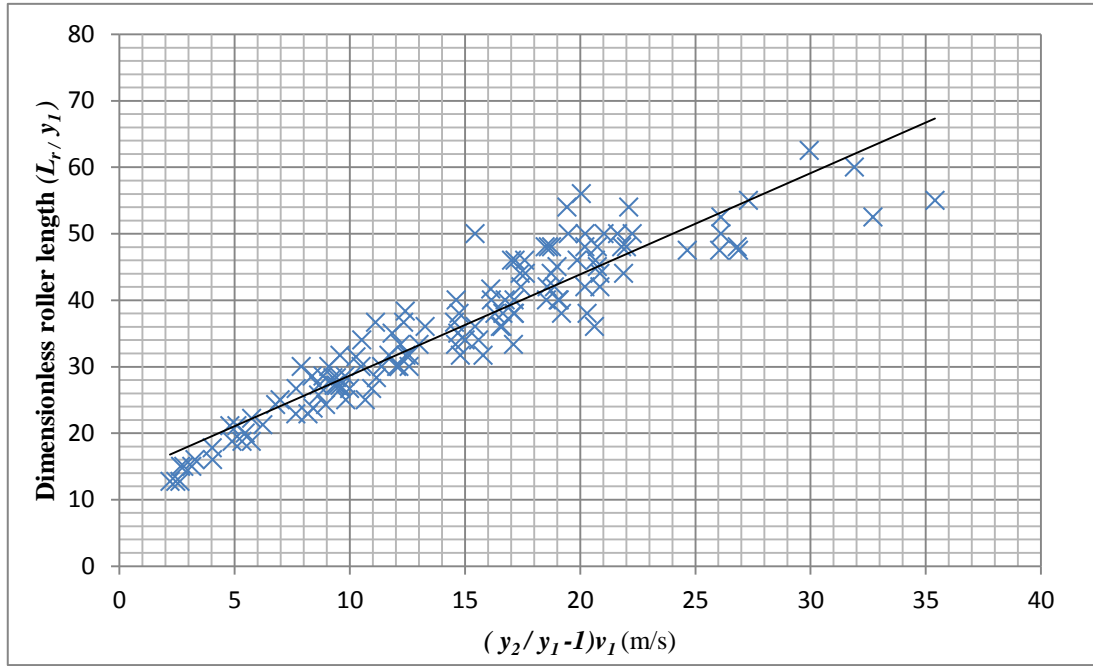


Figure 4.29: Relationship between dimensionless roller length, L_r/y_1 and $(y_2/y_1 - 1)v_1$ for all K_s values (Hughes and Flack, 1984)

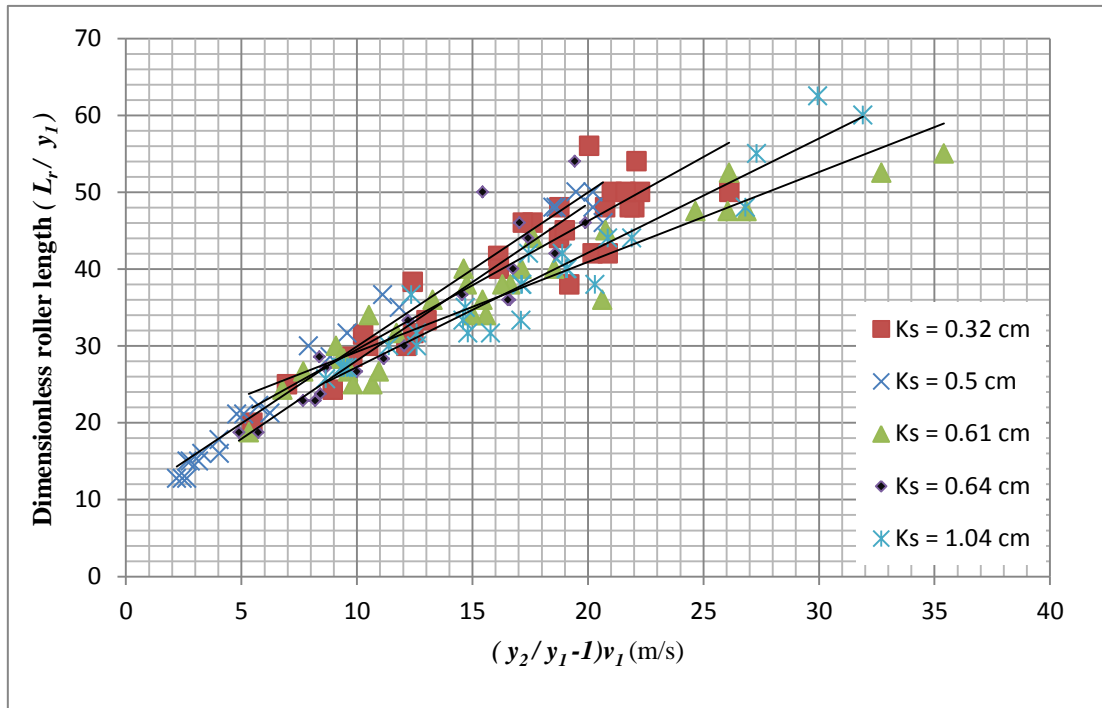


Figure 4.30: Relationship between dimensionless roller length, L_r/y_1 and $(y_2/y_1 - 1)v_1$ for different K_s values separately (Hughes and Flack, 1984)

Table 4.10: Generated equations for dimensionless roller length

figure number; dimensionless roller length	roughness height, K_s (cm)	equation type	coefficients of equation, a_6, b_5 ; correlation coefficient, R^2 ; MAPE (%)	data set reference	
4.27; L_r/y_1	All K_s values		$a_6=0.815, b_5^*=9.16$ $R^2=0.7634$; MAPE=7.9		
4.28; L_r/y_1	0.46		$a_6=1.2319, b_5=3.73$ $R^2=0.83$; MAPE=10.06		
4.28; L_r/y_1	0.82	$\frac{L_r}{y_1} = a_6 \left(\frac{y_2}{y_1} - 1 \right) v_1 + b_5$	$a_6=1.063, b_5=6.85$ $R^2=0.6961$; MAPE=9.39	Carollo et al., (2007)	
4.28; L_r/y_1	1.46		$a_6=0.6828, b_5=10.10$ $R^2=0.9292$; MAPE=4.45		
4.28; L_r/y_1	2.39		$a_6=0.5801, b_5=12.50$ $R^2=0.8309$; MAPE=3.55		
4.28; L_r/y_1	3.2		$a_6=0.7329, b_5=9.12$ $R^2=0.9327$; MAPE=4.63		
4.29; L_r/y_1	All K_s values		$a_6=2.0038, b_5=9.90$ $R^2=0.9753$; MAPE=9.05		
4.30; L_r/y_1	0.32		$a_6=1.67, b_5=12.82$ $R^2=0.8575$; MAPE=6.65		
4.30; L_r/y_1	0.5	$\frac{L_r}{y_1} = a_6 \left(\frac{y_2}{y_1} - 1 \right) v_1 + b_5$	$a_6=2.0038, b_5=9.90$ $R^2=0.9753$; MAPE=6.82	Hughes and Flack, (1984)	
4.30; L_r/y_1	0.61		$a_6=1.1694, b_5=17.53$ $R^2=0.8878$; MAPE=7.39		
4.30; L_r/y_1	0.64		$a_6=2.0386, b_5=7.73$ $R^2=0.8643$; MAPE=7.59		
4.30; L_r/y_1	1.04		$a_6=1.4862, b_5=12.40$ $R^2=0.9256$; MAPE=4.91		

* b_5 is a constant

Considering R^2 and MAPE values, it can be said that suggested Equation (4.3) is reliable to calculate dimensionless roller length for the datasets and retarding coefficient K .

Obtaining equations from dimensionless roller length (L_r/y_1) versus $(y_2/y_1 - 1)v_1$, leads to gain “ K ” value which is retarding force coefficient in Equation 3.50. In above obtained equations, coefficient “ a_6 ” gives $(1/K)$ amount for all kind of K_s values.

Chapter 5

CONCLUSION

This study introduced a solution for the hydraulic jump on a rough bed by integrating the drag force equation into the momentum equation (Eq. 3.20). Using the Initially, it is assumed that the well-known Belanger's equation is not satisfactorily representing the relationship between conjugate depth and Froude numbers. Under this assumption, momentum equation is rewritten to integrate the effect of surface friction on physical behavior of the hydraulic jump. The resultant relationship given by Equation 3.23 was successful to help deriving a relationship between different parameters enrolled in the friction effects on hydraulic jump. Using the experimental results of previous studies like Carollo et. al. (2007), Hughes and Flack (1984), Ead and Rajaratnam (2002), and Evcimen (2005), the parameters like dimensionless roughness effect, $(K_s / \Delta E)$ and dimensionless drag effect, (β) were analyzed and evaluated. The results show that Drag force has a significant effect on hydraulic jumps on rough surfaces. It was important to define a relationship for drag coefficient, C_D , in terms of β parameter. The semi-empirical equation of roller length (L_r) is improved by means of drag force equation. The semi-empirical relationship was showing that the coefficient of roller length increases as roughness of surfaces increases.

Regarding the magnitudes of mean absolute percentage error, (MAPE) and coefficient of determination (R^2), it can be concluded that the power type equation

(Eq. 4.1) is satisfying the relationship between β and $K_s/\Delta E$ in all experimental results except Hughes-Flack's datasets and Evcimen's dataset except when $K_s = 1$ cm. Also equation (Eq. 4.1) expressed a good relationship between β and $K_s/\Delta E$ for different hydraulic jump conditions; for oscillating jump condition in Carollo's experimental results when $K_s = 3.2$ cm and in Hughes-Flack's experimental results when $K_s = 0.32$ cm; for steady jump condition, in Carollo's experimental results; and also for strong jump condition in Evcimen's experimental results when $K_s = 0.6$ cm and $K_s = 2$ cm.

MAPE and R^2 magnitudes show that, Fr_1 and β follow a good power relationship for most of datasets except Evcimen's experimental results which is following a linear relationship and the reason is due to the strong jump condition ($Fr_1 > 9$) of experiments.

The results of regression analysis depicted good correlation between α and β ($R^2=0.83\sim 0.97$) when simulated with the dataset of Carollo's experimental results. The MAPE of the simulated data of regression equations were also approving the good correlation of the results.

Considering MAPE and R^2 values, it can be said that there is a good power type relationship between C_D and F_d in results of Hughes-Flack experiments and also for smaller K_s values in Carollo's experimental result except $K_s = 2.39$ and $K_s = 3.2$ cm.

With respect to regression and error analysis dimensionless roller length, (L_r/y_1) and $K/\Delta E$ are obeying a reliable power type relationship for both Hughes-Flack's and Carollo's Experimental results.

MAPE and R^2 values show that there is a strong linear relationship between dimensionless roller length, (L_r/y_1) and $(y_2/y_1 - 1)v_1$ for both Carollo and Hughes-Flack's datasets and this linear equation produces coefficient K values for all K_s values. Totally, it can be said that, generated equations 4.2 and 4.3 are satisfying both Hughes-Flack's and Carollo's experimental results very well.

Even though in most of the analyses good trends are obtained between the parameters, yet it is not possible to obtain only one equation representing the effect of bed roughness on the magnitudes of dimensionless drag effect, or dimensionless roller length. It is expected that in the future studies, the outcomes of this study can be further developed with new generation models of optimization theories like artificial neural network or genetic algorithm to simulate all the variables in one relation.

REFERENCES

- Abbaspour, A., Farsadizadeh, D., Hosseinzadeh A. D., Sadraddini, A. A. (2009). Numerical study of hydraulic jumps on corrugated beds using turbulence models. *Turkish J. Eng. Env. Sci.*, 33 (2009), 61 – 72.
- Afzal, N., Bushra, A., Seena, A. (2011). Analysis of turbulent hydraulic jump over a transitional rough bed of a rectangular channel: universal relations. *Journal of Engineering Mechanics*. 137(12), pp. 835-845.
- Alhamid, A. A., Negm, A. M., (1996). Depth ratio of hydraulic jump in rectangular stilling basins. *Journal of Hydraulic Research*. 34(5), pp. 597-604.
- Armstrong, J. S. (1985). Long-range Forecasting: From Crystal Ball to Computer, 2nd. ed. Wiley.
- Bidone, G. (1819, December 12). observations on the height of hydraulic jump in 1818. meeting of the Royal Academy of Science of Turin and later incorporated as a part of [2], pp. 21-80.
- Carollo, F. G., Ferro, V., and Pampalone, V. (2007). Hydraulic Jumps on Rough Beds. *Journal of Hydraulic Engineering*. Vol. 133, No. 9, pp. 989-999.
- Chanson, H. (2004). Hydraulics of open channel flow : An Introduction. (Butterworth-Heinemann, Oxford, UK), 2nd Edition, pp. 51-63

Chow, V. T. (1959). *Open Channel Hydraulics*. (McGraw-Hill International: New York, USA).

Chow, V. T. (1973). *Open Channel Hydraulics*. (McGraw-Hill International: New York, USA).

Ead, S. A., and Rajaratnam, N. (2002). Hydraulic Jumps on Corrugated Beds. *Journal of Hydraulic Engineering*. 138(7), 656-663.

Ebrahimi S, Salmasi F, Abbaspour A. (2013). Numerical Study of Hydraulic Jump on Rough Beds Stilling Basins. *J. Civil Eng. Urban*. 3(1), 19-24.

Evcimen, T. U. (2005). The Effect of Prismatic Roughness Elements on Hydraulic Jump. M. Sc. Thesis, Middle East Technical University, Department of Civil Engineering, Ankara, Turkey.

Glantz, Stanton A., Slinker, B. K. (1990). *Primer of Applied Regression and Analysis of Variance*, McGraw-Hill, pp. 187-287.

Hager, W. H., Bremen, R., and Kawagoshi, N. (1990). Classical hydraulic jump: length of roller, *Journal of Hydraulic Research*. IAHR, 28(5), 591-608.

Hager, W. H. (1992). *Energy dissipater and hydraulic jump*. *Kluwer academic publishers*. Dordrecht, Netherlands.

Hughes, W. C., and Flack, J. E. (1984). Hydraulic Jump Properties over a Rough Bed. *Journal of Hydraulic Engineering*. 110(12), pp. 1755-1771.

Khan, Aman U., Bartley, H. W. (2003). Case studies in public budgeting and financial management. New York, N.Y: Marcel Dekker.

Munson, B. R., Young, D. F., Okiishi, T. H., Huebsch, W. W., (1990). Fundamentals of Fluid Mechanics. (John Wiley & Sons, Inc.)

Rajaratnam, N. (1968). Hydraulic Jumps on Rough Beds. *Transaction, Engineering Inst. of Canada*, Vol. 11, No. A-2, pp. 1-8.

USBR. (1955). Research Studies on Stilling Basins. Energy Dissipators and Associated Appurtenances, US Bureau of Reclamation, Hydraulic Laboratory Report No. HYD-399.

Waller, Derek J. (2003). Operations Management: A Supply Chain Approach. Cengage Learning Business Press.

Zhao, Q., Misra, S. K., Svendsen, I. A., Kirby, J. T. (2004). Numerical study of a turbulent hydraulic jump. 17th ASCE Engineering Mechanics, June 13-16, 2004, University of Delaware, Newark, DE.

APPENDICES

Appendix 1: Hughes, W.C and Flack, J.E's (1984) Data

Hydraulic jump characteristics on artificially roughened beds in a rectangular horizontal flume with smooth side walls were measured by Hughes and Flack (1984). The test beds they used in their experiments were 0.305 wide each. The two types of roughness elements used were a series of parallel square bars aligned perpendicularly to the direction of the flow and closely packed gravel particles cemented to the base. A flume, which was made up of just a plexiglas surface, served as a control section by providing a smooth surface. The flume discharge, q , the upstream depth, y_1 , the tailwater or conjugate depth, y_2 , and the jump length, L_j , were measured during experiments. Two square bars (strip roughness) test beds were constructed using 3.18 mm and 6.36 mm square Plexiglas bars, with roughness elements spacing to height ratios of 4 and 3.75, respectively. Three gravel test beds were fabricated for $d_{50} = 4.4$ mm, 6.4 mm and 11.3 mm. 200 hydraulic jumps with the upstream Froude numbers ranging from 3.0 to 10.0 were observed throughout the testing period.

The measured experimental data is tabulated below

TABLE A.1 Hughes and Flack's data for smooth bed
(Hughes and Flack, 1984)

Q (ft ³ /s)	y ₁ (feet)	y ₂ (feet)	L _j (feet)	Fr ₁
0,34	0,082	0,256	1,30	2,53
0,33	0,069	0,292	1,50	3,23
0,33	0,061	0,315	2,00	3,89
0,33	0,057	0,331	2,20	4,30
0,33	0,054	0,338	2,50	4,71
0,33	0,041	0,377	2,80	6,95
0,35	0,073	0,285	1,40	3,12
0,36	0,060	0,328	1,80	4,27
0,35	0,054	0,354	2,10	4,93
0,35	0,048	0,374	2,40	5,82
0,34	0,043	0,381	2,70	6,80
0,38	0,068	0,325	1,60	3,78
0,38	0,059	0,354	2,00	4,73
0,38	0,054	0,374	2,40	5,37
0,37	0,047	0,407	2,80	6,47
0,41	0,074	0,335	1,70	3,64
0,41	0,065	0,361	2,00	4,40
0,41	0,061	0,394	2,10	4,81
0,40	0,052	0,423	2,60	6,02
0,41	0,060	0,387	2,30	4,91
0,41	0,064	0,371	-	4,48
0,41	0,071	0,344	1,90	3,87
0,41	0,080	0,322	1,60	3,23
0,41	0,065	0,348	2,00	4,35
0,41	0,065	0,371	2,20	4,37
0,41	0,058	0,377	2,20	5,14
0,40	0,049	0,420	2,70	6,59
0,40	0,057	0,397	2,50	5,25
0,41	0,062	0,371	2,20	4,67
0,41	0,067	0,351	1,90	4,16

TABLE A.2: Hughes and Flack's data for $z=0.32$ cm
(Hughes and Flack, 1984)

Q (ft ³ /s)	y ₁ (feet)	y ₂ (feet)	L _i (feet)	Fr ₁
0,43	0,08	0,34	1,60	3,44
0,42	0,06	0,39	1,90	5,34
0,43	0,06	0,39	1,90	4,86
0,42	0,05	0,42	2,10	7,06
0,42	0,05	0,41	2,20	6,03
0,42	0,05	0,43	2,40	7,49
0,42	0,05	0,43	2,40	7,42
0,41	0,05	0,44	2,50	7,38
0,42	0,05	0,43	2,40	7,06
0,42	0,05	0,42	2,20	6,55
0,42	0,05	0,43	2,40	6,06
0,42	0,05	0,41	2,10	7,49
0,43	0,06	0,39	2,00	4,86
0,42	0,06	0,39	1,80	5,21
0,42	0,05	0,40	1,90	7,09
0,45	0,08	0,38	2,00	3,80
0,45	0,06	0,43	2,50	6,17
0,45	0,06	0,43	2,40	6,18
0,45	0,05	0,44	2,80	6,65
0,45	0,06	0,43	2,50	5,16
0,45	0,06	0,42	2,40	5,03
0,45	0,07	0,41	2,10	4,72
0,45	0,07	0,40	2,00	4,54
0,45	0,05	0,44	2,70	7,33
0,45	0,06	0,44	2,70	7,08
0,45	0,07	0,41	2,20	4,62
0,45	0,05	0,43	2,50	7,16
0,44	0,07	0,38	1,70	4,42
0,44	0,05	0,47	2,50	8,04
0,43	0,07	0,37	1,70	3,88
0,43	0,06	0,40	2,00	5,42
0,43	0,05	0,41	2,30	6,32
0,43	0,05	0,41	2,40	6,74
0,43	0,05	0,43	2,50	7,36
0,43	0,05	0,41	2,30	6,17
0,43	0,06	0,40	2,30	5,17

TABLE A.3: Hughes and Flack's data for $d_{50}=0.5$ cm
(Hughes and Flack, 1984)

Q (ft ³ /s)	y ₁ (feet)	y ₂ (feet)	L _i (feet)	Fr ₁
0,49	0,11	0,32	1,40	2,40
0,49	0,10	0,32	1,50	2,61
0,52	0,10	0,35	1,60	2,96
0,51	0,09	0,35	1,90	3,40
0,51	0,09	0,37	2,00	3,56
0,48	0,10	0,32	1,60	2,73
0,48	0,11	0,31	1,40	2,34
0,48	0,10	0,30	1,50	2,55
0,43	0,09	0,31	1,60	2,71
0,44	0,10	0,29	1,50	2,55
0,45	0,09	0,32	1,60	2,77
0,46	0,09	0,35	1,90	3,20
0,46	0,09	0,32	1,60	3,04
0,46	0,11	0,29	1,40	2,34
0,38	0,06	0,35	1,90	4,68
0,35	0,06	0,32	1,80	4,30
0,41	0,05	0,41	2,40	7,26
0,41	0,06	0,36	1,90	4,44
0,41	0,06	0,37	-	4,66
0,4	0,06	0,38	2,10	5,24
0,4	0,06	0,37	2,20	5,08
0,4	0,05	0,42	2,30	7,22
0,43	0,05	0,40	2,10	5,97
0,42	0,05	0,40	2,30	5,95
0,44	0,05	0,42	2,40	6,51
0,43	0,05	0,42	2,40	6,46
0,43	0,05	0,42	2,50	6,81
0,44	0,05	0,43	2,50	6,88
0,44	0,07	0,38	2,00	4,36
0,44	0,08	0,36	1,70	3,64

TABLE A.4: Hughes and Flack's data for $d_{50}=0.61$ cm
(Hughes and Flack, 1984)

Q (ft ³ /s)	y ₁ (feet)	y ₂ (feet)	L _i (feet)	Fr ₁
0,40	0,07	0,34	1,70	3,84
0,40	0,05	0,39	1,90	6,33
0,40	0,05	0,41	2,20	6,33
0,40	0,06	0,34	1,80	4,60
0,34	0,04	0,37	2,10	9,15
0,34	0,05	0,35	1,80	5,72
0,34	0,05	0,32	1,70	4,80
0,42	0,06	0,34	1,50	5,40
0,41	0,08	0,33	1,50	3,48
0,41	0,06	0,35	1,60	5,35
0,41	0,05	0,37	1,70	6,30
0,41	0,05	0,38	1,90	5,78
0,41	0,06	0,37	1,90	5,35
0,40	0,05	0,40	2,00	6,33
0,41	0,04	0,43	2,10	9,70
0,41	0,04	0,40	1,90	8,37
0,41	0,04	0,43	2,20	10,50
0,35	0,06	0,31	1,60	4,35
0,35	0,04	0,36	1,80	7,50
0,35	0,05	0,32	1,70	5,04
0,35	0,04	0,37	1,90	8,64
0,36	0,06	0,33	1,70	4,86
0,42	0,05	0,38	1,80	6,05
0,41	0,06	0,35	1,70	4,60
0,42	0,05	0,39	1,90	6,20
0,41	0,04	0,41	1,90	8,40
0,41	0,05	0,40	2,00	6,85
0,41	0,05	0,36	2,00	6,10
0,41	0,05	0,40	1,80	7,62
0,42	0,05	0,38	1,70	5,88
0,41	0,06	0,35	1,60	4,70
0,41	0,06	0,35	1,50	4,80

TABLE A.5: Hughes and Flack's data for $z=0.64$ cm
(Hughes and Flack, 1984)

Q (ft ³ /s)	y ₁ (feet)	y ₂ (feet)	L _i (feet)	Fr ₁
0,44	0,08	0,36	1,60	3,42
0,44	0,07	0,38	1,90	4,27
0,44	0,05	0,40	2,30	6,29
0,44	0,06	0,39	2,00	5,24
0,44	0,05	0,39	2,00	6,37
0,50	0,08	0,40	1,90	4,30
0,50	0,06	0,43	2,20	5,57
0,42	0,08	0,32	1,50	3,33
0,42	0,06	0,35	1,60	4,88
0,42	0,08	0,34	1,50	3,60
0,42	0,06	0,36	1,70	5,27
0,42	0,07	0,36	1,60	4,04
0,41	0,05	0,38	1,80	6,51
0,41	0,06	0,38	2,00	4,79
0,41	0,05	0,39	2,30	7,56
0,41	0,05	0,40	2,10	6,86
0,41	0,06	0,38	1,80	5,33
0,41	0,05	0,38	1,80	6,48
0,42	0,07	0,36	1,60	4,32
0,42	0,07	0,38	2,10	4,11
0,42	0,05	0,39	2,50	5,87
0,42	0,05	0,41	2,70	6,98
0,42	0,05	0,39	2,20	5,96
0,42	0,06	0,38	1,90	4,68
0,42	0,05	0,40	2,20	6,43
0,42	0,07	0,37	2,00	4,27

TABLE A.6: Hughes and Flack's data for $d_{50} = 1.04$ cm
(Hughes and Flack, 1984)

Q (ft ³ /s)	y ₁ (feet)	y ₂ (feet)	L _i (feet)	Fr ₁
0,49	0,06	0,40	2,00	6,08
0,49	0,06	0,42	2,00	6,73
0,49	0,05	0,42	2,10	7,29
0,49	0,06	0,42	1,90	6,21
0,49	0,05	0,43	1,90	6,91
0,46	0,05	0,39	2,10	6,63
0,46	0,05	0,40	2,10	6,98
0,47	0,06	0,37	1,80	5,20
0,48	0,06	0,38	1,80	5,57
0,47	0,05	0,45	2,40	8,67
0,47	0,04	0,45	2,40	9,00
0,43	0,05	0,38	2,00	7,48
0,43	0,05	0,39	1,90	6,52
0,42	0,05	0,40	2,00	7,04
0,42	0,04	0,42	2,20	8,31
0,42	0,04	0,43	2,50	8,88
0,42	0,06	0,39	2,20	5,30
0,46	0,07	0,37	1,80	4,41
0,46	0,07	0,38	1,90	4,60
0,46	0,06	0,42	2,10	5,78
0,46	0,05	0,43	2,20	7,45
0,46	0,06	0,41	1,90	5,99
0,46	0,06	0,39	1,90	5,40
0,46	0,07	0,37	1,90	4,88
0,46	0,07	0,38	1,90	4,66
0,46	0,05	0,39	1,90	6,51

Appendix 2: Ead, S.A and Rajaratnam, N.'s (2002) Data

Ead and Rajaratnam (2002) conducted eleven experiments to study hydraulic jumps on corrugated beds. They used a flume that was 0.446 m wide, 0.60 m deep and 7.6 m long, and had plexiglas sides. In order to ensure that the crests of the corrugations were at the same level as the upstream bed on which the supercritical flow takes place, two corrugated aluminum sheets were installed on the bed of the flume in a certain way. These sheets had sinusoidal corrugations of the wavelength, s , of 68 mm perpendicular to the flow direction, and amplitudes, k_s , of 13 and 22 mm. In seven of the experiments, the initial depth, y_1 , measured above the crest level of the corrugations on the plane bed, was equal to 25.4 mm while it was 50.8 mm in four. All the experiments were conducted for a range of upstream Froude number from 4.0 to 10.0.

The measured experimental data is tabulated below

TABLE A.7: Ead and Rajaratnam's data for $k_s=1.3$ and 2.2 cm
(Ead and Rajaratnam, 2002)

K_s (cm)	s (mm)	q ($m^3/s/m$)	y_1 (cm)	y_2 (cm)	L_j (cm)	Fr_1
1,3	68,00	0,05	2,54	10,40	41,00	4,00
1,3	68,00	0,06	2,54	12,80	48,00	5,00
1,3	68,00	0,08	2,54	14,50	54,00	6,00
1,3	68,00	0,09	2,54	18,80	75,00	7,00
1,3	68,00	0,10	2,54	20,00	85,00	8,00
1,3	68,00	0,11	2,54	23,30	102,00	9,00
1,3	68,00	0,13	2,54	26,30	109,00	10,00
1,3	68,00	0,14	5,08	21,00	88,00	4,00
1,3	68,00	0,21	5,08	31,00	129,00	5,80
2,2	68,00	0,14	5,08	21,00	82,00	4,00
2,2	68,00	0,21	5,08	31,00	129,00	5,80

Appendix 3: Evcimen, T.U.'s (2005) Data

Evcimen (2005) observed the effects of rectangular prismatic roughness elements on hydraulic jump characteristics. A horizontal, rectangular open channel, which was 25.3 cm wide, 43.2 cm deep and 1000 cm long, was used in the studies. The entry and outlet of the channel was made of concrete, whereas the middle section was fiberglass, and 364 cm long. The roughness elements were located in the fiberglass part of the channel. An adjustable weir placed at the end of channel controlled the tailwater depth. The roughness elements were constructed using fiberglass. The heights of roughness elements were 0.6 cm, 1 cm and 2 cm. All the roughness elements had a width of 25 cm and a length of 1 cm. The longitudinal distance between two roughness elements were taken as 4 cm and 9 cm, respectively (Figure A.1). The incoming Froude number was between 6.8 and 16.6. A total of 81 measurements were made.

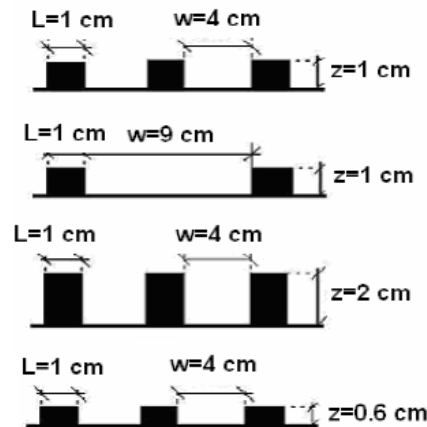


Figure A.1 Rectangular prismatic bars used in the experiments (Evcimen, 2005)

TABLE A.8: Evcimen's data for smooth bed (Evcimen, 2005)

y_1 (cm)	y_2 (cm)	Q (lt/s)	L_j (cm)	Fr_1
1,30	21,22	15,12	134,00	12,87
1,28	23,38	15,12	148,00	13,18
1,30	22,98	16,13	141,00	13,73
1,30	24,43	16,13	146,00	13,73
1,29	25,95	16,94	164,00	14,59
1,32	23,18	16,94	164,00	14,10
1,32	24,32	18,25	161,00	15,19
1,29	28,21	18,25	169,00	15,72
1,29	20,67	13,50	131,00	11,63
1,30	18,12	13,50	123,00	11,49
1,68	14,58	11,97	96,00	6,94
1,70	13,56	11,97	89,00	6,82
1,70	15,22	13,35	112,00	7,60
1,68	16,23	13,35	110,00	7,74
1,69	17,21	14,40	112,00	8,27
1,70	15,65	14,40	117,00	8,20
1,72	18,43	16,14	126,00	9,03
1,67	22,48	16,14	128,00	9,44
1,70	22,54	16,74	144,00	9,53
1,71	21,45	16,74	145,00	9,45

TABLE A.9: Evcimen's data for z=1 cm, w=4 cm (Evcimen, 2005)

y₁ (cm)	y₂ (cm)	Q (lt/s)	L_i (cm)	Fr₁
1,11	14,75	10,52	69,00	11,35
1,07	15,20	10,42	61,00	11,89
1,08	17,08	11,70	69,00	13,16
1,08	16,60	11,70	78,00	13,16
1,33	17,79	13,60	75,00	11,19
1,35	19,00	15,00	76,00	12,07
1,38	20,06	16,24	79,00	12,64
1,37	14,87	12,35	61,00	9,72
1,34	14,02	10,52	54,00	8,56
1,37	17,43	13,78	74,00	10,84

TABLE A.10: Evcimen's data for z=1 cm, w=9 cm (Evcimen, 2005)

y₁ (cm)	y₂ (cm)	Q (lt/s)	L_i (cm)	Fr₁
1,36	12,74	13,78	38,00	8,49
1,46	13,08	10,68	53,00	8,88
1,54	15,56	12,41	42,00	9,25
1,44	14,98	14,01	58,00	10,23
1,35	13,76	14,01	58,00	10,03
1,28	13,39	12,46	66,00	9,47
1,02	14,44	10,86	77,00	13,39
1,21	14,73	10,93	51,00	11,54
1,23	16,14	13,36	59,00	12,36
1,28	15,76	13,36	41,00	11,64
1,21	15,43	12,03	80,00	11,41
1,18	14,32	10,61	46,00	10,45
1,66	16,86	15,03	58,00	8,87
1,75	18,32	16,41	59,00	8,95
1,82	18,25	17,77	48,00	9,13
1,93	17,75	17,77	56,00	8,36
1,78	16,05	16,46	48,00	8,74
1,73	17,24	15,20	61,00	8,43
1,65	20,47	17,92	81,00	10,67
1,81	20,08	19,31	67,00	10,01

TABLE A.11: Evcimen's data for $z=2$ cm, $w=4$ cm (Evcimen, 2005)

y_1 (cm)	y_2 (cm)	Q (lt/s)	L_j (cm)	Fr_1
1,36	14,22	12,78	68,00	10,17
1,34	15,84	12,78	67,00	10,39
1,29	16,74	12,78	66,00	11,01
1,29	16,42	14,21	64,00	12,24
1,32	17,54	14,21	68,00	11,82
1,34	17,88	14,21	61,00	11,56
1,36	19,54	15,57	67,00	12,39
1,34	17,34	15,57	72,00	12,67
1,30	21,34	15,57	98,00	13,26
1,07	15,42	12,15	73,00	13,85
1,05	16,75	12,15	81,00	14,25
1,04	17,11	12,15	86,00	14,46
1,06	18,12	13,52	80,00	15,64
1,08	17,45	13,52	70,00	15,21
1,10	18,65	13,52	77,00	14,79
1,11	20,04	14,80	85,00	15,97
1,09	20,52	14,80	88,00	16,41
1,08	18,98	14,80	91,00	16,64
1,75	16,21	14,81	65,00	8,07
1,74	17,32	14,77	74,00	8,12
1,67	16,46	14,77	79,00	8,64
1,68	15,44	16,31	87,00	9,45
1,75	16,14	16,31	77,00	8,89
1,75	18,50	16,31	72,00	8,89
1,78	16,25	17,46	72,00	9,28
1,74	20,25	17,46	81,00	9,60
1,74	16,84	17,46	91,00	9,60

TABLE A.12: Evcimen's data for $z=0.6$ cm, $w=4$ cm (Evcimen, 2005)

y_1 (cm)	y_2 (cm)	Q (lt/s)	L_j (cm)	Fr_1
1,30	17,48	14,04	70,00	11,95
1,29	17,24	14,04	84,00	12,09
1,29	21,13	16,48	97,00	14,20
1,30	23,46	18,69	102,00	15,91
1,34	22,37	18,69	85,00	15,21
1,35	22,38	18,69	96,00	15,04
1,29	21,54	17,93	97,00	15,45
1,76	20,54	19,03	96,00	10,29
1,71	20,67	19,03	78,00	10,74
1,75	20,41	19,03	85,00	10,37
1,71	18,38	16,76	89,00	9,46
1,68	18,96	16,76	85,00	9,71
1,73	16,99	16,76	74,00	9,29
1,72	18,22	15,75	69,00	8,81
1,71	17,23	14,63	76,00	8,25
2,04	17,79	16,84	66,00	7,29

TABLE A.12 (Continued)				
y_1 (cm)	y_2 (cm)	Q (lt/s)	L_j (cm)	Fr_1
1,99	17,69	16,84	72,00	7,57
1,95	17,22	16,84	80,00	7,81
1,98	19,45	19,30	88,00	8,74
1,96	19,78	19,30	93,00	8,87
1,97	18,22	19,30	96,00	8,81
1,98	17,45	17,89	79,00	8,10
1,95	16,98	17,89	83,00	8,29
1,94	18,28	17,89	87,00	8,35

Appendix 4: Carollo, F.G, Ferro, V. and Pampalone, V.'s (2007)

Data

Carollo, Ferro, and Pampalone (2007) carried out an experimental study on horizontal rectangular rough beds. The experiments were conducted in a 14.4 m long, 0.6 m wide and 0.6 m deep rectangular flume made of glass. The measuring reach was 3 m long. Closely packed crushed gravel particles were cemented to the bottom of the flume. The median diameter, d_{50} , was used as roughness heights, k_s , which were taken as 0.46 cm, 0.82 cm, 1.46 cm, 2.39 cm and 3.20 cm for each experiment, respectively. 408 test runs were conducted using discharges ranging from 17.4 to 73.1 lt/s, and incoming Froude numbers ranging from 1.9 to 9.9.

The measured experimental data is tabulated below:

TABLE A.13: Carollo, Ferro and Pampalone's data for smooth bed
(Carollo, Ferro and Pampalone, 2007)

d_{50} (cm)	y_1 (cm)	y_2 (cm)	Q (lt/s)	L_r (cm)	Fr_1	d_{50} (cm)	y_1 (cm)	y_2 (cm)	Q (lt/s)	L_r (cm)	Fr_1
-	6,99	16,15	64,94	34,00	1,87	-	3,59	12,35	35,41	38,00	2,77
-	6,84	16,72	64,55	32,00	1,92	-	3,32	12,06	33,54	47,00	2,95
-	6,94	16,52	65,28	-	1,90	-	3,25	11,98	32,70	32,00	2,97
-	6,51	16,00	59,93	36,00	1,92	-	3,12	11,71	31,48	35,00	3,04
-	6,49	16,13	59,66	32,00	1,92	-	2,94	11,42	30,03	43,00	3,17
-	5,40	12,57	46,93	35,00	1,99	-	2,83	11,23	28,45	30,00	3,18
-	7,09	16,71	70,60	25,00	1,99	-	2,78	11,05	27,79	41,00	3,19
-	5,68	14,58	51,13	34,00	2,01	-	2,84	11,23	28,87	34,00	3,21
-	6,14	15,98	57,76	41,00	2,02	-	2,52	10,72	25,79	34,00	3,43
-	6,35	15,79	61,04	30,00	2,03	-	2,44	10,48	24,57	31,00	3,43
-	5,74	15,33	53,24	40,00	2,06	-	4,11	18,38	53,87	51,00	3,44
-	5,38	14,69	49,01	43,00	2,09	-	2,27	10,39	23,40	40,00	3,64
-	5,22	12,06	47,07	27,00	2,10	-	3,20	16,31	39,91	50,00	3,71
-	5,52	14,92	51,18	37,00	2,10	-	3,49	17,59	47,29	51,00	3,86
-	5,11	12,49	46,02	33,00	2,12	-	2,03	9,95	21,52	31,00	3,96
-	6,17	16,29	61,63	35,00	2,14	-	4,13	21,93	64,51	72,00	4,09
-	5,59	15,42	53,65	34,00	2,16	-	1,87	10,13	19,80	39,00	4,12
-	5,82	15,24	57,52	33,00	2,18	-	3,83	21,63	61,41	85,00	4,36
-	4,84	14,00	44,02	41,00	2,20	-	3,53	21,17	57,96	70,00	4,65
-	4,96	13,77	45,67	36,50	2,20	-	3,08	18,87	47,64	57,00	4,69
-	6,44	16,86	67,57	34,00	2,20	-	2,92	18,67	45,20	60,00	4,82
-	5,92	16,24	59,82	37,00	2,21	-	3,32	20,75	54,91	60,00	4,83
-	6,40	17,17	67,55	35,00	2,22	-	2,28	15,66	33,19	56,00	5,13
-	6,17	16,47	65,38	31,00	2,27	-	3,42	23,45	61,69	82,00	5,19
-	5,46	15,05	54,43	35,00	2,27	-	2,63	17,97	41,76	56,00	5,21
-	5,07	14,70	49,56	36,00	2,31	-	3,18	22,94	57,76	90,00	5,42
-	5,30	14,85	53,88	38,00	2,35	-	2,30	16,98	36,45	70,00	5,56
-	4,21	13,18	39,45	38,00	2,43	-	2,91	22,65	54,57	86,00	5,85
-	5,20	15,38	54,37	42,00	2,44	-	2,13	16,77	34,70	58,00	5,94
-	4,14	12,75	39,26	31,00	2,48	-	2,65	22,06	50,99	80,00	6,29
-	4,67	14,08	47,03	35,00	2,48	-	2,38	21,78	47,47	77,00	6,88
-	3,98	12,65	37,15	46,00	2,49	-	2,20	20,78	43,48	80,00	7,09
-	4,50	14,22	45,39	44,00	2,53	-	2,01	19,62	39,09	82,00	7,30
-	4,37	12,85	43,43	32,00	2,53	-	2,20	21,93	45,50	70,00	7,42
-	4,07	13,59	40,74	39,00	2,64	-	1,91	19,57	38,05	78,00	7,67
-	3,67	12,53	36,33	35,00	2,75						

TABLE A.14: Carollo, Ferro and Pampalone's data for gravel beds
(Carollo, Ferro and Pampalone, 2007)

d_{50} (cm)	y_1 (cm)	y_2 (cm)	Q (lt/s)	L_r (cm)	Fr_1	d_{50} (cm)	y_1 (cm)	y_2 (cm)	Q (lt/s)	L_r (cm)	Fr_1
0,46	5,65	16,04	57,80	-	2,29	1,46	3,68	19,15	58,77	62,00	4,43
0,46	5,49	16,06	58,26	-	2,41	1,46	3,76	20,42	60,97	67,00	4,45
0,46	5,07	16,08	57,71	-	2,69	1,46	3,47	18,56	54,06	62,00	4,45
0,46	4,69	17,70	57,83	66,00	3,03	1,46	3,31	18,10	53,76	61,00	4,75
0,46	4,75	18,26	60,50	62,00	3,11	1,46	2,66	14,95	38,89	49,00	4,77
0,46	4,57	17,88	57,65	61,00	3,14	1,46	3,07	16,25	49,03	57,00	4,85
0,46	4,66	18,55	60,49	64,00	3,20	1,46	3,47	20,25	60,74	60,00	5,00
0,46	4,25	19,63	60,26	65,00	3,66	1,46	3,00	17,02	49,31	61,00	5,05
0,46	4,19	19,38	60,12	68,00	3,73	1,46	3,38	20,06	60,61	-	5,19
0,46	4,15	19,24	60,21	69,00	3,79	1,46	2,89	16,95	48,84	-	5,29
0,46	3,93	18,41	55,64	62,00	3,80	1,46	2,68	18,08	46,75	58,00	5,67
0,46	3,86	18,98	55,01	67,00	3,86	1,46	2,93	19,23	54,10	64,00	5,74
0,46	4,06	19,71	60,26	65,00	3,92	1,46	2,63	16,84	46,41	56,00	5,79
0,46	3,73	18,51	54,69	-	4,04	1,46	2,71	17,56	49,21	53,00	5,87
0,46	3,60	18,95	55,58	70,00	4,33	1,46	2,60	16,68	46,25	53,00	5,87
0,46	3,39	18,12	51,61	66,00	4,40	1,46	3,06	20,73	60,26	63,00	5,99
0,46	3,31	18,18	50,70	50,00	4,48	1,46	2,83	19,04	54,13	-	6,05
0,46	3,29	18,47	51,03	54,00	4,55	1,46	2,63	17,58	48,81	60,00	6,09
0,46	3,57	19,84	59,45	55,00	4,69	1,46	2,54	16,59	46,79	59,00	6,15
0,46	3,53	20,70	59,70	74,00	4,79	1,46	2,29	15,38	40,57	48,00	6,23
0,46	3,49	20,29	59,30	52,00	4,84	1,46	2,54	17,53	48,31	60,00	6,35
0,46	3,12	17,90	50,33	66,00	4,86	1,46	2,52	17,14	48,64	54,00	6,47
0,46	3,44	19,90	58,75	53,00	4,90	1,46	2,32	16,71	43,10	54,00	6,49
0,46	3,08	18,06	49,88	65,00	4,91	1,46	2,69	19,46	54,22	67,00	6,54
0,46	3,26	19,73	54,75	63,00	4,95	1,46	2,63	18,27	53,22	57,00	6,64
0,46	3,26	19,47	54,86	68,00	4,96	1,46	2,16	14,98	40,57	47,00	6,80
0,46	3,41	20,89	59,29	76,00	5,01	1,46	2,43	17,88	48,83	57,00	6,86
0,46	3,01	18,10	50,34	50,00	5,13	1,46	2,56	19,35	53,65	63,00	6,97
0,46	3,35	20,70	59,34	73,00	5,15	1,46	2,13	16,95	42,94	60,00	7,35
0,46	3,00	17,97	50,29	67,00	5,15	1,46	2,11	16,42	43,08	52,00	7,48
0,46	3,32	20,18	58,66	71,00	5,16	1,46	2,05	16,02	42,69	50,00	7,74
0,46	3,13	18,94	54,01	61,00	5,19	1,46	1,98	15,76	41,36	54,00	7,90
0,46	2,99	18,18	50,62	50,00	5,21	1,46	1,84	15,61	40,15	55,00	8,56
0,46	3,09	18,94	53,39	62,00	5,23	1,46	1,77	15,22	38,68	58,00	8,74
0,46	2,67	17,45	43,29	62,00	5,28	2,39	4,97	12,10	54,35	-	2,61
0,46	2,95	18,29	50,37	55,00	5,29	2,39	4,55	12,14	54,35	-	2,98
0,46	2,65	16,77	42,89	64,00	5,29	2,39	2,08	12,94	39,07	45,00	6,93
0,46	2,82	17,98	47,08	58,00	5,29	2,39	2,04	13,04	38,22	48,00	6,98
0,46	3,23	20,83	58,91	71,00	5,40	2,39	1,98	13,34	37,12	-	7,09
0,46	3,02	19,97	53,46	71,00	5,42	2,39	2,48	16,72	52,26	61,00	7,12
0,46	3,02	19,54	53,95	70,00	5,47	2,39	5,39	12,11	54,32	-	2,31
0,46	2,88	18,46	50,33	56,00	5,48	2,39	4,38	12,24	54,09	-	3,14
0,46	2,74	17,69	47,48	68,00	5,57	2,39	4,28	13,42	53,91	-	3,24
0,46	2,82	18,20	49,66	69,00	5,58	2,39	4,56	14,54	60,20	-	3,29
0,46	2,96	19,55	53,78	60,00	5,62	2,39	4,49	15,14	61,15	-	3,42
0,46	2,69	17,84	46,93	60,00	5,66	2,39	4,10	13,31	53,98	-	3,46
0,46	2,68	17,19	46,75	58,00	5,67	2,39	4,47	15,51	61,63	-	3,47

TABLE A.14 (Continued)

d ₅₀ (cm)	y ₁ (cm)	y ₂ (cm)	Q (lt/s)	L _r (cm)	Fr ₁	d ₅₀ (cm)	y ₁ (cm)	y ₂ (cm)	Q (lt/s)	L _r (cm)	Fr ₁
0,46	2,53	16,75	42,88	58,00	5,67	2,39	3,87	15,33	53,65	-	3,75
0,46	2,27	15,57	36,51	61,00	5,68	2,39	4,16	16,00	60,27	-	3,78
0,46	2,66	18,48	47,12	70,00	5,78	2,39	4,11	15,87	61,07	-	3,90
0,46	2,48	17,11	42,94	59,00	5,85	2,39	4,07	16,43	61,26	70,00	3,97
0,46	2,42	16,73	42,52	64,00	6,01	2,39	3,72	13,49	53,93	-	4,00
0,46	2,42	16,37	42,73	66,00	6,04	2,39	3,72	16,46	55,96	63,00	4,15
0,46	2,65	18,47	49,53	67,00	6,11	2,39	3,33	16,21	52,30	60,00	4,58
0,46	2,54	17,76	47,09	70,00	6,19	2,39	2,75	12,20	39,34	49,00	4,59
0,46	2,32	16,87	41,37	65,00	6,23	2,39	3,55	18,05	59,96	67,00	4,77
0,46	2,51	18,25	46,56	64,00	6,23	2,39	2,95	14,04	46,37	56,00	4,87
0,46	2,74	19,31	53,19	69,00	6,24	2,39	3,28	17,20	55,59	63,00	4,98
0,46	2,57	19,02	49,86	60,00	6,44	2,39	3,48	17,77	60,88	72,00	4,99
0,46	2,15	16,36	38,69	62,00	6,53	2,39	2,66	13,30	40,76	47,00	5,00
0,46	2,24	16,47	41,14	65,00	6,53	2,39	3,40	17,66	60,68	70,00	5,15
0,46	2,26	16,56	42,14	67,00	6,60	2,39	2,39	12,19	36,04	41,00	5,19
0,46	2,05	15,00	36,46	58,00	6,61	2,39	2,80	14,60	46,05	55,00	5,23
0,46	2,38	17,86	46,58	67,00	6,75	2,39	3,18	16,94	55,95	65,00	5,25
0,46	2,07	16,27	39,12	63,00	6,99	2,39	2,45	12,98	39,06	48,00	5,42
0,46	2,10	16,29	40,15	63,00	7,02	2,39	3,12	17,77	56,24	66,00	5,43
0,46	1,75	14,04	31,58	58,00	7,26	2,39	3,24	17,98	59,73	69,00	5,45
0,46	2,13	17,46	42,94	64,00	7,35	2,39	2,97	16,55	52,71	51,00	5,48
0,46	1,44	11,82	24,71	48,00	7,61	2,39	2,52	14,32	41,35	50,00	5,50
0,46	1,84	15,22	36,02	61,00	7,68	2,39	2,91	16,82	51,49	62,00	5,52
0,46	1,61	13,59	29,60	56,00	7,71	2,39	2,71	15,33	46,45	56,00	5,54
0,46	1,69	13,58	31,87	54,00	7,72	2,39	2,50	14,06	41,38	49,00	5,57
0,46	1,21	11,39	21,76	50,00	8,70	2,39	2,30	13,13	36,91	45,00	5,63
0,46	1,11	10,80	19,16	44,00	8,72	2,39	2,30	12,37	36,91	44,00	5,63
0,82	3,47	16,86	43,12	53,00	3,55	2,39	2,26	12,66	36,27	44,00	5,68
0,82	3,56	16,59	44,94	55,00	3,56	2,39	2,65	15,51	46,05	57,00	5,68
0,82	6,75	19,06	73,16	67,00	2,22	2,39	2,43	13,98	40,72	47,00	5,72
0,82	6,53	19,15	70,56	70,00	2,25	2,39	2,35	12,11	39,06	44,00	5,77
0,82	6,25	19,34	70,47	69,00	2,40	2,39	2,34	13,38	39,08	48,00	5,81
0,82	6,00	20,06	70,71	69,00	2,56	2,39	2,42	13,33	41,17	49,00	5,82
0,82	5,87	19,55	70,29	73,00	2,63	2,39	2,58	14,00	45,33	57,00	5,82
0,82	5,41	18,90	63,37	66,00	2,68	2,39	2,93	17,51	56,17	67,00	5,96
0,82	5,28	16,06	63,84	70,00	2,80	2,39	2,87	17,78	55,92	63,00	6,12
0,82	5,14	18,82	63,29	70,00	2,89	2,39	2,30	13,12	40,77	44,00	6,22
0,82	5,10	18,98	63,42	70,00	2,93	2,39	2,13	12,53	36,92	42,00	6,32
0,82	4,98	19,63	63,28	74,00	3,03	2,39	2,45	14,91	46,05	57,00	6,39
0,82	4,71	18,80	58,40	71,00	3,04	2,39	2,92	18,26	60,20	68,00	6,42
0,82	4,69	18,72	60,13	70,00	3,15	2,39	2,65	16,33	52,53	53,00	6,48
0,82	4,45	18,80	58,04	67,00	3,29	2,39	2,15	12,85	38,69	44,00	6,53
0,82	4,69	20,23	63,37	76,00	3,32	2,39	2,59	16,38	51,15	58,00	6,53
0,82	4,41	18,93	58,13	66,00	3,34	2,39	2,35	15,36	45,70	53,00	6,75
0,82	4,35	19,51	57,29	66,00	3,36	2,39	2,02	12,15	36,47	43,00	6,76
0,82	4,38	19,60	58,05	64,00	3,37	2,39	2,30	15,49	45,16	53,00	6,89
0,82	4,38	18,97	58,57	76,00	3,40	2,39	2,14	14,03	40,53	48,00	6,89
0,82	4,23	19,58	57,88	65,00	3,54	2,39	1,98	13,46	38,69	49,00	7,39
0,82	3,26	16,74	44,25	54,00	4,00	2,39	2,17	15,42	45,17	52,00	7,52

TABLE A.14 (Continued)

d₅₀ (cm)	y₁ (cm)	y₂ (cm)	Q (lt/s)	L_r (cm)	Fr₁	d₅₀ (cm)	y₁ (cm)	y₂ (cm)	Q (lt/s)	L_r (cm)	Fr₁
0,82	3,22	16,82	44,19	55,00	4,07	2,39	1,88	13,85	36,72	-	7,58
0,82	3,83	20,22	57,75	75,00	4,10	2,39	2,34	16,42	52,27	62,00	7,77
0,82	2,69	13,87	35,40	41,00	4,27	2,39	2,11	15,03	45,16	50,00	7,84
0,82	3,65	19,51	57,53	66,00	4,39	2,39	1,80	13,75	38,26	48,00	8,43
0,82	3,79	21,14	61,70	60,00	4,45	2,39	1,75	14,05	38,02	-	8,74
0,82	3,07	17,60	45,39	57,00	4,49	3,2	3,93	16,09	56,37	53,00	3,85
0,82	3,58	19,09	57,41	63,00	4,51	3,2	3,98	16,05	58,04	58,00	3,89
0,82	2,95	16,43	42,94	53,00	4,51	3,2	4,06	16,10	60,42	63,00	3,93
0,82	3,74	21,09	61,98	73,00	4,56	3,2	3,98	16,80	59,39	58,00	3,98
0,82	3,00	17,23	45,31	58,00	4,64	3,2	2,13	13,50	39,08	47,00	6,69
0,82	3,38	19,47	54,77	65,00	4,69	3,2	2,27	14,91	43,32	50,00	6,74
0,82	2,58	15,57	36,68	42,00	4,71	3,2	2,34	16,02	46,75	55,00	6,95
0,82	2,85	16,20	42,95	53,00	4,75	3,2	2,75	18,58	59,90	61,00	6,99
0,82	2,48	14,06	34,94	47,00	4,76	3,2	6,27	12,76	61,96	-	2,10
0,82	2,83	16,98	45,00	60,00	5,03	3,2	6,24	13,33	61,81	-	2,11
0,82	2,81	17,22	44,79	58,00	5,06	3,2	5,78	13,66	61,63	-	2,36
0,82	3,13	19,28	54,01	60,00	5,19	3,2	5,73	13,83	61,60	-	2,39
0,82	2,65	16,16	42,56	47,00	5,25	3,2	5,44	13,26	59,13	-	2,48
0,82	1,93	12,51	26,76	43,00	5,31	3,2	5,41	13,46	58,88	-	2,49
0,82	2,11	14,45	30,76	56,00	5,34	3,2	5,38	13,43	59,10	-	2,52
0,82	1,50	10,50	18,54	30,00	5,37	3,2	5,51	13,91	61,25	-	2,52
0,82	2,33	15,63	36,49	51,00	5,46	3,2	5,34	14,42	61,22	-	2,64
0,82	2,27	15,22	35,54	48,00	5,53	3,2	5,06	14,19	58,82	-	2,75
0,82	2,19	14,79	33,86	50,00	5,56	3,2	4,89	14,54	58,73	52,00	2,89
0,82	1,88	13,30	28,05	52,00	5,79	3,2	4,88	14,85	58,55	53,00	2,89
0,82	1,74	12,45	25,28	45,00	5,86	3,2	4,41	15,63	58,48	55,00	3,36
0,82	1,35	9,21	17,36	29,00	5,89	3,2	4,26	15,68	58,00	53,00	3,51
0,82	2,16	14,89	35,38	58,00	5,93	3,2	3,89	16,21	57,96	57,00	4,02
0,82	1,58	11,05	22,28	40,00	5,97	3,2	3,91	16,92	59,14	58,00	4,07
0,82	1,34	9,18	17,55	24,00	6,02	3,2	3,89	16,30	60,12	63,00	4,17
0,82	1,69	11,82	24,98	42,00	6,05	3,2	3,73	16,43	59,84	60,00	4,42
0,82	1,56	11,01	22,45	37,00	6,13	3,2	3,60	17,11	59,95	61,00	4,67
0,82	1,68	12,65	26,64	53,00	6,51	3,2	3,29	16,19	53,61	58,00	4,78
0,82	1,27	9,08	17,51	25,00	6,51	3,2	3,23	16,35	56,95	58,00	5,22
0,82	1,25	8,98	17,44	18,00	6,64	3,2	3,32	17,03	60,59	61,00	5,33
0,82	1,57	12,25	25,55	45,00	6,91	3,2	3,16	17,04	56,90	63,00	5,39
0,82	1,59	13,25	26,45	45,00	7,02	3,2	3,28	17,60	60,39	62,00	5,41
0,82	1,50	11,88	24,89	43,00	7,21	3,2	2,98	15,97	53,46	60,00	5,53
0,82	1,50	12,11	25,27	43,00	7,32	3,2	2,86	16,69	50,63	57,00	5,57
0,82	1,45	11,42	24,81	40,00	7,56	3,2	2,76	15,97	49,98	58,00	5,80
0,82	1,42	12,10	25,31	42,00	7,96	3,2	3,03	18,09	58,08	58,00	5,86
0,82	1,36	11,75	24,89	38,00	8,35	3,2	3,05	17,52	60,16	63,00	6,01
1,46	4,76	18,17	61,87	66,00	3,17	3,2	2,81	16,36	53,38	58,00	6,03
1,46	4,69	18,58	61,84	65,00	3,24	3,2	2,72	17,30	53,03	59,00	6,29
1,46	5,68	13,17	56,22	-	2,21	3,2	2,70	16,85	53,03	60,00	6,36
1,46	5,49	13,69	55,60	-	2,30	3,2	2,92	18,19	59,92	62,00	6,39
1,46	5,44	13,14	55,80	-	2,34	3,2	2,83	18,60	57,89	59,00	6,47
1,46	5,22	13,78	56,26	-	2,51	3,2	2,53	15,19	49,99	58,00	6,61
1,46	5,19	15,42	55,99	65,00	2,52	3,2	2,73	17,50	56,37	63,00	6,65

TABLE A.14 (Continued)

d₅₀ (cm)	y₁ (cm)	y₂ (cm)	Q (lt/s)	L_r (cm)	Fr₁	d₅₀ (cm)	y₁ (cm)	y₂ (cm)	Q (lt/s)	L_r (cm)	Fr₁
1,46	5,00	14,73	54,63	-	2,60	3,2	2,40	15,77	49,68	55,00	7,11
1,46	5,27	17,57	62,75	67,00	2,76	3,2	2,25	15,27	46,62	54,00	7,35
1,46	5,22	17,00	62,08	66,00	2,77	3,2	2,52	17,29	56,46	59,00	7,51
1,46	4,75	14,56	54,47	-	2,80	3,2	1,93	14,51	37,94	53,00	7,53
1,46	5,06	18,07	62,67	70,00	2,93	3,2	1,87	13,75	37,15	52,00	7,73
1,46	4,71	18,42	62,62	70,00	3,26	3,2	2,19	16,09	47,14	55,00	7,74
1,46	4,62	18,56	61,58	66,00	3,30	3,2	2,54	18,46	59,19	-	7,78
1,46	4,51	18,71	61,92	66,00	3,44	3,2	2,54	17,88	59,34	60,00	7,80
1,46	4,43	18,95	61,15	68,00	3,49	3,2	1,91	13,19	38,89	46,00	7,84
1,46	4,43	18,76	61,50	68,00	3,51	3,2	2,31	16,47	52,72	59,00	7,99
1,46	3,98	17,91	54,16	64,00	3,63	3,2	2,07	15,94	45,45	57,00	8,12
1,46	4,16	18,79	61,71	67,00	3,87	3,2	1,94	14,59	43,11	50,00	8,49
1,46	3,98	18,62	59,24	72,00	3,97	3,2	1,73	13,55	36,82	52,00	8,61
1,46	3,70	17,56	53,90	62,00	4,03	3,2	2,00	16,22	46,03	58,00	8,66
1,46	3,90	18,63	58,76	68,00	4,06	3,2	1,71	13,05	36,60	54,00	8,71
1,46	3,45	16,96	49,37	63,00	4,10	3,2	1,96	15,12	46,62	55,00	9,04
1,46	3,69	18,50	54,75	65,00	4,11	3,2	2,02	16,28	49,53	57,00	9,18
1,46	3,97	19,42	61,24	63,00	4,12	3,2	1,80	15,65	42,52	54,00	9,37
1,46	3,63	18,26	54,07	68,00	4,16	3,2	1,80	13,90	42,71	50,00	9,41
1,46	3,63	17,45	54,07	61,00	4,16	3,2	1,58	12,71	36,24	44,00	9,71
1,46	3,82	18,87	58,51	60,00	4,17	3,2	1,63	13,17	38,44	48,00	9,83
1,46	3,39	16,32	49,03	58,00	4,18	3,2	1,63	12,83	38,68	48,00	9,89
1,46	3,73	18,71	59,30	66,00	4,38						